1-31-2019

Understanding MyD88-dependent and -independent Mechanisms of Phagosomal Signaling and Inflammation Elicited by Borrelia burgdorferi, the Lyme Disease Spirochete

Sarah Benjamin
University of Connecticut - Storrs, sabenjamin@uchc.edu

Understanding MyD88-dependent and -independent Mechanisms of Phagosomal Signaling and Inflammation Elicited by *Borrelia burgdorferi*, the Lyme Disease Spirochete

Sarah Jane Benjamin, PhD

University of Connecticut, 2019

ABSTRACT

Lyme disease is a tick-borne illness caused by the spirochete *Borrelia burgdorferi* (Bb). It is believed that the robust inflammatory response induced by the host's innate immune system is responsible for the clinical manifestations associated with Bb infection. The macrophage plays a central role in the immune response to many bacterial infections and is thought to play a central role in activation of the innate immune response to Bb. Previous studies have shown that following phagocytosis of spirochetes by macrophages, phagosome maturation results in degradation of *Bb* and liberation of bacterial lipoproteins and nucleic acids, which are recognized by TLR2 and TLR8, respectively, and elicit MyD88-mediated phagosome signaling cascades. Bone marrow-derived macrophages (BMDMs) from *MyD88*$^{-/-}$ mice show significantly reduced spirochete uptake and inflammatory cytokine production when incubated with *Bb ex vivo*. Paradoxically, additional studies revealed that Bb-infected *MyD88*$^{-/-}$ mice exhibit inflammation in joint and heart tissues. To determine the contribution of MyD88 to macrophage-mediated spirochete clearance, we compared wildtype (WT) and *MyD88*$^{-/-}$ mice using a murine model of Lyme disease. *MyD88*$^{-/-}$ mice showed increased Bb burdens in hearts 28 days

post infection, while H&E staining and immunohistochemistry showed significantly increased inflammation and greater macrophage infiltrate in the hearts of *MyD88*$^{-/-}$ mice. This suggests that Bb triggers MyD88-independent inflammatory pathways in macrophages to facilitate cell recruitment to tissues. Upon stimulation with Bb *ex vivo*, WT and *MyD88*$^{-/-}$ BMDMs exhibit significant differences in bacteria uptake, suggesting that MyD88 signaling mediates cytoskeleton remodeling and the formation of membrane protrusions to enhance bacteria phagocytosis. A comprehensive transcriptome comparison in Bb-infected WT and *MyD88*$^{-/-}$ BMDMs identified a large cohort of MyD88-dependent genes that are differentially expressed in response to Bb*,* including genes involved in actin and cytoskeleton organization (*Daam1*, *Fmnl1*). We also identified a cohort of differentially-expressed MyD88-independent chemokines (*Cxcl2*, *Ccl9*) known to recruit macrophages. We identified master regulators and generated networks which model potential signaling pathways that mediate both phagocytosis and the inflammatory response. These data provide strong evidence that MyD88-dependent and -independent phagosomal signaling cascades in macrophages play significant roles in the ability of these cells to phagocytose Bb and mediate infection.

Understanding MyD88-dependent and -independent Mechanisms of Phagosomal Signaling and Inflammation Elicited by *Borrelia burgdorferi*, the Lyme Disease Spirochete

Sarah Jane Benjamin

B.S., Colorado State University, **2012**

M.S., Colorado State University, **2013**

A Dissertation

Submitted in Partial Fulfillment of the

Requirements for the Degree of

Doctor of Philosophy

at the

University of Connecticut

2019

APPROVAL PAGE

Doctor of Philosophy Dissertation

Understanding MyD88-dependent and -independent Mechanisms of Phagosomal Signaling and Inflammation Elicited by *Borrelia burgdorferi*, the Lyme Disease Spirochete

Presented by

Sarah Jane Benjamin, B.S., M.S.

Major Advisor_____

Juan C. Salazar, MD, MPH

Associate Advisor_____

Justin D. Radolf, MD

Associate Advisor_____

Melissa J. Caimano, PhD

Associate Advisor_____

Lynn Puddington, PhD

University of Connecticut

2019

ACKNOWLEDGMENTS

To Dr. Juan Salazar: You haves been the most incredible mentor and made this work possible through your unwavering support. You have encouraged independence and passion in my research, are always there in times of crisis, and have always been respectful and understanding. Thank you for helping me embrace the failures and celebrate the successes; you have taught me more than I could have ever hoped for.

To my Thesis Committee Members (Drs. Justin Radolf, Melissa Caimano, Lynn Puddington, and Kamal Khanna): Thank you all for contributing your scientific intellect and investing time for review and discussion. Your efforts helped make this work possible.

To my fellow labmates Dr. Kelly Hawley and Carson Karanian: You made the long experiments fun and the miserable moments bearable. Thank you for your patience and sharing your science expertise with me. It is through your teachings that I have been able to complete this work.

To Drs. Paola Vera-Licona and Laura Haynes: You both have been incredible role models for me. Thank you for always being available to listen, always wanting to help, and never letting me give up.

To my mother (Stacy), my father (John) and my brother (Tyler): Thank you for being my motivation to complete this process. You have always encouraged to keep moving forward and never give up on my dreams. My greatest gift in life has been having you there.

To my friends: There are too many things to list. You turned my experience in graduate school from negative to positive. Thank you all for reminding me that life is supposed to be fun.

TABLE OF CONTENTS

CHAPTER 1: INTRODUCTION

LYME DISEASE PREVALENCE AND CLINICAL MANIFESTATIONS

Lyme disease (LD) is the most common vector-borne illness in the United States (US). In 2017 there were 29,513 confirmed cases and 13,230 probable cases reported (CDC 2016). LD is most prevalent in the northeastern and north Midwestern regions of the US. Clinical manifestations range along a spectrum in severity and presentation and vary from patient to patient (**Figure 1**) (CDC 2016). Classic manifestations of LD include presentation of the characteristic bullseye rash know as *erythema migrans*, fever, aches, fatigue and other flu-like symptoms. Approximately 30% of patients develop arthritis, while smaller percentages of patients develop other severe manifestations including carditis (1%), meningitis (2%) and facial palsy (9%) (CDC 2016). Fatal myocarditis is a rare event, with only nine cases being reported between 1985 and 2018 (CDC 2016, Muehlenbachs, Bollweg et al. 2016). Despite receiving proper antibiotic treatment, a subset of LD patients develops what is termed Post Treatment Lyme Disease Syndrome (PTLDS) (CDC 2016). This syndrome develops in approximately 20% of LD cases and does not correlate with antibiotic treatment (Adrion, Aucott et al. 2015). PTLDS is indicated by a variety of symptoms that are not specific to Lyme disease, such as muscle aches and chronic fatigue (CDC 2016). Another subset of patients develop what is termed antibiotic-refractory Lyme arthritis. This presents in patients as persistent inflammatory arthritis even following antibiotic treatment for Lyme disease, and is potentially due to excessive inflammation or immune dysregulation (Steere and Arvikar 2015). Because of the variety of clinical manifestations seen in patients, it is widely accepted that the individual immune

response to infection is what drives human disease presentation (Bockenstedt 2010, Radolf, Caimano et al. 2012).

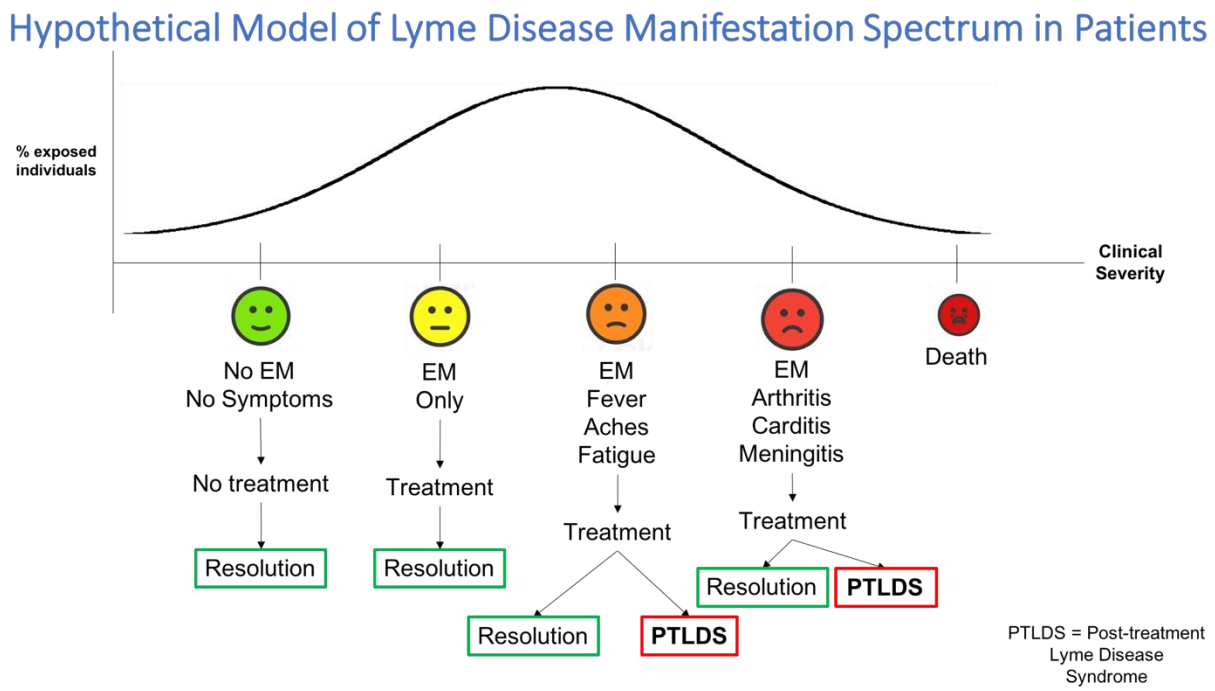

Figure 1: Spectrum of Clinical Manifestions in Lyme Disease. Clinical severity scale is plotted according to percentage of exposed individuals.

ETIOLOGIC AGENT OF LYME DISEASE

LD is caused by infection with the spirochetal bacterium *Borrelia burgdorferi* (Bb). There are at least 18 genospecies of *Borrelia burgdorferi* sensu lato, 3 of which cause most human infections (Mead 2015). In North America *Borrelia burgdorferi* sensu stricto cause Lyme disease, which is often distinguished by development of arthritis. The other two Borrelia strains that cause most disease in humans are *Borrelia garinii* and *Borrelia afezelii*, which are more prevalent in Europe (Radolf, Caimano et al. 2012, Steere, Strle et al. 2016). *Borrelia garinii* is distinguished more by presentation of neuroborreliosis and *Borrelia afezelii* is distinguished more by presentation with dermatologic conditions (Steere, Strle et al. 2016).

MOLECULAR ARCHITECTURE OF BB

There are multiple components of spirochetes that contribute to their recognition by innate immune cells. Bb, an extracellular pathogen, has a unique helical wave morphology with unique membrane and metabolic characteristics that differ from both gram-negative and gram-positive bacteria (Radolf, Goldberg et al. 1995). Bb does not contain coding material for lipopolysaccharide (LPS) and thus does not engage TLR4 (Norgard, Arndt et al. 1996, Fraser, Casjens et al. 1997). It also does not contain coding material for any toxins that may contribute to pathogenesis, The Bb spirochete forms a helical wave that contains both inner and outer membranes. In the periplasmic space between the outer and inner membranes there is a peptidoglycan layer and a flagellum that wraps around the cell between the outer membrane and the peptidoglycan layer. The flagella are anchored to

motors at either end of the spirochete that are controlled by chemotaxis proteins, which control direction of cell movement. The inner membrane of Bb contains inner membrane lipoproteins, sugar transport systems and ABC transporters. Finally, there are export systems that span the inner membrane, the periplasmic space, and the outer membrane. The genome of Bb consists of a linear chromosome, 12 linear plasmids, and 9 circular plasmids. (Fraser, Casjens et al. 1997). The outer membrane is abundant in a variety of lipoproteins. These include outer surface proteins (Osps), decorin-binding proteins (Dbps), and complement regulator-acquiring surface proteins (CRASPs) (Kenedy, Lenhart et al. 2012). Bb also has porins, which are β-barrel proteins that span the outer membrane.

OUTER SURFACE PROTEINS:

OspA/B: OspA and OspB contribute to Bb persistence in ticks. Both lipoproteins are expressed when Bb colonizes the tick midgut and are downregulated when the tick begins to feed (Pal, de Silva et al. 2000, Schwan and Piesman 2000). OspA binds to the tick receptor for OspA (TROSPA) (Pal, Li et al. 2004). Bb mutants deficient in OspA fail to survive in the tick midgut (Yang, Pal et al. 2004).

OspC: Expression of OspC is induced within 36 hours of tick feeding and is essential for transmission into the mammalian host but is not required for dissemination within the host (Schwan 2003, Tilly, Krum et al. 2006).

COMPLEMENT REGULATOR-ACQUIRING SURFACE PROTEINS:

CRASPs are Bb lipoproteins on the outer membrane that bind host complement proteins in the serum. Bb CRASP proteins include the OspE-related proteins CspA and CspZ (Kraiczy, Hellwage et al. 2004, Hartmann, Corvey et al. 2006). These proteins bind Factor H and Factor H-like protein-1 (FH and FH-1 respectively) (Hellwage, Meri et al. 2001), which are negative regulators of complement. Binding of the proteins on the Bb membrane helps the spirochete evade host complement.

TRANSMISSION AND LIFE CYCLE OF BB

Transmission of Bb in North America is through the black-legged deer tick, *Ixodes scapularis*. Humans are considered "dead-end" hosts or incidental hosts because they are not natural reservoirs for Bb (Radolf, Caimano et al. 2012). The most common mammalian reservoir is the white-footed mouse *Peromyscus leucopus*. Bb maintains a natural enzootic cycle between a tick vector and mammalian reservoir, typically small rodents. Naïve larvae become infected when they feed on an infected mammalian host. After feeding, the infected larvae molt into nymphs, which then feed on a second mammalian host. If this mammalian host is uninfected the infected nymph will transmit Bb into the bloodstream via the tick salivary stream. After feeding nymphs will molt into adult ticks and females will feed on larger mammalian hosts, which are typically white-tailed deer. Adult males do not feed. In addition to feeding, adult ticks breed on white-tailed deer. However, deer are non-competent hosts for Bb and do not become infected or transmit the spirochetes (Kurtenbach, Hanincova et al. 2006).

DISSEMINATION OF BB IN THE MAMMALIAN HOST

Despite secretion of salivary proteins to inhibit chemotaxis, immune cells are actively recruited to the bite site. Blister fluid analysis of EM lesions shows recruitment of dendritic cells, macrophages, lymphocytes and neutrophils. Recruitment of these cells results in cytokine and chemokine production as part of the inflammatory response. However, Bb is still able to disseminate via the hematogenous route in the mammalian host, but does not reach high levels in the blood (Wormser 2006). Instead, Bb first travels to target tissues by traversing the extracellular matrix or crossing tissue barriers. Target tissues for Bb dissemination that can result in severe clinical manifestations include heart, joint and brain (Steere and Glickstein 2004). Interactions with the host vasculature through fibronectin and various fibronectin-binding proteins expressed on Bb (such as Bbk32) contribute to the spirochete's ability to cross the extracellular matrix (Hyde, Weening et al. 2011). As an additional measure to cross the extracellular matrix, Bb also produces a bacterial protease (BbHtrA) which can cleave aggrecan, fibronectin and decorin (Russell, Delorey et al. 2013). Cleavage of these proteins degrades the extracellular matrix to promote invasion of the spirochete. Bb also expresses decorin-binding proteins (ie DbpA) which also contribute to its interactions with the host vasculature and contribute to dissemination (Guo, Brown et al. 1998). Binding to decorin plays a critical role in colonization, since decorin-defcient mice are resistant to infection and Bb that do not express DbpA fail to colonize target mouse tissues after inoculation (Fortune, Lin et al. 2014). Once Bb has disseminated through the human host it seeks to invade target tissues through interactions with endothelial cells. Proteins expressed on the outer membrane of Bb show affinity to integrins expressed on host endothelial cells. The most

well-defined interaction is that of Bb protein P66 with B1 and B3 integrins (Skare, Mirzabekov et al. 1997, Coburn, Magoun et al. 1998). P66 is not expressed in Bb during tick colonization and Bb strains with mutant P66 can infect mammalian hosts but are unable to survive longer than 48 hours, even in the absence of inflammatory cells (Curtis, Hahn et al. 2018). This suggests an important role for P66 in transmission (Ristow, Miller et al. 2012).

IMMUNE CELLS IN RESPONSE TO BB INFECTION

Adapted from (Cervantes, Hawley et al. 2014)

Unlike the reservoir hosts, humans mount significantly inflammatory responses to the spirochete that result in development of symptoms. Human infection with Bb induces both innate and adaptive immune responses, and it is believed that the innate immune response to the spirochete plays an important role in the severity of clinical manifestations during early LD (Bockenstedt 2010, Radolf, Caimano et al. 2012). A great amount of research has been done on the involvement of different parts of the innate and adaptive immune responses relating to infection with Bb. In the innate response, monocytes, macrophages, dendritic cells, Natural Killer cells (NK cells), NK-T cells and neutrophils have all been demonstrated to play an active role in the host response (Bockenstedt 2010, Radolf, Caimano et al. 2012, Cervantes, Hawley et al. 2014, Steere, Strle et al. 2016). T-cells and B-cells play a critical role in the adaptive immune response. Excluding the macrophage, the specific roles of each cell type have been described in more detail below. Because of the significance of macrophages in these studies, they will be reviewed in greater detail in the next section.

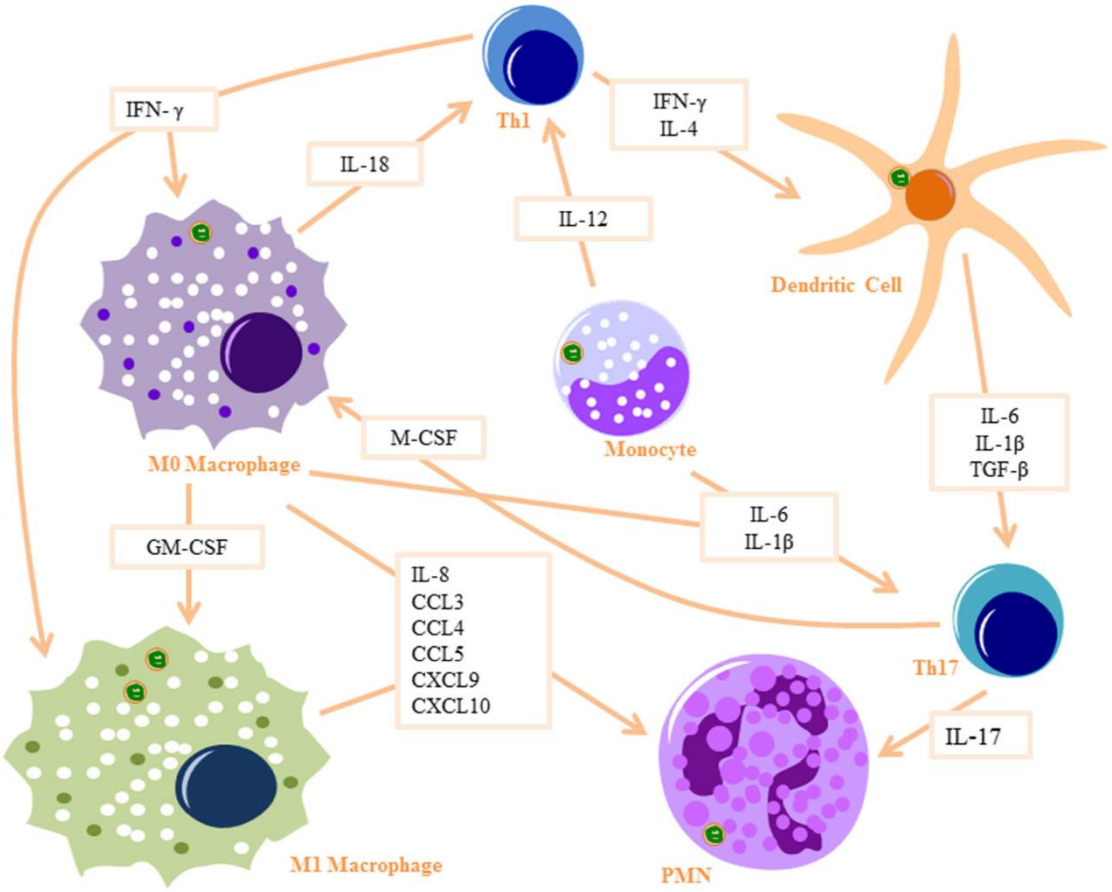

Figure 2: Innate signaling cascade in response to Bb Phagocytosis. Monocytes produce IL-12 to activate Th1 cells and IL6 and IL-1β to activate Th17 cells. Monocytes differentiate into macrophages when stimulated with IFN-γ (produced by Th1 cells) and M-CSF (produced by Th17 cells) and differentiate into dendritic cells when stimulated with IL-4 and IFN-γ. M0 macrophages produce IL-18 to activate Th1 cells and IL-6 and IL-1β to activate Th17 cells, as well as several PMN recruitment chemokines. They also differentiate into M1 macrophages when stimulated with GM-CSF and IFN-γ. Dendritic cells produce IL-6, IL-1β, and TGF-β to activate Th17 cells. Th17 cells produce IL-17, which is a strong PMN attractant. Part of images from Motifolio drawing toolkit (www.motifolio.com) were utilized in the figure preparation.

Figure adapted from (Cervantes, Hawley et al. 2014)

Monocytes: Monocytes contribute to the innate immune response through pro-inflammatory cytokine production after phagocytosis. These cytokines include IL-6, TNF-alpha, and IL-12. The increased IL-6 production helps induce Th17 helper cell differentiation which leads to neutrophil recruitment through IL-17 production. Production of TNFα helps facilitate recruitment of leukocytes and neutrophils by increasing vascular permeability at sites of infection. Finally, production of IL-12 drives Th1 differentiation, which results in increased IFNγ production that helps activate macrophages.

Dendritic Cells: Dendritic cells are very early responders to sites of Bb infection. Characterization of these cells after phagocytosis of Bb showed increased expression of CD40, CD80, CD83, CD86 and HLA-DR. Like monocytes, dendritic cells produce IL-6, TNFα and IL-12 in response to Bb. They also produce TGFβ, which helps Th17 differentiation, and IL-8, a neutrophil chemoattractant. To help regulate the inflammatory response, dendritic cells produce IL-10 which downregulates proinflammatory mediators. Finally, dendritic cells play a critical role in Bb antigen presentation to T-cells, which induces the adaptive immune response.

NK Cells and NKT Cells: While very little work has been published studying the effect of Bb on NK cells, there have been several studies characterizing the role of NKT cells in Bb infection. NKT cells have an important role in Bb clearance, since studies show that depleting NKT cells in mice results in higher bacterial burdens. NKT cells produce IFNγ in response to Bb, which aids in macrophage activation.

Neutrophils: Neutrophils are not only early responders to site of Bb infection, but also play an important role in development of Lyme arthritis. This has been shown in both mice, where they have been shown to play a significant role in arthritis development and severity, and in humans, where they are the primary cell type present in synovial fluid. In response to Bb, neutrophils make several inflammatory cytokines and chemokines that aid in both macrophage and T-cell activation.

T cells: T cells are important sources of IFNγ and are recruited to erythema migrans lesions in humans (Salazar, Pope et al. 2003). While they are not required for development of arthritis or carditis, Th1 cells are the predominant infiltrate in patients with Lyme arthritis and can exacerbate the severity of arthritis in the absence of B cells(Steere and Glickstein 2004). The regulation and function of regulatory cells is also disrupted in patients with Lyme arthritis (Vudattu, Strle et al. 2013). They also play a role in controlling Bb infection, since mice lacking T cells show higher spirochete burdens. CD4+ and CD8+ T cells can be activated by TLR signaling in response to Bb ligands, in addition to being activated by antigen presentation (Whiteside, Snook et al. 2018).

B cells: B cells can be activated by Bb both dependently and independently of helper CD4+ T cells (Hastey, Ochoa et al. 2014). Bb has been shown to migrate to lymph nodes to activate B cells via costimulation of their receptors (Tunev, Hastey et al. 2011). In addition, B-cells have been shown to make highly specific antibodies to Bb in both mice and humans, producing both IgM and IgG. However, the process of affinity maturation is not effective, and the humoral response is short-lived (Elsner, Hastey et al. 2015). This

antibody production plays an important role in recognizing bacteria peptides leftover from degradation and may contribute to arthritis severity.

Macrophages: Macrophages are highly phagocytic professional antigen presenting innate immune cells. They contain the machinery necessary to bind, engulf and degrade Bb. The macrophage is a principle component of the innate immune response and has been observed at sites of Bb infection (Salazar, Pope et al. 2003, Shin, Strle et al. 2010, Lasky, Olson et al. 2015). In humans, macrophages are recruited to sites of Bb infection in early stages and have been identified in EM lesions of patients with acute LD. They produce large amounts of chemokines at EM lesions in response to Bb. Macrophages also play a prominent role in the pathogenesis of murine Lyme carditis, and their recruitment to heart tissue is important in bacterial clearance (Montgomery, Booth et al. 2007). However, the mechanisms behind how these signaling cascades allow macrophages to initiate effective internalization and mediate inflammation are not well characterized.

INFLAMMATORY RESPONSES TRIGGERED BY BB

There are multiple Bb ligands that can trigger an innate immune response in the human host. Lipoproteins isolated from Bb were shown to be activators of both human and murine immune cells, even before the discovery of TLRs (Brandt, Riley et al. 1990, Radolf, Norgard et al. 1991). More importantly, the response elicited by macrophages stimulated with Bb lipoproteins or LPS (absent on the Bb outer membrane) was very similar (Radolf, Arndt et al. 1995, Radolf, Goldberg et al. 1995, Norgard, Arndt et al. 1996). Bb lipoproteins

contain triacyl peptides that can be recognized by TLR2/1 heterodimers (Hirschfeld, Kirschning et al. 1999, Wooten, Ma et al. 2002). Triacylation of lipoproteins is required for them to be localized to the Bb outer membrane and occurs in the spirochete through addition of first a diacylglyceride moiety onto a cysteine residue in the N-terminal region. This embeds the lipoprotein in the inner membrane and is followed by addition of a third fatty acid chain which facilitates transportation to the outer membrane. TLR2 recognizes the diacylglyceride moiety while TLR1 contains a hydrophobic pocket (absent in TLR6) that can recognize the additional fatty acid chain (Schenk, Belisle et al. 2009). The response is also enhanced by interaction of CD14 with the Bb PAMP-TLR2 complex. Early experiments investigating the role of CD14 on immune cell activation suggested that surface exposure of lipoproteins on the Bb outer membrane is important in initiating an immune response (Sellati, Bouis et al. 1999). However, the absence of CD14 results in more severe inflammatory responses both *in vitro* using human and murine cells and *in vivo* using CD14-/- mice (Benhnia, Wroblewski et al. 2005).

Following the discovery of Bb lipoprotein recognition by TLR2, it was discovered that in human cells a more significant immune response is elicited against live intact Bb rather than lysed or heat-killed spirochetes (Moore, Cruz et al. 2007). This is due to the location of the lipoprotein lipid moiety which serves as the TLR2 PAMP; it is embedded in the Bb outer membrane and tethers it to the surface. As a result, minimal recognition occurs at the cell surface (Moore, Cruz et al. 2007, Shin, Isberg et al. 2008, Salazar, Duhnam-Ems et al. 2009, Schenk, Belisle et al. 2009). Instead, principal recognition of Bb TLR2 ligands occurs within macrophage endosomal structures when the spirochete is phagocytosed, and its fragile outer membrane is compromised (Moore, Cruz et al. 2007, Shin, Isberg et

al. 2008). Thus, while some engagement of TLR2 is at the cell surface, the majority of Bb lipoprotein recognition occurs in the phagosome by endosomal TLR2 (Salazar, Duhnam-Ems et al. 2009, Cervantes, Dunham-Ems et al. 2011). In the absence of TLR2, murine macrophages do not show any defect in uptake of Bb (Salazar, Duhnam-Ems et al. 2009). However, mice lacking TLR2 show increased spirochete burdens in ankle, ear and heart tissue two and four weeks post Bb infection (Wooten, Ma et al. 2002).

In addition to Bb lipoprotein recognition by TLR2, other bacterial ligands are released into the phagosome for recognition by endosomal TLRs. As the spirochete is degraded, nucleic acids are released into the phagosomal compartment. These include Bb DNA and Bb RNA. Bb RNA is recognized by TLR7 in mouse cells and TLR8 in human cells (Petzke, Brooks et al. 2009, Cervantes, La Vake et al. 2013). Bb DNA is recognized by TLR9 (Shin, Isberg et al. 2008). Engagement of these TLRs by their Bb ligands results in production of type I interferons.

TLR2, TLR7, TLR8 and TLR9 appear to make the most significant contribution to Bb recognition by immune cells. Other endosomal TLRs appear to make a minimal, if any impact on initiating an immune response. The lack of LPS in Bb prevents recognition by TLR4. Pre-stimulation of macrophages with TLR3 ligands has no significant impact on cytokine response (Shin, Miller et al. 2009), indicating that TLR3 engagement and signaling do not appear to significantly contribute to the Bb inflammatory response. While Bb does have flagella located in the periplasmic space that can be recognized by TLR5,

cytokine production in macrophages pretreated with siRNA against TLR5 show no defect in phagocytosis or cytokine production (Shin, Isberg et al. 2008).

When taken together, the work described above defines a concept known as “phagosomal signaling”, which refers to the signaling cascades that are emitted from phagosomes due to recognition of ligands that are only accessible within the acidic environment of the phagosome. Phagosomal signaling emphasizes that because of the unique bacterial structure it is necessary for Bb to be taken up and degraded for significant recognition by the host immune system (Cervantes, Hawley et al. 2014) and is critical in the innate immune response to Bb because borrelial PAMPs are not exposed for recognition at the surface. To compensate for this, TLRs are recruited to phagosomes containing Bb. The TLRs that recognize Bb ligands all utilize the adaptor protein MyD88, making it a critical component in triggering inflammatory signaling in response to the spirochete.

THE ADAPTOR PROTEIN MYD88

MyD88 is the principle adaptor protein for TLR signaling. Once the TLRs bind to their ligand and heterodimerize, MyD88 binds to the cytoplasmic domain of the TLR and creates a scaffold for IRAK-1 and IRAK-4 to bind. This complex recruits TRAF-6, an E3 ubiquitin ligase that adds polyubiquitin chains in collaboration with TRICA-1, an E2 ubiquitin ligase. The addition of polyubiquitin chains onto both TRAF-6 and NEMO allow recruitment and activation of TAK1. Once activated, TAK1 phosphorylates IκB on NFκB and targets it for degradation. This activates NFκB and allows it to translocate into the

nucleus to induce proinflammatory cytokine production. Signaling cascades initiated by engagement of these TLRs are mediated by binding the adaptor protein MyD88. The TLRs involved in recognizing Bb utilize MyD88 to trigger phagosomal signaling cascades, making this adaptor protein a crucial element in mediating the inflammatory response to Bb. Nevertheless, the key host components involved downstream of these MyD88-mediated phagosome signals and their effects have not been well studied in the context of Bb infection.

MyD88 has been shown to be implicated in multiple processes relating to bacterial recognition and clearance. Previous studies have shown that MyD88 has no effect on bacterial binding (Blander and Medzhitov 2004). Murine macrophages lacking MyD88 show markedly diminished uptake of several bacterial species, including Bb (Takeuchi, Hoshino et al. 2000, Edelson and Unanue 2002, Blander 2007, Shin, Isberg et al. 2008, Ip, Sokolovska et al. 2010, Shen, Kawamura et al. 2010). Links between MyD88 signaling and proteins associated with phagocytosis have been studied (reviewed in the following section). The absence of MyD88 also results in a defect in phagosome maturation and acidification. In the absence of MyD88, degradation of multiple bacteria strains is also impaired due to inefficient acidification of phagosomes (Blander and Medzhitov 2004). However, in the context of Bb infection, lysosome maturation markers are recruited to Bb-containing phagosomes in macrophages lacking MyD88 (Shin, Isberg et al. 2008). The degree of phagosome maturation and acidification required to expose Bb ligands from the bacteria cell envelope for recognition is not known. Murine macrophages lacking MyD88 also show diminished production of NFκB-triggered pro-inflammatory cytokines,

such as TNFα and IL-6, when stimulated with different bacterial species, including Bb (Edelson and Unanue 2002, Shin, Isberg et al. 2008).

Paradoxically, mice lacking MyD88 show comparable levels of inflammation to WT mice in heart and joint tissue when infected with Bb (Bolz, Sundsbak et al. 2004, Liu, Montgomery et al. 2004, Behera, Hildebrand et al. 2006). This Bb-induced inflammation in MyD88-/- mice in joint tissues consists of a cell infiltrate that is more neutrophilic compared to WT mice (Bolz, Sundsbak et al. 2004). Comparable levels of inflammation in Bb-infected WT and MyD88-/- mice also suggests that the macrophage may help drive additional MyD88-independent inflammatory responses (Behera, Hildebrand et al. 2006). Bb-infected MyD88-/- mice also show significantly higher bacterial burdens in joint and bladder tissues (Bolz, Sundsbak et al. 2004, Liu, Montgomery et al. 2004, Behera, Hildebrand et al. 2006), which is not surprising given that the absence of MyD88 in macrophages also results in reduced spirochete uptake (Shin, Isberg et al. 2008). Increased pathogen burdens is a common phenotype in MyD88-/- when they are infected with multiple bacteria species (Ribes, Regen et al. 2013).

PHAGOCYTOSIS OF BB

Phagocytosis is a highly dynamic process that involves multiple cell processes. The events leading to phagosome formation can be summarized in four discrete steps: dynamic probing, particle binding that induces receptor clustering, phagocytic cup formation, and phagosome sealing (Levin, Grinstein et al. 2016, Niedergang and Grinstein 2018). Probing of the cell membrane results in surface receptor clustering when a phagocytic target is recognized. The receptor cluster allows for recruitment of kinases

such as Syk, which phosphorylates phagocytic receptors for activation, and PI3K, which converts PtdIns(4,5)P2 (PIP2) on the plasma membrane to PtdIns (3,4,5)P3 (PIP3). High levels of PIP3 in the plasma membrane initiate recruitment of guanine exchange factors (GEFs) and Rho-GTPases such as Rac1 and Cdc42. These proteins, through the WAVE or WASP protein complex, recruit and activate Arp2/3 for actin polymerization (Takenawa and Suetsugu 2007, Devreotes and Horwitz 2015). This results in two membrane protrusions that form a phagocytic cup around the target for uptake into the cell.

There are three different forms of phagocytosis that have been studied with Bb; opsonin-mediated phagocytosis, conventional phagocytosis, and coiling phagocytosis (**Figure 3**) (Cervantes, Hawley et al. 2014). Opsonin-mediated phagocytosis is mediated by the binding of opsonin antibodies to Bb and then triggering phagocytosis through ligation of Fc receptors expressed on the surface of professional immune phagocytes. Opsonic-mediated phagocytosis can occur with Bb and has been shown to play a role in pathogen burden and arthritis severity (Belperron, Liu et al. 2014), but professional immune phagocytes do not require opsonic antibodies to efficiently phagocytose Bb (Hawley, Cruz et al. 2017). Conventional phagocytosis requires the presence of a surface receptor that recognizes Bb and triggers membrane ruffling so that the spirochete is enveloped and sinks into the cell. inding of Bb to macrophages is mediated by surface integrins. Several surface integrins have been identified as receptors for Bb, including complement receptor 3 (CR3) and $\alpha 3\beta 1$ (Behera, Hildebrand et al. 2006, Hawley, Martin-Ruiz et al. 2013). Once attached, the mechanism by which Bb is phagocytosed is complex and can occur by either a sinking or coiling mechanism (Naj, Hoffmann et al. 2013, Cervantes, Hawley

et al. 2014). Both mechanisms require actin cytoskeleton rearrangement to internalize Bb into the endosome, where degradation takes place (Naj and Linder 2015). However, the mechanisms behind how these signaling cascades allow macrophages to initiate effective internalization and mediate inflammation are not well characterized. Coiling phagocytosis requires cell remodeling in order to occur. The cell protrudes a pseudopod out of the plasma membrane that can bend around the bacteria in a hook-like fashion. These pseudopod protrusions are the result of F-actin polymerization that is regulated by GTPases, Cdc42, Rac1. The WASP and Arp2/3 complexes are also involved. In the context of Bb phagocytosis, the formin proteins Daam1, Fmnl1 and mDia1 have been shown to play a role in the branching of actin filaments (Williams, Weiner et al. 2018).

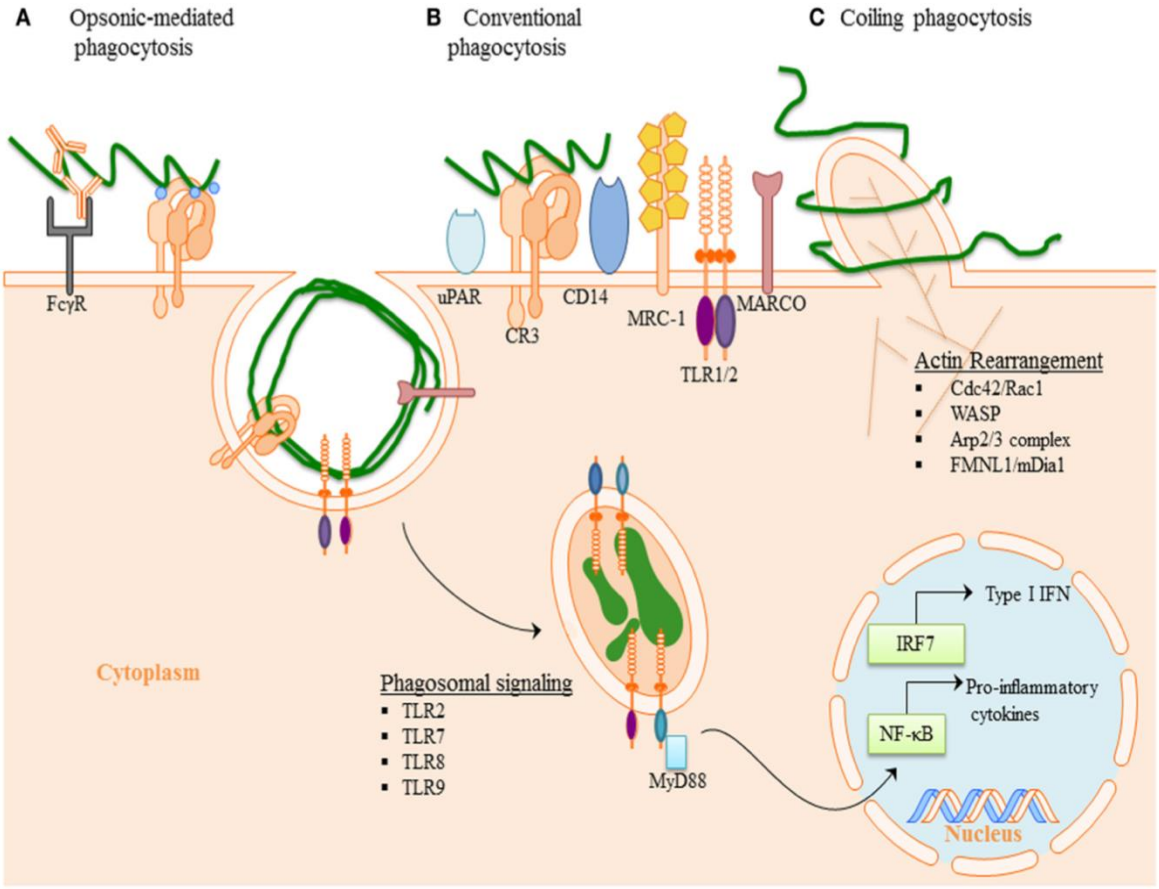

Figure 2: Phagocytosis of *Borrelia burgdorferi*. (A) Opsonic-mediated phagocytosis—complement factors, such as C3b and iC3b, bound to the surface of Bb can interact with complement receptors and mediate phagocytosis. Additionally, the immune cells Fc-receptors have the ability to bind to the opsonic antibodies that coat Bb and internalize the pathogen. (B) Conventional phagocytosis—the direct interaction of surface receptors with Bb, such as integrins and C-type lectins, allows for tether of the spirochete to the cell surface. Various PRRs induced signal cascade initiates formation of the phagocytic cup and spirochete engulfment. (C) Coiling phagocytosis—the preferred mechanism of spirochete internalization in which the phagocytic cell uses filopodial protrusions that capture Bb. The filopodial enwrap the spirochete and convert into coiling pseudopods. During this dynamic process FMNL1, mDai1 Arp2/3 complex, and WASP are involved in actin rearrangement of the cell, which then facilitates subsequent phagocytosis of Bb. Following internalization of Bb, the spirochete is degraded within the phagosome thus exposing additional PAMPs to PRR with in the phagosome. The phagosomal signals initiated by Bb generates a robust inflammatory response, including the induction of pro-inflammatory genes and Type I IFNs.

Figure adapted from (Cervantes, Hawley et al. 2014)

MURINE MODELS OF LD

Bb infection has been modeled in 5 different strains of laboratory mice; C3H/He, SWR, C57BL/6, SJL and BALB/c (Barthold, Beck et al. 1990, Barthold, Persing et al. 1991, Armstrong, Barthold et al. 1992, de Souza, Smith et al. 1993). Currently, the most common mouse strains studied are C57BL/6 and C3H/He, with genetic modifications based off these strains. In humans, carditis and arthritis are considered severe clinical manifestations that can be modeled in murine infection and are most commonly evaluated in mice. Of the strains evaluated, C3H/He mice display the most severe arthritis (Barthold, Persing et al. 1991). Bb disseminates to multiple tissues when inoculated in mice, including bladder, ear, skin, heart, joint, lymph node and spleen. Despite having high burdens during the initial stages of infection, C57BL/6 mice remain relatively asymptomatic with no joint swelling or weight loss. C3H/He mice development severe arthritis as indicated by ankle swelling, but still manage to reduce spirochete loads in tissues 3 weeks post infection.

SUMMARY OF THESIS CONTENT

The primary goal of the work presented in this dissertation is to understand how MyD88 mediates macrophage recognition and clearance of Bb both in vivo and ex vivo. Through murine infection, macrophage stimulation in culture, and computational analysis we have gained mechanistic insights into MyD88-dependent and -independent effects on inflammation and Bb uptake.

In Chapter 3 we define the role of MyD88 on Bb burdens, immune cell infiltrate, activated macrophage infiltrate, and inflammatory transcript response in target tissues. We identify

several chemokines that are produced in the absence of MyD88 and may contribute to cell recruitment during Bb infection. Here we show using a murine model of LD that MyD88 plays a role in inflammation severity in heart, but not joint tissue and is not required for immune cell recruitment. However, the presence of MyD88 is associated with Bb clearance from multiple tissues in the mouse, including heart and tibiotarsal joint. We also show that there are tissue-specific chemokine responses, resulting in different types of cell infiltrate and inflammation severity in the absence of MyD88. Taken together, our findings underscore the importance of the macrophage in Bb recognition and clearance and identify key MyD88-dependent components that play a significant role in mediating these processes.

In Chapter 4 we examine the effect of MyD88 on macrophage binding and uptake. We also characterize the colocalization of key receptors with Bb-containing phagosomes and confirm that MyD88 is not necessary for sufficient degradation of Bb. Finally, we show that production of MyD88-dependent chemokines is phagocytosis-dependent. Using an *ex vivo* murine macrophage system, we show that in the context of Bb stimulation, MyD88 signaling enhances, but is not required, for bacterial uptake and is not required for phagosome maturation.

In Chapter 5 we perform a comprehensive analysis of RNA sequencing data and identify MyD88-dependent genes involved in Bb uptake. We also characterize MyD88-independent inflammatory pathways through identification of master regulator proteins. Using an RNA-sequencing approach, we demonstrate that uptake of Bb by macrophages induces robust MyD88-independent inflammatory responses via phagocytosis-dependent production of chemokine proteins that can mediate cell recruitment to tissues. Taken

together, our findings underscore the importance of the macrophage in Bb recognition and clearance and identify key MyD88-dependent components that play a significant role in mediating these processes.

This body of work progresses the field of Bb immunology by proposing mechanisms that link MyD88 signaling with enhanced phagocytosis of Bb. It also identifies potential targets that can be tested and translated in human cells to better understand what inflammatory pathways contribute to Lyme disease severity in humans.

CHAPTER 2: MATERIALS AND METHODS

MICE:

Female 6-8-week-old C57BL/6J wild-type (WT) and C57BL/6J MyD88-/- (MyD88-/-) mice (Adachi, Kawai et al. 1998) used in these studies were obtained from breeding colonies maintained in the UConn Health (UCH) Center for Comparative Medicine facility according to protocols approved by the UCH Institutional Animal Care and Use Committee. Original WT breeding pairs were purchased from The Jackson Laboratory (Bar Harbor, Maine). Original MyD88-/- breeding pairs were kindly provided by Dr. Egil Lien at the University of Massachusetts with permission from Dr. S. Akira in Osaka, Japan. Disruption of the murine MyD88 gene was confirmed through PCR (Adachi, Kawai et al. 1998). WT and MyD88-/- mice were maintained on the antibiotic Sulfatrim (sulfomethoxazole [40 mg/mL] + trimethoprim [8 mg/mL]) diluted in water 1:50, which have been previously shown to not impact the degree of Bb infection (Liu, Montgomery et al. 2004).

BACTERIAL STRAINS:

Low-passage virulent wild-type strain 297 (Steere, Grodzicki et al. 1984) or a strain 297 isolate containing a stably-inserted copy of green fluorescent protein (GFP) under the control of the constitutively-expressed *flaB* promoter (Bb914) (Dunham-Ems, Caimano et al. 2009) were maintained in Barbour-Stonner-Kelly (BSK)-II media supplemented with 6% normal rabbit serum (Dunham-Ems, Caimano et al. 2009) and gentamicin (50 μg/μl). For temperature-shift, cultures were grown at 23°C for at least one week prior to being

shifted to 37°C as previously described(Dunham-Ems, Caimano et al. 2009). Spirochetes were counted by dark-field microscopy using a Petroff-Hausser counting chamber (Hausser Scientific) and diluted in BSK-II for experimental use. For *ex vivo* experiments, spirochetes were centrifuged at 3300 x g for 20 minutes at 4°C and suspended in DMEM (Gibco, 15630-080) supplemented with sodium pyruvate (Gibco, 11360-070) and HEPES (Gibco, 15630-080). After resuspension the cultures were counted by darkfield and diluted accordingly.

MOUSE INOCULATION:

Sex- and age-matched WT and MyD88-/- mice (6 mice per genotype per experiment) were injected intradermally with either 1 x 10^5 temperature-shifted Bb diluted in BSK-II or an equal volume of media alone and then sacrificed 14, 28, or 58 days post-infection. Infection was confirmed at 2 weeks post-infection by serology and culturing of ear tissue in BSK-II. Cultures were examined weekly for spirochetes by darkfield microscopy for at least 4 weeks. Serum was tested against Bb strain 297 whole cell lysates via chemiluminescent immunoblot using goat anti-mouse HRP-conjugated IgG (GE NA931) as previously described (Dunham-Ems, Caimano et al. 2012).

QUANTITATION OF BB BURDENS IN MOUSE TISSUES:

Mouse heart, tibiotarsal joint, bladder, skin, and ear tissues were harvested at the time of sacrifice. Skin for DNA isolation was taken from the abdomen of the mouse. Tissues were digested overnight in 0.1% Collagenase Type I in PBS (Gibco, 17100-017) at 37°C, then further digested with proteinase K solution (200 mM NaCl, 20 mM Tris-HCl pH 8.0, 50

mM EDTA, 1% SDS, 0.2 mg/mL Proteinase K (Machery-Nagel, 740506) in dH_2O) overnight at 56°C. DNA from 200μL of digested tissue was isolated using a genomic DNA purification kit (Machery-Nagel, 740952) according to manufacturer's instructions. Spirochete burdens were quantitated by qPCR using TaqMan-based assays for Bb *flaB* and murine nidogen (*nido*) as previously described. The primers and probe used to detect *flaB* were flaB-F (5-CTTTTCTCTGGTGAGGGAGCTC-3') and flaB-R (5'-GCTCCTTCCTGTTGAACACCC-3') and flaB-probe (5'-FAM-CTTGAACCGGTGCAGCCTGAGCA-3'-BHQ1). The primers and probe used for *nidogen* were nidogen-F (5'-CCCCAGCCACAGAATACCAT-3'), nidogen-R (5'-AAAGGCGCTACTGAGCCGA-3'), and nidogen-probe (5'-FAM-CCGGAACCTTCCCACCCAGC-3'-BHQ1). The copy numbers for *flaB* and *nidogen* genes were calculated by the Bio-Rad software (Version 3.1) based on standard curves (10^7 – 10^2 copies) generated from cloned versions of the corresponding amplicon as previous described. *flaB* copy numbers were normalized to *nidogen*. General statistical analysis was performed using GraphPad Prism 4.0 (GraphPad Software, San Diego, CA), using an unpaired Student *t* test. For each experiment, both the standard deviation and the standard error of the mean were calculated. *p* values of <0.05 were considered significant.

HISTOPATHOLOGY:

Mouse tibiotarsal joints and hearts were fixed for one week in 10% buffered formalin. Joints were decalcified using 8% formic acid for 48 hours after fixation. Tissues were then embedded in paraffin and 5 μm sections were cut using a microtome and floated on to

glass slides using a 40°C water bath. Tissues were stained in hematoxylin solution for 90 seconds and Eosin Y solution for 18 seconds. Joints were scored on a scale of increasing severity from 1-3 by a pathologist in a blinded fashion for arthritis severity. Hearts were scored on a scale of increasing severity from 1-3 by a pathologist in a blinded fashion according to type and volume of cell infiltrate. General statistical analysis was performed using GraphPad Prism 4.0 (GraphPad Software, San Diego, CA), using an unpaired Student *t* test. For each experiment, both the standard deviation and the standard error of the mean were calculated. *p* values of <0.05 were considered significant.

RNA ISOLATION FROM MOUSE TISSUES:

Mouse tibiotarsal joints and hearts were homogenized using an electric homogenizer with toothed blades in tissue lysis buffer (Machery-Nagel, 740962) containing beta-mercaptoethanol (diluted 1:100) (Bio-Rad, 161-0710) and Triton-X-100 (diluted 1:100) (Fisher, BP151-100). RNA was isolated from tissue lysates using a Nucleospin RNA Kit (Midi column, Machery-Nagel, 740962) according to the manufacturer's instructions for fibrous tissues. RNA was quantified using a Nanodrop spectrometer (Thermo-Fisher). cDNA was generated from 2.5 nanograms total RNA using a High-capacity cDNA Reverse Transcriptase kit (Applied Biosystems, 4368814) according to manufacturer's instructions. Gene-specific qRT-PCR analyses were performed as previously described (Cervantes, La Vake et al. 2013). Expression levels for selected genes (Table S1) were normalized to *Gapdh* (Mm99999915_g1) and the fold changes in gene expression relative to the unstimulated or uninfected control were calculated using the $2^{-\Delta\Delta Ct}$ method (Schmittgen and Livak 2008). Statistical analysis of the differences in fold changes was

performed using GraphPad Prism 4.0 (GraphPad Software, San Diego, CA), using an unpaired Student *t* test. For each experiment, both the standard deviation and the standard error of the mean were calculated. *p* values of <0.05 were considered significant.

BMDM STIMULATION:

Bone marrow-derived macrophages (BMDMs) were isolated from 6-8-week-old WT and MyD88-/- mice as described previously (Salazar, Duhnam-Ems et al. 2009). Single cell macrophage suspensions were seeded into either 12-well tissue culture-treated plates at a concentration of 10^6 cells/ml per well or 10^5 cells/500 μL per well in 8-chamber cell microscopy slides. Slides and plates were then incubated overnight at 37°C/5% CO_2 to allow cell adherence before experimentation. Cells were incubated for either 1, 4 or 6 hours at 37°C/5% CO_2 with live GFP-Bb at multiplicities of infection (MOIs) of either 10 or 100. Stimulation media was DMEM supplemented with 1% sodium pyruvate and 1% HEPES. For stimulations looking at the effect of Bb uptake, Cytochalasin D (Sigma, C8273-1MG) was added to wells at a concentration of 10 μg/mL and incubated at 37°C for 1 hour before addition of Bb. At the end of the incubation period, culture supernatants were collected and stored at −80°C until cytokine analysis. Cells stimulated in chamber slides were processed for confocal microscopy. Cell stimulated in 12-well plates were processed for RNA extraction. All culture media and reagents utilized in the stimulation experiments were confirmed to be free of LPS contamination (<10 pg/ml) by Limulus amoebocyte lysate assay quantification (Cambrex, MA).

CONFOCAL MICROSCOPY:

After stimulation BMDMs were fixed in 2% paraformaldehyde with 0.05% Triton-X-100 (Fisher, BP151-100) for 10 minutes. Slide wells were then incubated with 5% bovine serum albumin (BSA) solution in PBS overnight at 4°C to block non-specific antibody binding. The next day, cells were stained with different combinations of anti-GFP (Thermo Scientific A-21311, 1:100), phalloidin conjugated with Alexa Fluor 647 (Biolegend 424205, 1:20), anti-MyD88 (Santa Cruz 11356, 1:100), anti-TLR2 (eBioscience 14-9021-82, 1:100), anti-TLR7 (R&D MAB7156, 1:100) and anti-LAMP-1 (eBioscience 14-1071-82, 1:100). A secondary antibody was used to detect anti-MyD88, anti-TLR2, and anti-LAMP-1 (Molecular Probes Alexa Fluor 568, A11036) (1:200). Incubations with primary and secondary antibodies were done for 1 hour each at room temperature and slide wells were washed following each incubation three times with PBS supplemented with 0.5% Tween-20, with a final wash in distilled H_2O before mounting. After antibody staining slides were mounted using Vectashield mounting medium (Vector H-1000) and imaged using a Zeiss 880 confocal microscope. Image processing and analysis were performed using ImageJ (NIH, v1.41b). Colocalization values were determined by first analyzing profile plots in Image ("Plot Profile") across ten different phagosomes for each cell genotype and then calculating the average difference between the fluorescence intensity curves of the markers of interest (i.e., LAMP-1 and Bb). Uptake percentages were calculated by imaging 100-200 cells using a confocal microscope and then measuring the ratio of cells containing at least one internalized spirochete to the total number of cells imaged for each condition, represented as %Bb-positive BMDMs.

WESTERN BLOTTING OF BMDM SUPERNATANTS AND LYSATES:

Protein lysates were generated from BMDM cell culture lysates and supernatants after Bb stimulation. In these experiments, adenosine triphosphate (ATP) (Sigma, 3A6419-1G) was added to WT BMDMs (already stimulated with Bb) 1 hour prior to harvest for generation of lysates. Supernatants were treated with an equal volume of methanol and ¼ volume of chloroform, vortexed and spun at 16,000 x g for 10 minutes. After removal of the upper phase 500 μL of methanol was added to the intermediate phase which was then vortexed and spun at 16,000 x g for 10 minutes. The pellets were then dried at room temperature, resuspended in 30 μL of 2x Laemmli buffer and incubated in a 37°C water bath until proteins became soluble. Stimulated BMDMs were lysed using RIPA buffer at -80°C and spun at maximum speed for 10 minutes. Protein pellets were resuspended in 2x Laemmli buffer. Lysates were boiled at 99°C for 10 minutes and run on a 12.5% SDS-PAGE gel at 140V for 1 hour (5 μL per lane, 15 lanes). Protein from the gel was then transferred to a nitrocellulose membrane (Bio-Rad 162-0177) at 20V for 20 minutes. Membranes were incubated overnight at 4°C with primary antibodies for either β-actin (Sigma A5441, 1:2000), IL-1β (R&D AF401NA, 1:800) or Caspase-1 (Adipogen AG-20B-0042, 1:1000) diluted in milk block solution. Membranes were then washed 5 times for 5 minutes each in wash buffer and incubated with goat anti-mouse HRP-conjugated IgG (GE NA931) diluted 1:5000 (β-actin and Caspase-1) or 1:1000 (IL-1β) in milk block for 2 hours at room temperature. Washes were then repeated as described above and membranes were incubated in HyGlo spray chemilunescent substrates (Denville Scientific, E2400) for 5 minutes and imaged on a Bio-Rad ChemiDoc MP imaging system.

CYTOKINE ANALYSIS:

The Cytokine Bead Array Mouse Inflammation kit (BD Biosciences 552364) was used according to manufacturer's instructions for simultaneous measurement of IL-6, IL-10, MCP-1, IFNγ, TNFα, and IL-12p70 in supernatants from stimulated BMDMs. General statistical analysis was performed using GraphPad Prism 4.0 (GraphPad Software, San Diego, CA), using an unpaired Student *t* test. For each experiment, both the standard deviation and the standard error of the mean were calculated. *p* values of <0.05 were considered significant.

IDENTIFICATION OF DIFFERENTIALLY EXPRESSED GENES BY RNA-SEQUENCING:

Total RNA was extracted from three biological replicates of WT and MyD88-/- BMDMs, either unstimulated or stimulated for 6 hours with Bb at MOI 10:1 or MOI 100:1. RNA was isolated using the total RNA isolation kit (Macherey-Nagel) and was used as input for the Ovation RNA-seq V1 kit (NuGen, San Carlos, CA). cDNA output was analyzed for correct size distribution with an Experion Standard Sensitivity RNA chip and quantified using a Qubit Fluorometer (Invitrogen, Carlsbad, CA). Strand-specific sequencing libraries were produced using the NuGen Encore NGS Library I kit. Libraries were multiplexed and sequenced on an Illumina HiSeq 2500 at The Jackson Laboratory Genomic Medicine Sequencing Core. 2X50bp paired-end reads from each individual library were mapped with Tophat2 RNA-Seq spliced reads mapper (version 2.0.5) (Kim, Pertea et al. 2013) with parameter settings adjusted to suit strand-specific pair-end reads. The resulting bam files were used as input to the HTSeq high-throughput sequencing data analysis package

(Lister, Gregory et al. 2009) to quantify the read counts mapped to all genes in UCSC mm9 mouse gene annotation set. Mapped read counts were normalized using DESeq2 (function: *estimateSizeFactor*) (Anders and Huber 2010). Genes were considered expressed if the number of reads was above the 25th percentile for the normalized data set. For quality control, only replicates with Pearson correlation coefficient above 0.9 on their FPKM values were considered (**Figure 1**). Expressed genes were then further analyzed for differential gene expression using the DEseq2 package with FDR cutoff: 0.1. Differential gene expression was calculated in WT BMDMs stimulated 10:1 with Bb relative to unstimulated WT BMDMs and MyD88-/- BMDMs stimulated 100:1 with Bb relative to unstimulated MyD88-/- BMDMs. Differentially expressed genes (DEGs) were classified as either upregulated or down regulated based on log2 fold change compared to the unstimulated control, which was calculated in R statistical software using package "DESeq2". Determined DEGs were then separated into five groups based on their expression profiles; WT (all DEGs in WT BMDMs), MyD88-/- (all DEGs in MyD88-/- BMDMs), MyD88-dependent (all DEGs in WT but not MyD88-/- BMDMs), MyD88-independent (all DEGs in both WT and MyD88-/- BMDMs), and MyD88-exclusive (all DEGs in MyD88-/- but not in WT BMDMs).

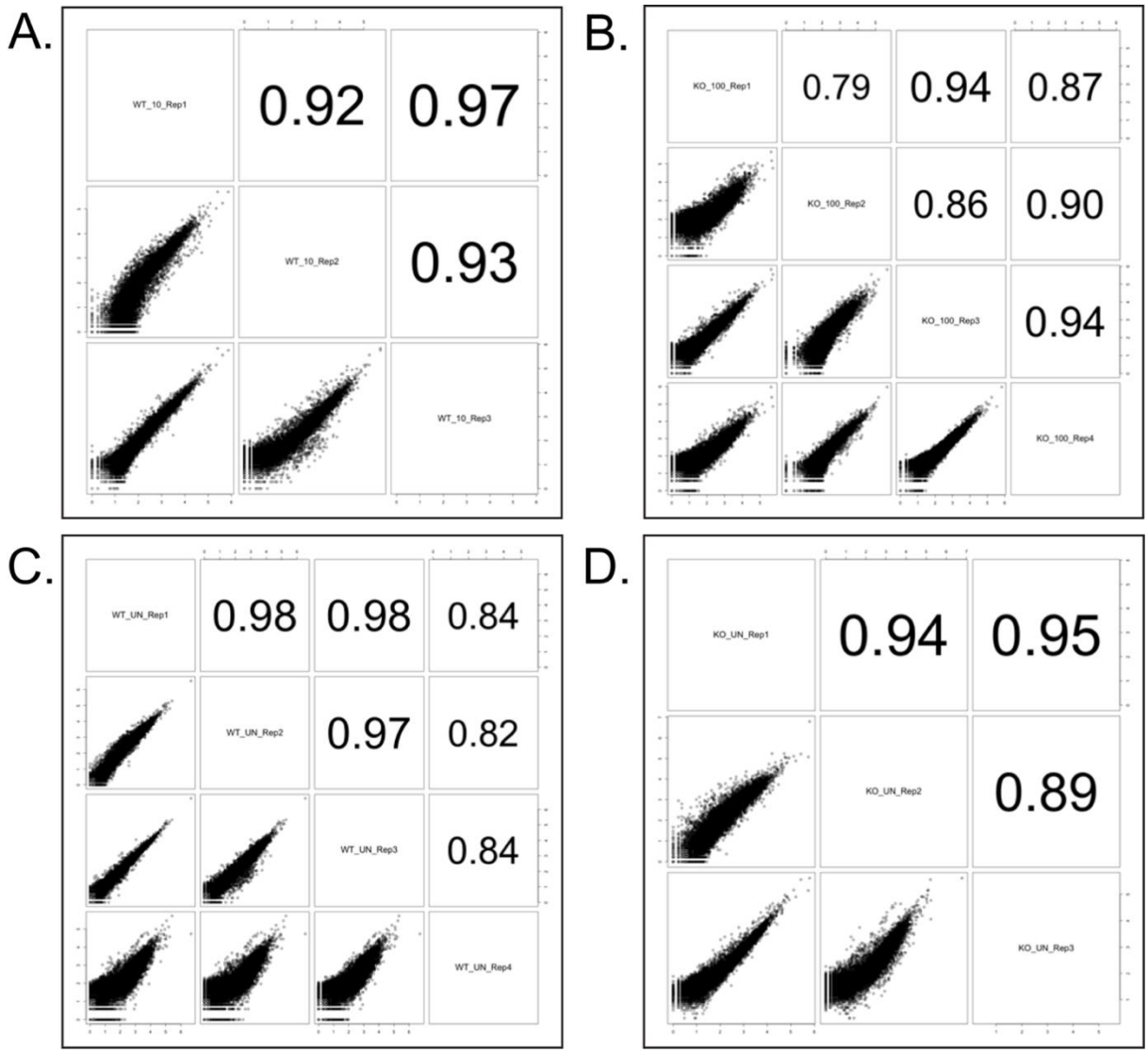

Figure 1: Correlation of reads of RNA sequencing data. (A-D) Correlation of reads of RNA isolated from Bb-stimulated BMDMs. WT BMDMs were stimulated at a MOI 10:1 for 6 hours (A). MyD88-/- BMDMs were stimulated at a MOI 100:1 for 6 hours (B). To calculate differential expression, reads from the stimulated samples were normalized to unstimulated BMDMs of the same genotype; WT (C) or MyD88-/- (D)

Identification of Enriched Transcription Binding Sites and Master Regulator Analysis:

Transcription factor binding sites in promoters of differentially-expressed genes were analyzed using known DNA-binding motifs described in the TRANSFAC library (Matys, Kel-Margoulis et al. 2006), release 2017.2, available in the GeneXplain software (http://genexplain.com). Binding site enrichment analysis for each one of our sets of DEGs was carried out as part of a GeneXplain dedicated workflow. The background consisted of 300 mouse house-keeping genes and the TRANSFAC mouse Positional Weight Matrices PWM (motifs) for binding site prediction with p-value<0.001 score cutoff. Promoters were extracted by the workflow with a length of 600 bp (−500 to +100) and an enrichment fold of 1.0.

Master regulatory molecules were searched for in signal transduction pathways upstream of the identified TFs. The GeneXplain workflow available for this analysis was used in conjunction with the GeneWays database. Parameters set included a maximum radius of 10 steps upstream of the TF nodes, the DEG lists from the respective group as context genes and a Z-score cutoff of 1.0. All transcription factors and master regulators used in the network analysis had confirmed expression in respective conditions using the total gene expression lists from the RNA-sequencing data set.

Gene Ontology (GO) Enrichment Analysis:

A Gene Ontology (GO) enrichment analysis was performed for the different sets of DEGs, transcription factors, and master regulators using the TRANSPATH (Krull, Pistor et al. 2006) database through GeneXplain software. Input sets were the DEGs, transcription

factors, or master regulators from either the MyD88-dependent, MyD88-independent, or MyD88-privative groups. Focus was directed to the Gene Ontology (GO) biological processes output. GO biological processes related to Bb uptake, inflammation, and chemotaxis were identified by first reviewing previous studies for any genes involved in response to Bb relating to these phenotypes. Enrichment analysis was done on these genes to identify GO biological processes that hit at least 60% of the genes on the list, generating a list of relevant GO biological processes. Then an intersection was performed between the list of GO biological processes identified using our DEG, transcription factor, or master regulator lists, and the GO biological processes identified from the relevant genes. Heat maps of expressed genes hits in each biological process were done in R statistical software using package “ggplots”.

NETWORK RECONSTRUCTION AND NETWORK ANALYSIS:

Networks were constructed joining the three identified layers on the networks: DEGs, TFs and MRs. The subnetworks were extracted from identified master regulators of interest. From the MyD88-dependent master regulator group, effort was directed on linking MyD88 with transcription factors that had binding sites in the promoter regions of the MyD88-dependent DEGs enriched in uptake biological processes. These transcription factors were identified using the TRANSPATH database with the enriched DEGs of interest as input. The output list of transcription factors was intersected with the list of transcription factors that were only expressed in WT BMDMs. Networks were assembled and analyzed using Cytoscape software (Shannon, Markiel et al. 2003). To extract the desired subnetworks, we used OCSANA (Vera-Licona, Bonnet et al. 2013) within the BiNOM

plugin (Zinovyev, Viara et al. 2008) in Cytoscape 2.8.3. MyD88 was considered as a source node and transcription factors from the intersected list as target nodes. For MyD88-privative chemotaxis subnetwork construction the same analysis pipeline was applied. MyD88-privative master regulators significantly enriched in chemotaxis were used as source nodes and MyD88-privative transcription factors enriched in chemotaxis were used as targets.

CHAPTER 3: THE ROLE OF MYD88 IN MURINE INFLAMMATION DURING INFECTION WITH *BORRELIA BURGDORFERI*

IMPORTANCE

The macrophage is an essential element of the inflammatory cell infiltrate in tissues of mice experimentally infected with Bb (Montgomery, Booth et al. 2007, Hawley, Navasa et al. 2012), but its role in spirochetal clearance and tissue inflammation, as well as the importance of MyD88 in these processes, has not been well characterized. The purpose of the following experiments was to investigate whether MyD88 affects macrophage infiltrate into tissues during Bb infection and how this contributes to inflammation severity, tissue response and bacterial clearance.

RESULTS

MyD88 signaling significantly reduces bacterial load in tissues of Bb-infected mice.

To determine the role of MyD88 in Bb clearance from infected tissues, we first used a well-defined murine model of LD that enables investigation of cell populations in tissues, transcript responses and bacterial clearance. For these experiments we needle-inoculated WT and MyD88-/- mice with Bb and quantitated bacterial burdens in heart, patellofemoral joints, bladder, ear and skin tissues at 14-, 28- and 56-days post-infection (DPI). By 14 days, all experimentally infected mice seroconverted based on immunoblot analysis (data not shown). As shown in **Figure 1**, Bb disseminated to all tissues in both WT and MyD88-/- mice. In heart tissue, MyD88-/- mice showed significantly increased

bacterial burdens compared to WT mice at 14 and 28 DPI (**Figure 1A**); this difference was not significant by 56 DPI. The overall Bb burdens in heart tissue were lower than the other tissues studied (**Figure 1**). In patellofemoral joint, tibiotarsal joint, bladder, ear and skin tissues, burdens in WT and MyD88-/- mice were comparable at 14 DPI, but significantly higher in MyD88-/- mice at 28 and 56 DPI (**Figure 1B-E**). We also saw a significant decrease in bacterial burdens in WT mice in all tissues except heart between 14 and 56 DPI (**Figure 1B-E**). Taken together, our results substantiate that MyD88 signaling is essential for Bb control in murine joint, skin, bladder and ear tissue. However, our results also show that in heart tissue MyD88-independent mechanisms can also mediate effective, though delayed, bacterial clearance.

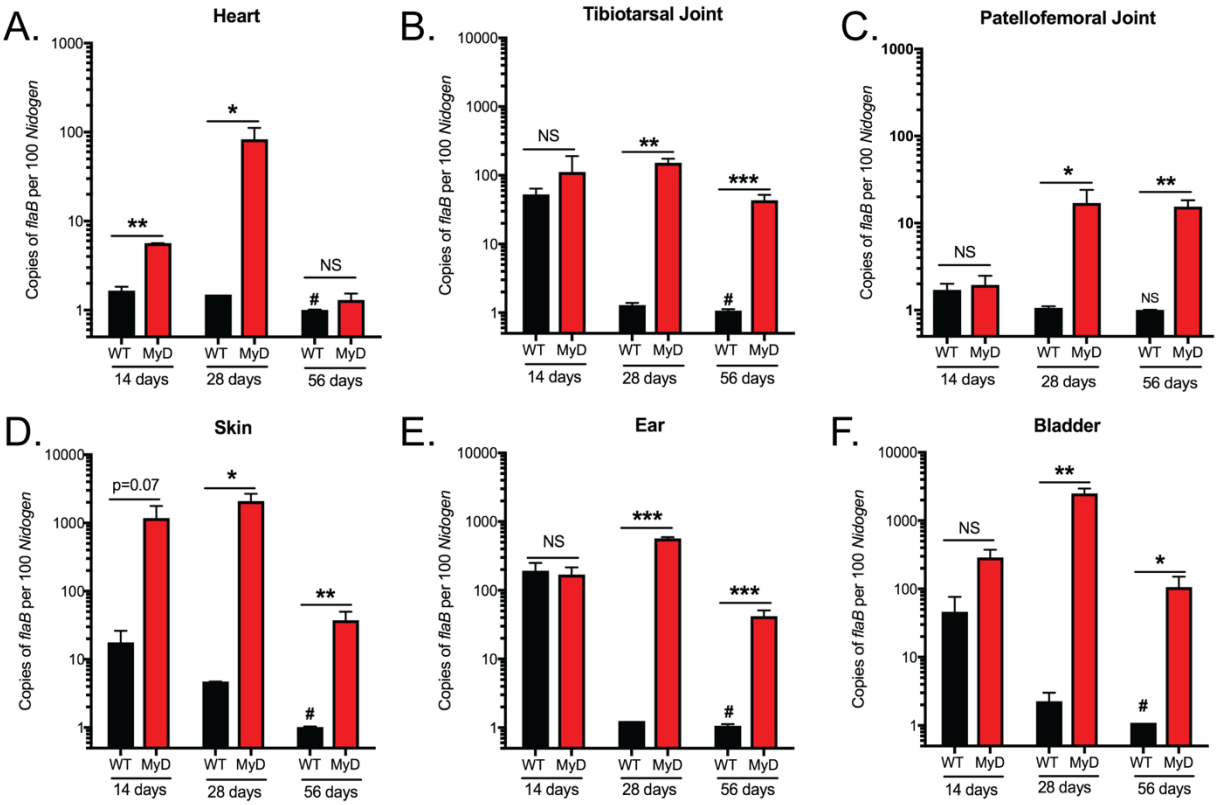

Figure 1: MyD88-/- mice show increased Bb burdens 28 and 56 DPI (A-F) Bb burdens in selected mouse tissues as determined by RT-PCR. Mice were syringe-inoculated with 10^5 Bb914 and sacrificed 14, 28 or 56 DPI. DNA was isolated from WT (black bars) and MyD88-/- (red bars) mice. Copies of *flaB* were normalized to *Nidogen* amplified from total tissue DNA in heart (A), tibiotarsal joint (B), patellofemoral joint (C), skin (D), ear (E), and bladder (F). n=3-5 mice per group *p-value<0.05, **p-value<0.01, NS=not significant, $^{\#}$p-value<0.05 using Mann-Whitney test against WT 14 DPI burden values

Bb-driven MyD88-independent mechanisms are associated with inflammation severity in heart tissue.

To study the severity of inflammation in Bb-infected murine hearts, we first examined the cellular infiltrates at 14 and 28 DPI by hematoxylin and eosin (H&E) staining. The histopathology of infected hearts consisted of lymphocytes, plasma cells, macrophages, reactive mesothelial cells, and fibroblasts. In more intensely inflamed heart tissue, neutrophils were also a significant component of the cellular infiltrate (**Figure 2A**). Inflammation was primarily evident in connective tissue at the heart base, especially around the root of the aorta, and in the atrial epicardium with some involvement of the atrial myocardium, valve leaflets and ventricular epicardium. Similar numbers of WT (2/5) and MyD88-/- (2/5) infected mouse hearts had evidence of low-grade inflammation (scores of 0-1) by 14 DPI (**Figure 2A**). Infected WT hearts showed stromal cell thickening at the base (**Figure 2A, top panels**), whereas a neutrophil infiltrate was clearly evident in the heart of one MyD88-/- infected mouse 14 DPI (**Figure 2A, inset**). Importantly, inflammation scores between the two genotypes were not significantly different at 14 DPI (**Figure 2B**). By contrast, 28 DPI the majority of MyD88-/- mice (4/5) showed significantly increased cellular infiltrates (**Figure 2C, bottom panels**) and high inflammation scores (**Figure 2D**), whereas only 2/5 WT mice revealed evidence of inflammation. Hearts from MyD88-/- mice also revealed the presence of neutrophils as part of the inflammatory infiltrate (**Figure 2C, bottom panels and inset**) whereas WT mice did not. (**Figure 2C, top panels**).

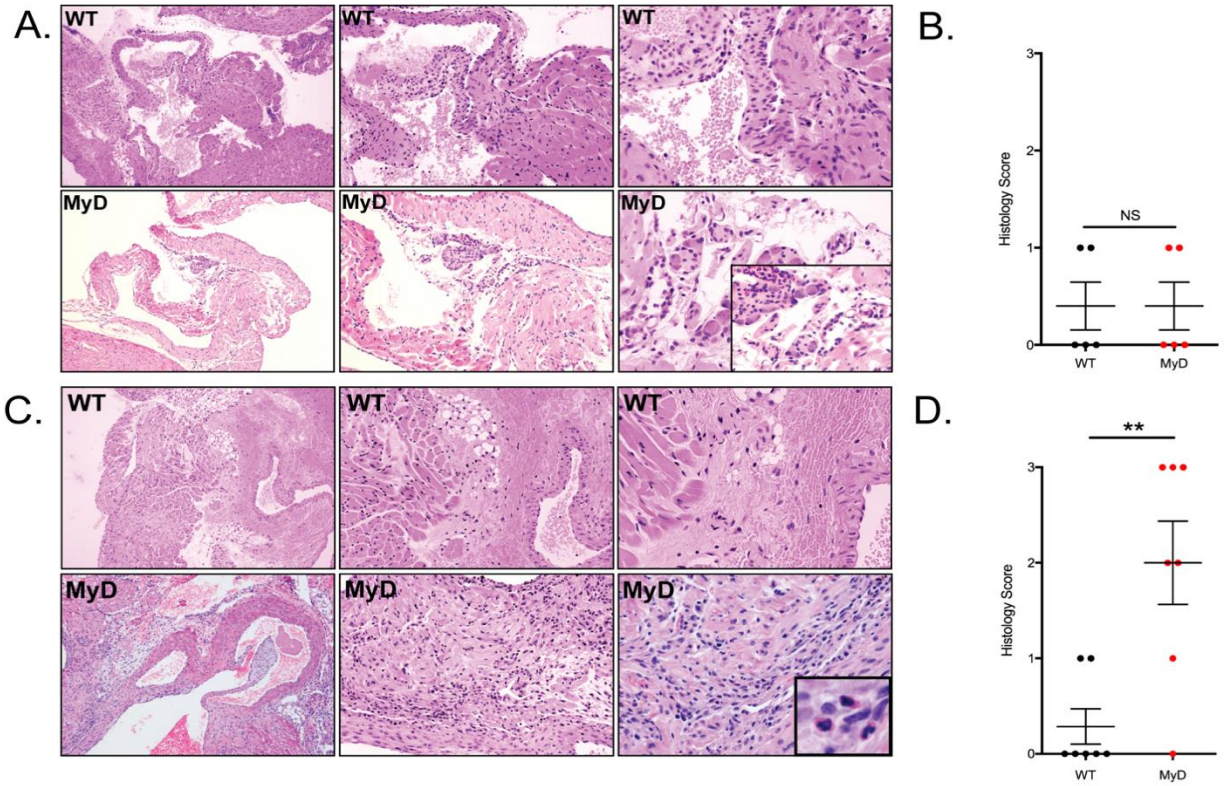

Figure 2: MyD88-/- mice show increased inflammation severity and macrophage infiltrate 28 days post Bb-infection. (A and C) Representative images of H&E staining of heart tissue sections from WT and MyD88-/- mice syringe-inoculated with 10e5 Bb at 14 DPI (A) and 28 DPI (C). Images are of increasing magnification from left to right (10x, 20x, 40x, inset is 60x). Sections are 5 μm. (B and D). Compilation of inflammation scores for WT (black dots) and MyD88-/- (red dots) mice at 14 DPI (B) and 28 DPI (D) N=5 mice per group.

The absence of MyD88 affects expression of genes associated with inflammation but does not increase inflammation severity or infiltration of macrophages in joints.

We next examined joints using an approach similar to that described above for hearts. Inflamed joints had small numbers of neutrophils, lymphocytes, plasma cells and macrophages (**Figure 3A and 3C**). This infiltrate was most commonly evident in the joint capsule near the junction with the periosteum. More prominent mixed inflammatory infiltrates were generally present in the periarticular loose connective tissue, especially in fat and along the periosteum, extending from the joint. A low-grade immune cell infiltrate was observed in most WT (3/5) and all MyD88-/- (5/5) mouse joints 14 DPI (**Figure 3A**). Similar to heart tissue, no differences in inflammation score between WT and MyD88-/- joints were observed 14 DPI (**Figure 3B**). The number of WT (3/5) and MyD88-/- (5/5) mice presenting with inflammation 14 DPI also were comparable (**Figure 3B**). In contrast to hearts, inflammation severity in joints was minimal to mild at 28 DPI in both genotypes, with no appreciable differences in the cell types present (**Figure 3C, bottom panels**). Inflammation scores also were comparable between WT and MyD88-/- mice; no significant difference in the number of mice showing inflammation was noted (WT = 2/5, MyD88-/- = 3/5) (**Figure 3D**).

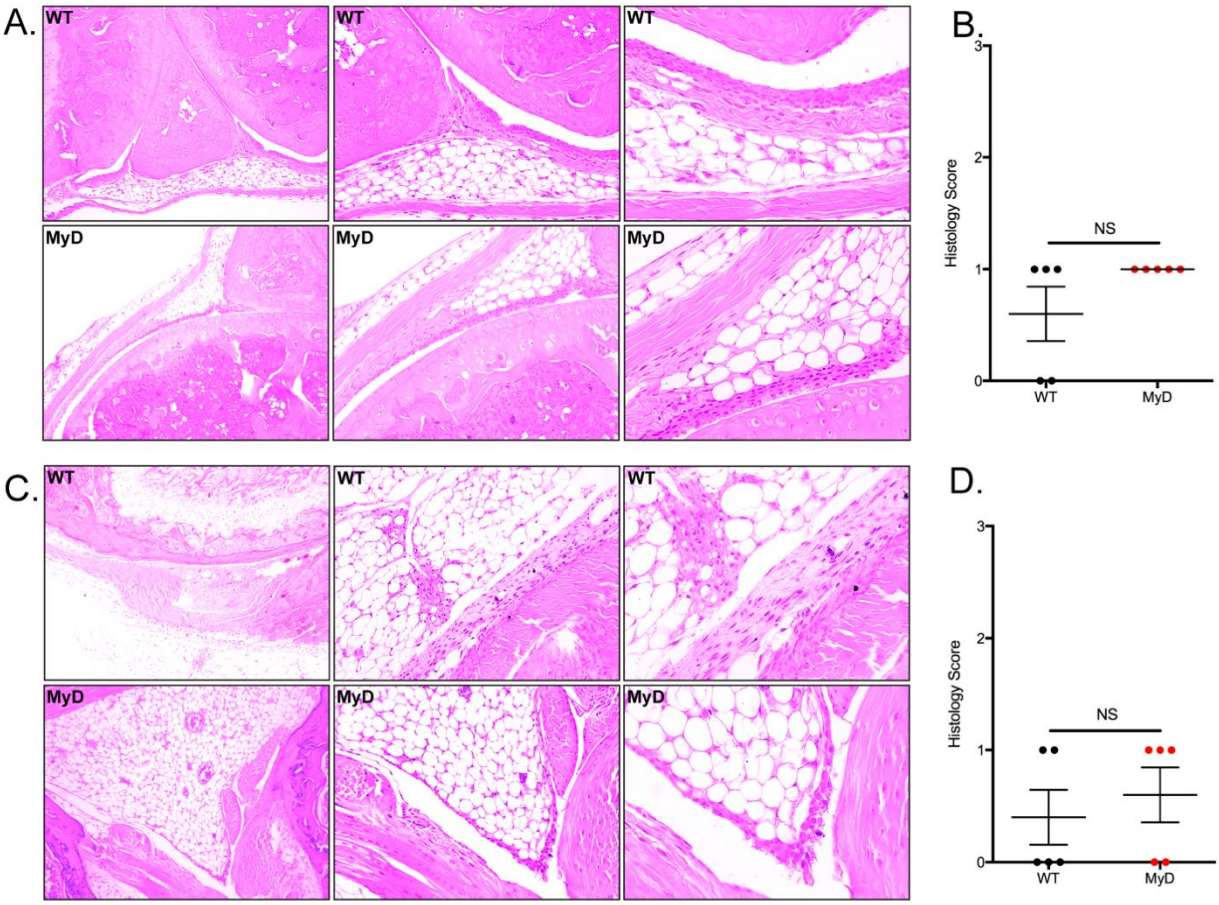

Figure 3: MyD88-/- mice show comparable inflammation and macrophage infiltrate in knee joint tissue 14 and 28 days post Bb-infection. (A and C) Representative images of H&E staining of knee joint tissue sections from WT and MyD88-/- mice syringe-inoculated with 10e5 Bb at 14 DPI (A) and 28 DPI (C). Images are of increasing magnification from left to right (10x, 20x, 40x). Sections are 5μm. (B and D) Compilation of inflammation scores for WT (black dots) and MyD88-/- (red dots) mice at 14 DPI (B) and 28 DPI (D) N=5 mice per group. *p-value<0.05, **p-value<0.01, NS=not significant

Macrophage infiltration is dramatically increased in MyD88-/- heart tissue but not joint tissue

Because macrophages are not easily distinguishable by H&E staining, we performed immunohistochemistry (IHC) analysis for Iba-1, a calcium channel marker known to be expressed in macrophages (Utans, Arceci et al. 1995). Both WT and MyD88-/- infected and uninfected hearts revealed Iba-1+ macrophages throughout the myocardium, as would be expected in normal murine hearts (Keller and Maniatis 1991, Utans, Arceci et al. 1995). By 14 DPI, small numbers of macrophage clusters were observed in the heart base in WT mice (**Figure 4A, top left**), while no increase in macrophages was observed in MyD88-/- hearts 14 DPI (**Figure 4A, top right**). On the other hand, 28 DPI MyD88-/- mouse hearts revealed a very dense macrophage infiltrate at the base (**Figure 4A, bottom right**). We also performed Iba-1 IHC on patellofemoral joint tissue sections and visualized a few macrophages in the periarticular space in both WT and MyD88-/- mice 14 DPI (**Figure 4B, top panels**) and 28 DPI (**Figure 4B, bottom panels**). However, no difference in the number of macrophages infiltrating joint tissue was apparent between the two genotypes at the time points studied. Our IHC findings suggest that although infiltration is delayed in the absence of MyD88, murine macrophages are significant contributors to the inflammatory response in heart tissue and, by extension, Lyme carditis.

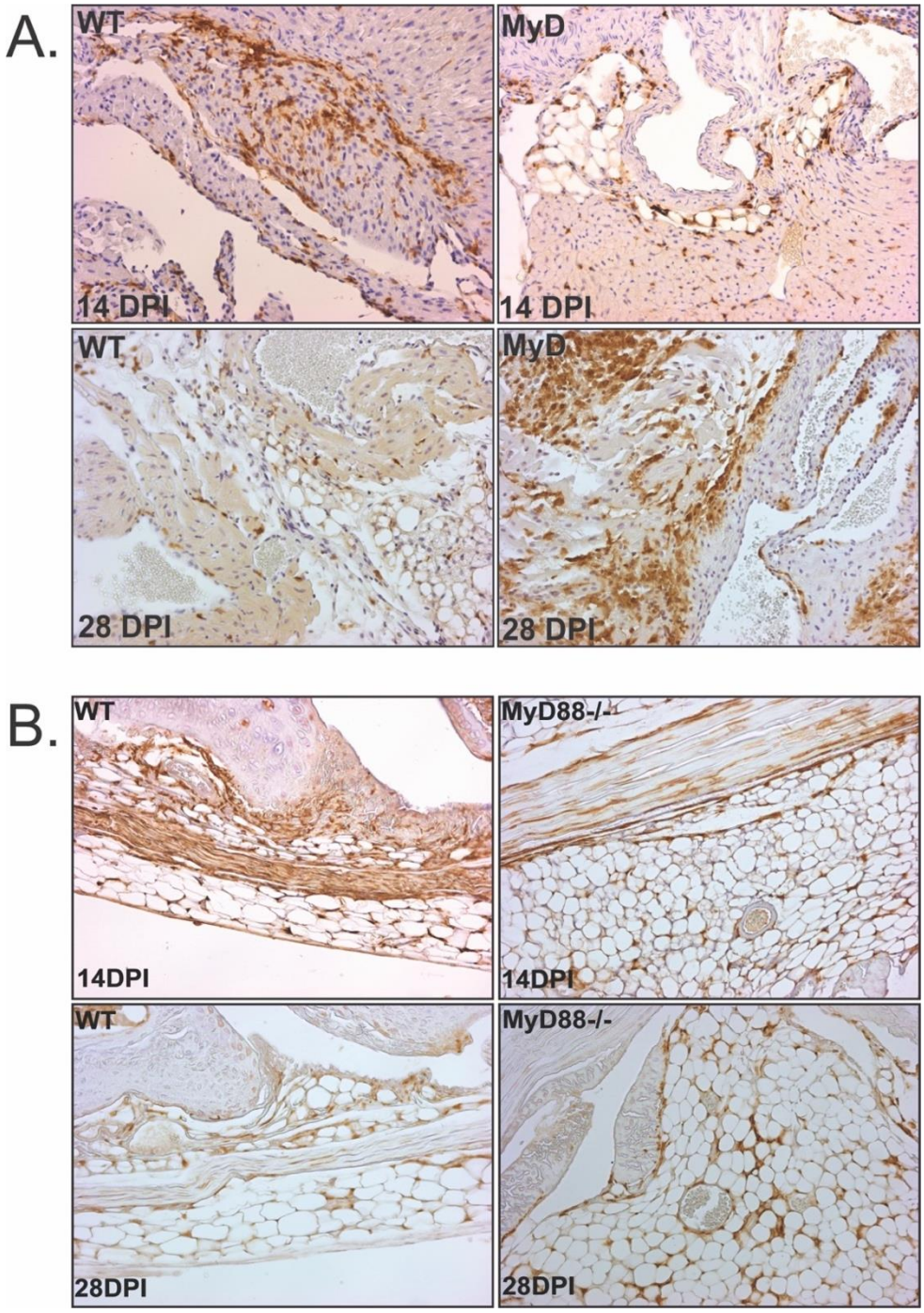

Figure 4: MyD88-/- mice show increased macrophage infiltrate 28 days post Bb-infection. (A) Iba-1 immunohistochemistry of heart tissue sections from Bb-infected WT and MyD88-/- mice. (B) Iba-1 immunohistochemistry of knee joint tissue sections from Bb-infected WT and MyD88-/- mice, magnification = 20x. Sections are 5μm.

The absence of MyD88 drives unique chemokine transcript expression profiles in heart tissue during Bb infection.

Our results above show that MyD88 signaling affects type and quantity of inflammatory cells recruited to heart tissue during Bb infection. To gain further insight into how these cells are responding to Bb, we performed RT-PCR of selected genes from total RNA isolated from heart tissues from Bb-infected mice. We focused on various groups of genes related to inflammation; NFκB-mediated cytokines (*Tnfa* and *Il1b*), type I interferons, components of the inflammasome (*Nod2*, *Nlrp3*, *Casp1*) and chemokines (*Ccl2*, *Ccl9*, *Cxcl2*, *Cxcl3*, *Cxcl10*). We also included *Aif1*, which translates into Iba-1, and *Itgam,* also known integrin alpha M or CD11b, which has been previously identified as a phagocytic receptor for Bb (Hawley, Olson et al. 2012). As shown in **Figure 5A**, significant transcriptional differences between WT and MyD88-/- mice were seen 14 DPI, with WT hearts showing marked upregulation of all genes tested in comparison to uninfected WT controls. In contrast to WT mice, several genes in MyD88-/- infected hearts were down-regulated at 14 DPI compared to uninfected controls, including *Ccl9*, *Cxcl2*, *Cxcl3* and *Cxcl10,* as well as genes involved in inflammasome activation (*Nod2*, *Nlrp3* and *Casp1*) (Figure 2F). However, four out of five MyD88-/- hearts showed upregulation of *Ccl2,* a macrophage-specific chemokine (Mantovani, Sica et al. 2004), and two MyD88-/- mouse hearts showed upregulation of *Itgam* at 14 DPI (**Figure 5A**). At 28 DPI, *Ccl2* and *Ccl9*, another macrophage-specific chemokine (Mantovani, Sica et al. 2004), were upregulated in all MyD88-/- heart tissues studied (**Figure 5B**). Three out of five MyD88-/- mice also showed upregulation of *Ifnb*. By contrast, *Ccl9*, *Ccl2* and *Ifnb* were down-regulated in WT hearts 28 DPI, and not surprisingly WT mice still showed significant up-regulation of

MyD88-dependent pro-inflammatory genes (i.e. *Tnfa)* (Adachi, Kawai et al. 1998) (**Figure 5B**). At 28 DPI, WT mice also showed upregulation of *Ncf2*, which codes for Neutrophil Cytosol Factor 2, a subunit of NADPH oxidase that can indicate the presence of neutrophils in the tissue (Mantovani, Sica et al. 2004), and *Aif1* (**Figure 5B**). All MyD88-/- mice showed down-regulation of *Ncf2* and *Aif1* at 28 DPI; this finding was surprising given the increased neutrophilic infiltrate and Iba-1-positive macrophage infiltrate seen in the MyD88-/- mice by IHC. Overall, these data suggest that in the absence of MyD88, cells in heart tissue show different inflammatory gene expression in response to Bb, with increased macrophage chemokine production that can facilitate their recruitment.

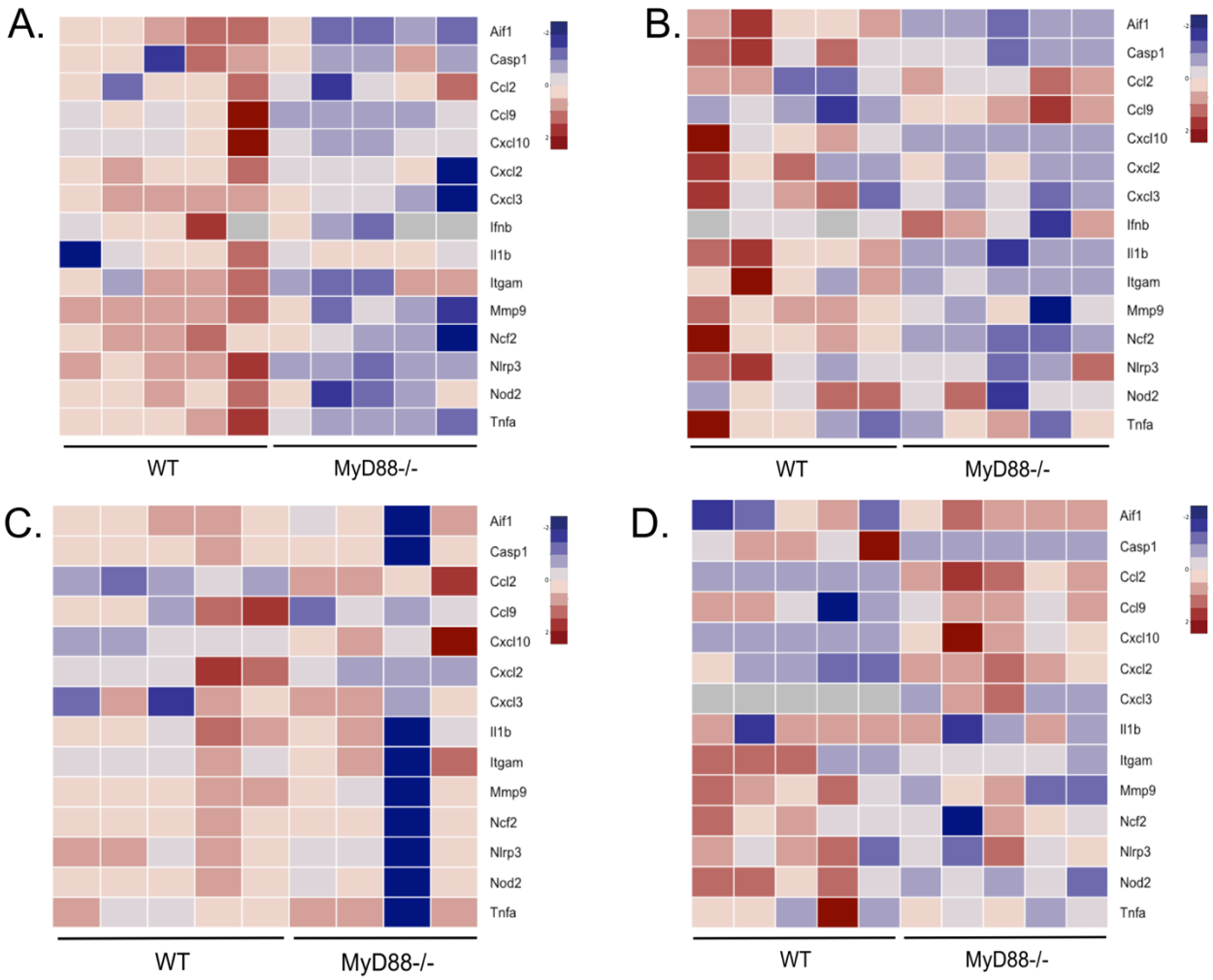

Figure 5: MyD88-/- mice show decreased proinflammatory cytokine production but increased tissue-specific chemokine production. (A and B) Compilation of multiple qRT-PCR gene amplifications from heart tissue RNA. Total RNA was isolated from Bb-infected WT and MyD88-/- mice 14 (A) and 28 (B) days post infection. (C and D) Compilation of multiple qRT-PCR gene amplifications from tibiotarsal joint tissue RNA. Total RNA was isolated from Bb-infected WT and MyD88-/- mice 14 (C) and 28 (D) days post infection. Gene amplification values were normalized to *Gapdh*. Heat map shows *z*-score relative to the row mean. *p-value<0.05, **p-value<0.01, NS=not significant

Transcript production of multiple chemokines are upregulated in MyD88-/- joint tissue during Bb infection.

We also performed targeted qRT-PCR on total RNA isolated from tibiotarsal joints of Bb-infected mice as described above for hearts. At 14 DPI we saw upregulation of inflammatory genes in both WT and MyD88-/- mice compared to respective uninfected controls, but no significant differences were observed between the two groups (**Figure 5C and 5D**). However, there were noticeable differences between WT and MyD88-/- mice at 28 DPI. WT mice showed upregulation of NFkB-mediated cytokines including *Tnfa*, *Il1b* and *Mmp9* (a matrix metalloproteinase shown to be upregulated in murine joint tissue in Bb infection (Gebbia, Coleman et al. 2001)) and inflammasome genes, which were downregulated in MyD88-/- mice (**Figure 5D**). By contrast, MyD88-/- mice showed significant upregulation of the chemokines *Ccl2*, *Ccl9*, *Cxcl2*, and *Cxcl10* (**Figure 5D**) compared to uninfected controls. These chemokines were downregulated overall in WT mice. Interestingly, *Cxcl2* and *Cxcl10* were not significantly upregulated in heart tissue at the same time point (**Figure 5B**). These chemokines have high affinity for the IL-8 receptor (Ahuja and Murphy 1996), and may facilitate recruitment of other inflammatory cells (besides macrophages) to joint tissue in the absence of MyD88. Despite the lack of macrophage infiltrate seen in joint tissue, *Aif1* was significantly upregulated in WT joints 14 DPI and MyD88-/- joints 28 DPI (**Figure 5D**). This is consistent with heart tissue, where *Aif1* was transcriptionally upregulated in absence of increased macrophage infiltrate (**Figure 5B**) and suggests that there is another cell type in the joint which could be upregulating Aif1 transcription (Pawlik, Kotrych et al. 2016). Taken together these data support that there are MyD88-independent tissue specific responses to Bb infection.

CHAPTER 4: THE ROLE OF MYD88 IN RECOGNITION AND UPTAKE OF BORRELIA BURGDORFERI BY MURINE MACROPHAGES

IMPORTANCE

Once spirochetes are phagocytosed by macrophages, recruitment of TLR and MyD88 proteins to the phagosome is essential to trigger MyD88-dependent signaling cascades. Importantly, we have demonstrated that in human monocytes TLR2 and TLR8 are recruited to endosomes containing Bb (Cervantes, Dunham-Ems et al. 2011). The purpose of the following experiments was to determine the effect of MyD88 on Bb uptake kinetics by macrophages, establish localization of TLR2, TLR7 and MyD88 to Bb-containing phagosomes, investigate the importance of MyD88 in phagosome maturation for spirochete degradation, and determine whether MyD88-independent signaling occurs from the phagosome.

RESULTS

MyD88-deficient macrophages show comparable binding but reduced uptake of Bb

To better understand the contribution of MyD88 to spirochete binding, uptake and degradation by macrophages, we transitioned into an *ex vivo* macrophage model using WT and MyD88-/- BMDMs co-incubated with Bb at MOIs of either 10:1 or 100:1 for 1, 4 or 6 hours. To quantify binding percentages, we imaged a minimum of 100 cells by confocal microscopy and from the images determined the number of cells with

spirochetes either attached to the surface or internalized (**Figure 1A, yellow and white arrows respectively**). We used the same confocal images and total cell numbers to quantify uptake percentages based on the number of cells with internalized spirochetes. The percentage of cells with spirochetes either bound or internalized was comparable between WT and MyD88-/- BMDMs at all three time points irrespective of MOI (**Figure 1B and 1C**). While macrophages of both genotypes were able to phagocytose Bb, MyD88-/- BMDMs showed significantly reduced spirochete uptake compared to WT BMDMs (**Figure 1D**). While increasing the MOI to 100:1 significantly enhanced uptake in both cell genotypes, MyD88-/- BMDMs never reached the phagocytic potential of their WT counterparts (**Figure 1E**).

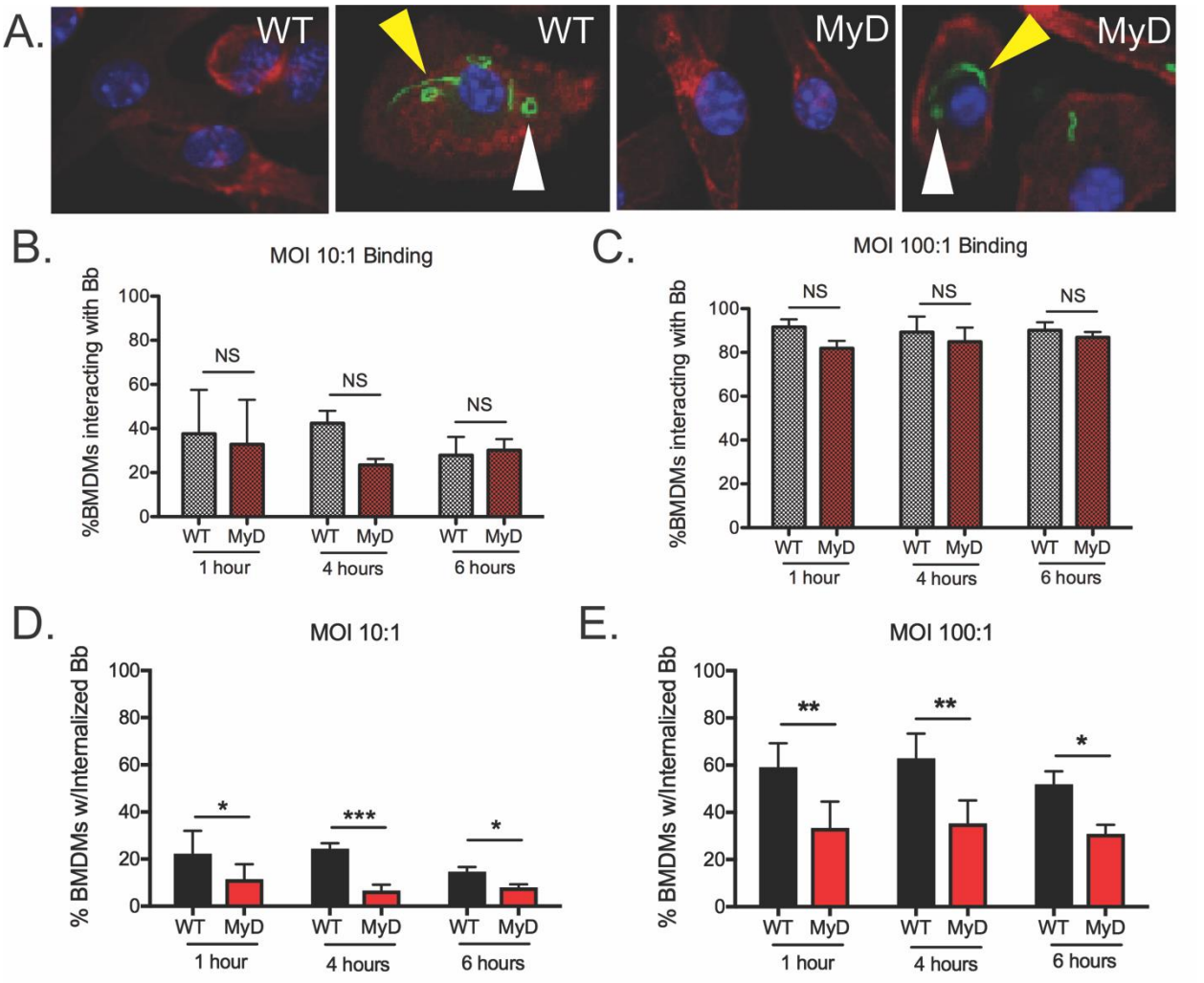

Figure 1: Quantitation of Bb binding and uptake by WT and MyD88-/- BMDMs. (A) Confocal images of WT and MyD88-/- BMDMs after 6 hours of stimulation with Bb at MOI 10:1, highlighting bound (yellow arrows) and internalized (white arrows) spirochetes. Green is Bb, red is actin and blue is cell nucleus. (B-C) Quantitation of bound (B) or internalized (C) spirochetes to WT (black bars) or MyD88-/- (red bars) BMDMs after 1, 4 or 6 hours of stimulation at a MOI of 10:1. (D-E) Quantitation of bound (D) or internalized (E) spirochetes to WT (black bars) or MyD88-/- (red bars) BMDMs after 1, 4 or 6 hours of stimulation at MOI 100:1. (F) Comparison of Bb internalization by WT BMDMs (black bars) at MOI 10:1 with MyD88-/- BMDMs (red bars) at MOI 100:1. n=3-5 mouse BMDM experiments per genotype *p-value<0.05, **p-value<0.01, ***p-value<0.001, NS=not significant

TLR2, TLR7 and MyD88 are recruited to Bb-containing phagosomes in macrophages

To determine whether in mouse macrophages TLRs also co-localize to phagosomes to contribute to inflammatory signaling, we next characterized co-localization of TLR2, TLR7 and MyD88 with phagosomes containing Bb in BMDMs. Given that murine TLR8 does not seem to utilize ssRNA as its ligand (Heil, Hemmi et al. 2004), we investigated the presence of TLR7 in the phagosome, which also utilizes bacterial ssRNA as its ligand. In addition, other groups have shown a prominent role for TLR7 in the Bb inflammatory response (Petzke, Brooks et al. 2009). By confocal microscopy, we showed that in WT BMDMs there is recruitment of MyD88 (**Figure 2A**) and TLR2 (**Figure 2B**) to Bb-containing phagosomes. Signals from MyD88 and TLR2 distinctly overlay with Bb-containing phagosomes in both coiled and degraded states (**Figure 2A and B, graphs**). However, greater fluorescence intensities of MyD88 and TLR2 were observed colocalizing with degraded phagosomes rather that coiled phagosomes, indicating that as more Bb ligand is exposed through phagosome maturation more of each of these markers are recruited. We also saw significant colocalization of TLR7 with Bb-containing phagosomes (**Figure 2C**). However, colocalization of TLR7 was only observed with degraded phagosomes (**Figure 2C**). In MyD88-/- BMDMs there is still recruitment of TLR2 to the phagosome (**Figure 3A**), but TLR2 recruitment is not associated with pro-inflammatory signaling due to the lack of functional MyD88 protein (Adachi, Kawai et al. 1998). We also saw no difference in colocalization of TLR2 (**Figure 3B**) or MyD88 (**Figure 3C**) with either elongated Bb on the cell surface, coiled Bb in early endosomes, or degraded Bb in late endosomes. There was also no difference in cell surface area

between WT and MyD88-/- BMDMs after Bb stimulation for 1 hour (**Figure 3E**). Taken together, these data confirm that endosomal TLR2, TLR7 and MyD88 colocalize to Bb-containing phagosomes to facilitate recognition of bacterial ligands and early response to infection.

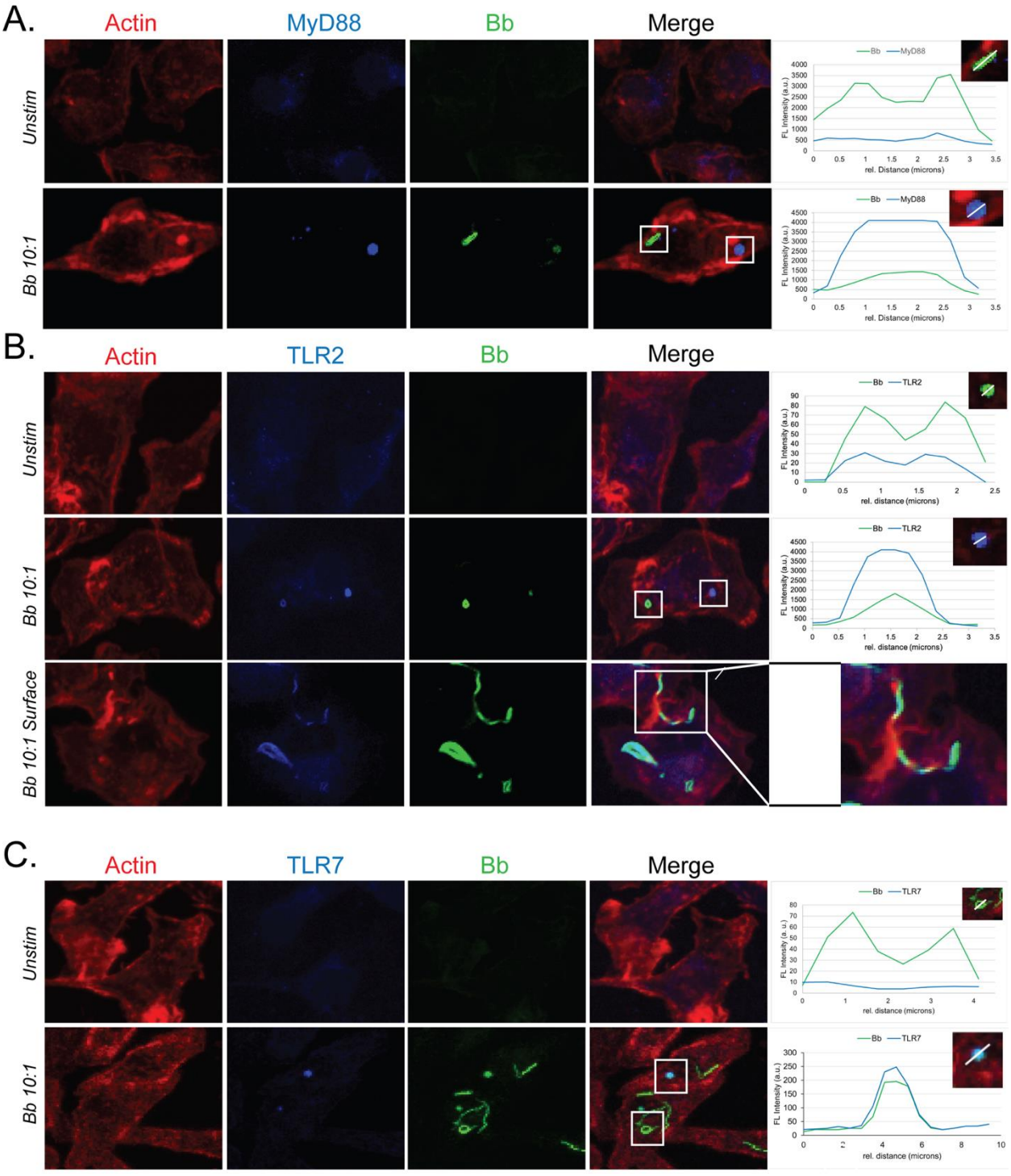

Figure 2: MyD88, TLR2 and TLR7 colocalize with Bb in phagosomes. (A-C) Confocal images and colocalization analysis of internalized Bb with MyD88 (A), TLR2 (B) or TLR7 (C) in WT BMDMs after stimulation at MOI 10:1. White box indicates phagosome depicted in inset. Large inset in (B) shows coiling pseudopod formation around Bb on cell surface. Graph shows the intensity of each indicated pixel marker across the white line (distance on x-axis). Green is Bb, blue is MyD88 (A), TLR2 (B) or TLR7 (7), and red is actin.

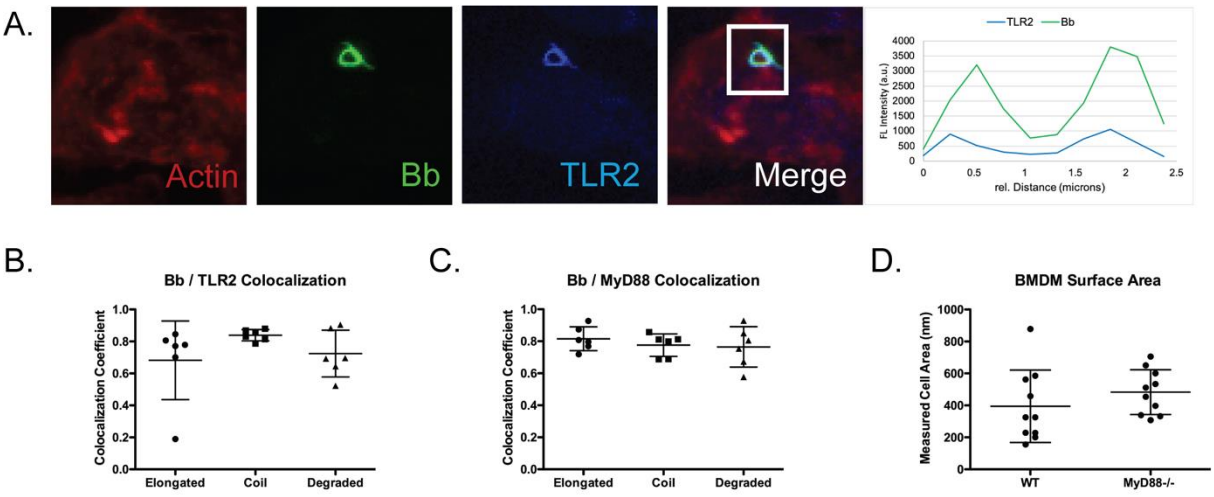

Figure 3: TLR2, MyD88 and TLR7 colocalize to both bound and degraded Bb in BMDMs. (A) Confocal images and colocalization analysis of internalized Bb with TLR2 in MyD88-/- BMDMs after 1 hour of stimulation at MOI 10:1. White box indicates phagosome depicted in inset. Graph shows the intensity of each indicated pixel marker across the white line (distance on x-axis). Green is Bb, blue is TLR2, and red is actin. (B-C) Quantitation of colocalization coefficients between Bb and TLR2 (B) or MyD88 (C) during different phagosome stages. (D) Measurement of cell surface area using Actin staining, comparing WT and MyD88-/- BMDMs after 1 hour of Bb stimulation.

Lack of MyD88 does not affect degradation of Bb in the phagosome

Given that both WT and MyD88-/- BMDMs bind and internalize Bb, we next sought to determine if spirochetes are similarly degraded in phagosomes with and without MyD88. Confocal images taken after a 6-hour stimulation at MOI 10:1 showed that both WT and MyD88-/- BMDMs contained Bb (GFP+) blebs within the cell actin matrix (**Figure 4A**). To assess phagosome maturation, we quantitated recruitment of Lysosome-Associated-Membrane-Protein-1 (LAMP-1), which is a marker of endosome maturation, to Bb-containing phagosomes by looking at colocalization of LAMP-1 and GFP fluorescence intensity (Westphal, Cheng et al. 2017). Both WT and MyD88-/- BMDMs showed comparable LAMP-1 and Bb colocalization in phagosomes (**Figure 4A, graphs**). Colocalization between Bb and LAMP-1 was measured in multiple phagosomes in BMDMs from both genotypes and no significant differences were found (**Figure 4B**). To test for the presence of phagosome leakage, we measured cleaved Caspase-1, which is indicative of inflammasome activation by recognition of lysosomal contents in the cytosol. Western blot analysis of WT BMDM cell lysates and supernatants showed no activation of Caspase-1 by stimulation of Bb alone (**Figure 4C**), which is consistent with previously published studies (Oosting, van de Veerdonk et al. 2011). However, in discordance with previous studies (Oosting, Berende et al. 2010), we did not see cleavage of IL-1β (**Figure 4C**). To confirm MyD88 signaling in response to Bb we also measured TNFα secretion after 1, 4 and 6 hours of incubation with spirochetes. We also confirmed lack of assembled inflammasome activation by staining WT BMDMs for ASC 30 minutes and 6 hours after Bb stimulation (**Figure 5B and 5D**). As a positive control, we also performed ASC staining on WT BMDMs stimulated with *Staphylococcus aureus* (Sa), which has been previously

shown to induce inflammasome activation (Sokolovska, Becker et al. 2013) (**Figure 5A and 5C**). While Sa induced high amounts of ASC in WT BMDMs both 30 minutes and 6 hours post-stimulation, Bb did not (**Figure 5**). This further confirms that Bb does not induce leakage of phagosome cargo into the cytosol. WT BMDMs showed significant increase in TNFα secretion in the presence of spirochetes, while MyD88-/- BMDMs did not make TNFα protein (**Figure 6A**). MyD88-/- BMDMs also did not secrete IL-6, IL-10 or IL-12 (**Figure 6**). In line with our experiments *in vivo* and consistent with prior studies by Behera *et al*. (2016), both WT and MyD88-/- BMDMs secrete the macrophage chemokine CCL2 (**Figure 6D)**. Taken together, these data suggest that even in the absence of MyD88 there is still uptake (although reduced) and sufficient degradation, creating potential for recognition of Bb ligands solely within the phagosome.

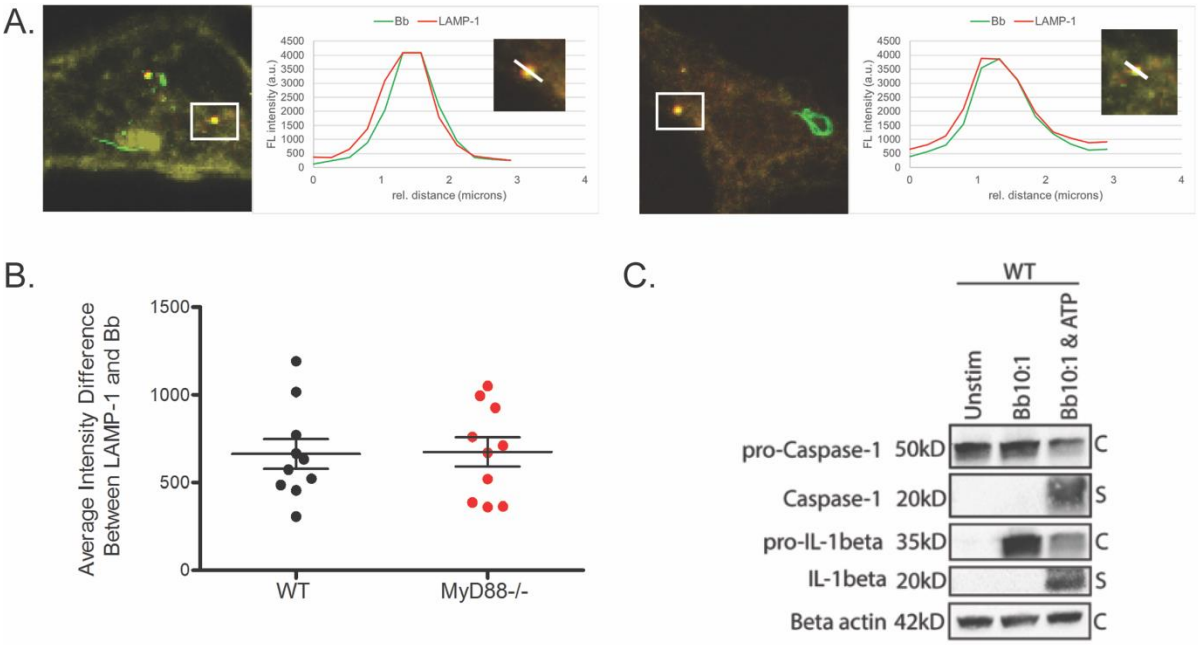

Figure 4: Colocalization of phagosome markers with internalized Bb in WT and MyD88-/- BMDMs. (A) BMDMs after 6 hours of stimulation with Bb at MOI 10:1, depicting colocalization of Bb-containing phagosomes with LAMP-1. White box indicates phagosome depicted in inset. Graph shows the intensity of each indicated pixel across the white line (distance on x-axis). Green is Bb, red is LAMP-1 and yellow is actin. (B) Quantitation of colocalization between Bb and LAMP-1 in 10 phagosomes of WT (black dots) and MyD88-/- (red dots) BMDMs by measuring intensity overlap between LAMP-1 staining and Bb staining. (C) Western blot of protein lysate isolated from WT BMDMs after 6-hour stimulation with Bb +/- ATP (C=cell lysate, S=supernatant).

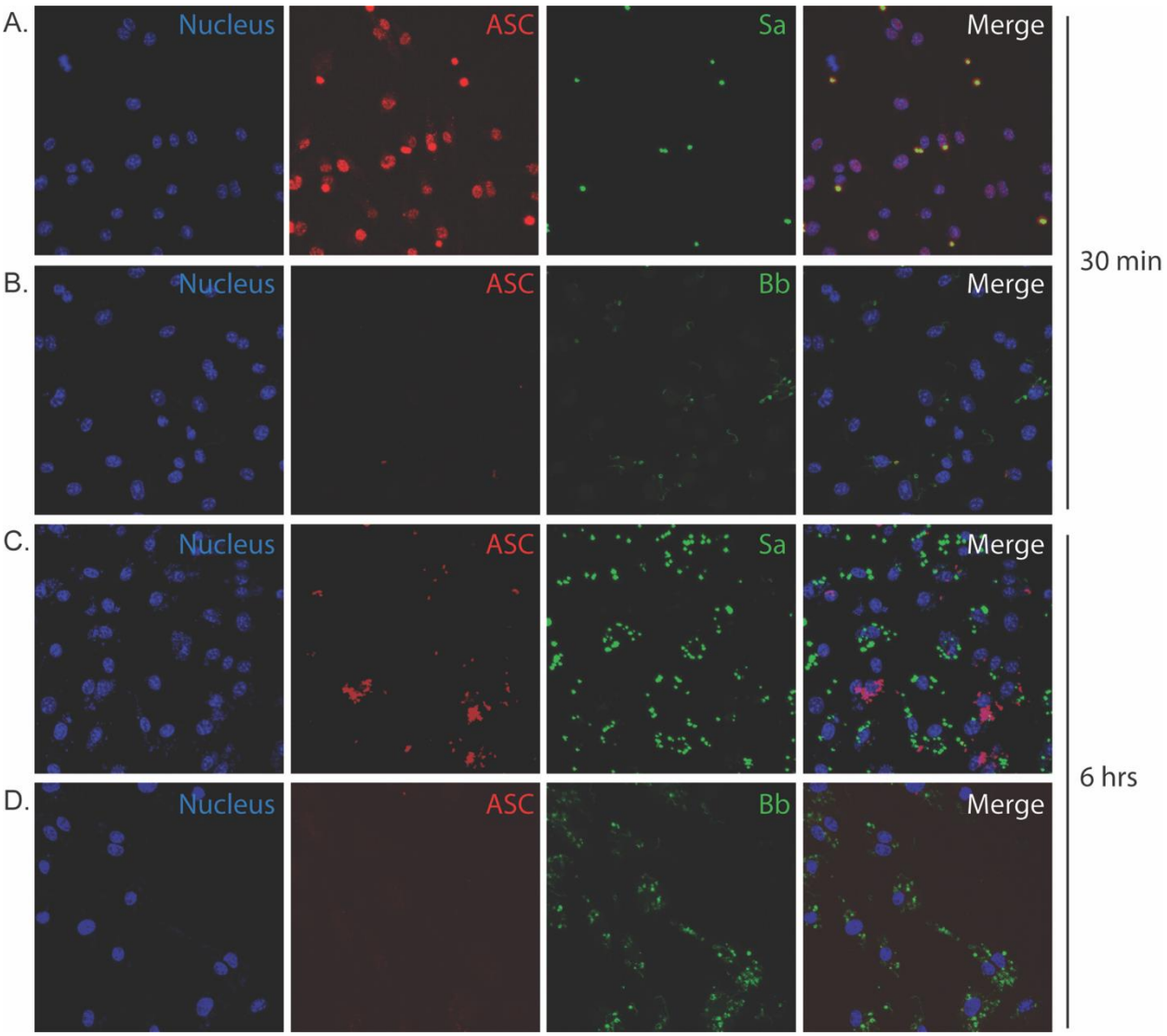

Figure 5: Bb does not induce ASC formation in BMDMs. (A-D) Confocal images (40x) of BMDMs stimulated with either Bb (B and D) or Sa (A and C) for 1 hour (A-B) or 6 hours (C-D). Blue is nucleus, red is ASC and green is the bacteria species.

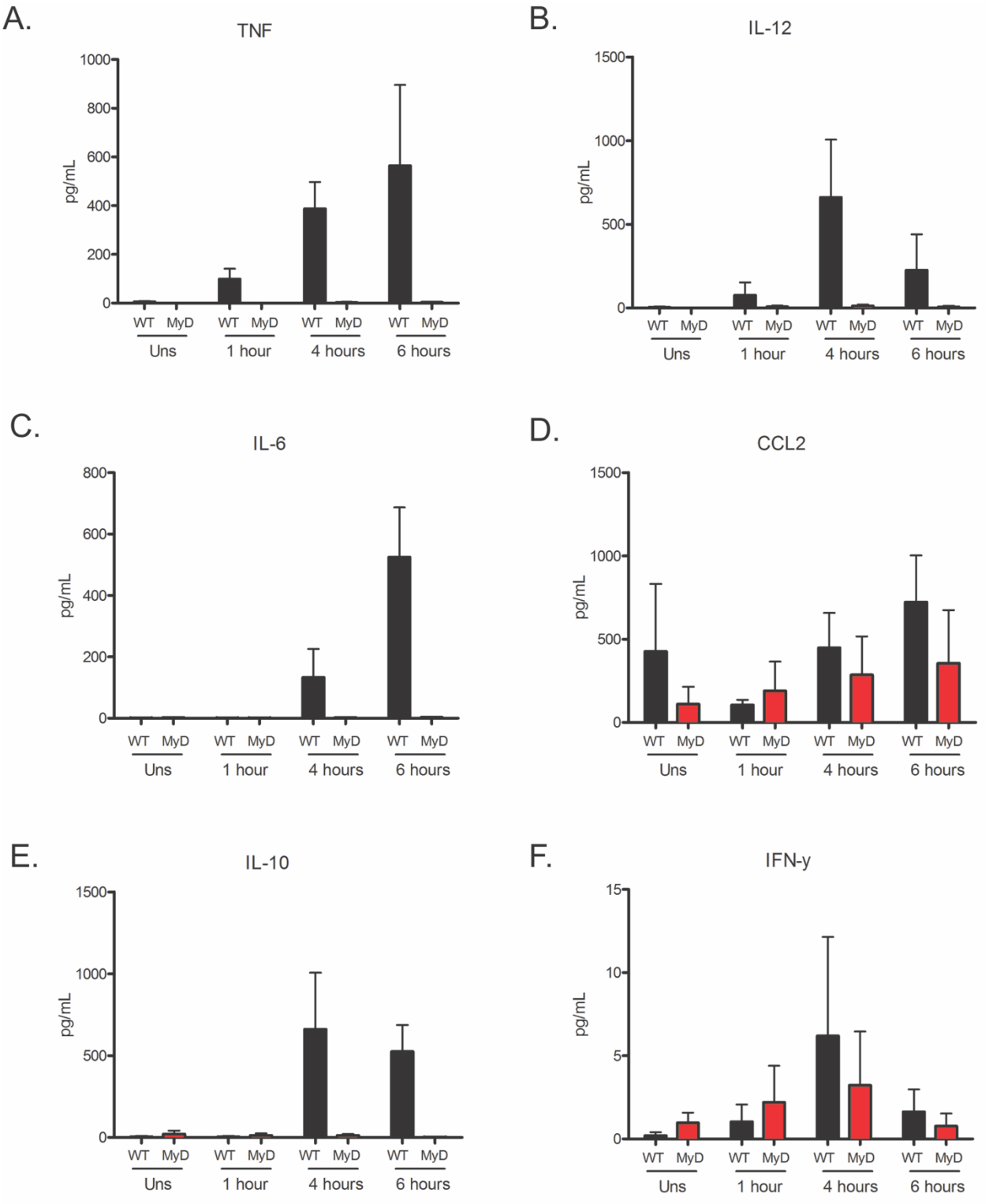

Figure 6: MyD88-/- BMDMs stimulated with Bb show abrogated cytokine production. (A-D) Quantification of CCL2 (A), IL-12 (B), IL-6 (C) and IL-10 (D) proteins in supernatant from WT and MyD88-/- (MyD) BMDMs stimulated with Bb at MOI 10:1 for 1, 4 or 6 hours. N= 3 mouse BMDM per genotype *p-value<0.05, **p-value<0.01, ***p-value<0.001, NS=not significant

Signaling cascades induced in the absence of MyD88 are still triggered from the phagosome

The signaling pathways described above illustrate potential mechanisms that inflammatory genes can be induced in the absence of MyD88. However, previous studies indicate that phagocytosis is critical to induce a robust cytokine response to the spirochete, even in the presence of MyD88 (Moore, Cruz et al. 2007). To determine whether MyD88-dependent inflammatory signals are enhanced by phagocytosis, we stimulated WT and MyD88-/- BMDMs with Bb in the presence or absence of Cytochalasin D, which blocks phagocytosis. We then measured transcript production of chemokines identified in our RNA-sequencing data as MyD88-independent and which also were significantly altered in the tissue microarray. Absence of Bb uptake in BMDMs in Cytochalasin-D treated cells was confirmed by confocal microscopy (data not shown). In WT BMDMs significant transcript reduction of *Ccl9* (**Figure 7A**), *Cxcl2* (**Figure 7B**), *Cxcl3* (**Figure 7C**), and *Cxcl10* (**Figure 7D**) was observed 1-, 4- and 6-hours post-stimulation. Similar reduction was also observed in MyD88-/- BMDMs at each time point (**Figure 7**). While there was a significant increase of MyD88-independent pro-inflammatory chemokines in both WT and MyD88-/- BMDMs, the increase was more pronounced in WT BMDMs. We also measured production of MyD88-dependent transcripts that we have previously shown to be abrogated in BMDMs pre-treated with Cytochalasin-D and stimulated with Bb (Moore, Cruz et al. 2007). Significant reduction of *Tnfa* (**Figure 7E**), and *Il6* (**Figure 7F** was observed in WT BMDMs pre-treated with Cytochalasin-D. As expected, production of these transcripts was not observed in MyD88-/- BMDMs (**Figure 7**). These results suggest that while, in response to Bb, pro-inflammatory chemokine

production by BMDMs does not require MyD88, it does require uptake of the spirochete into the phagosome for signaling cascades to be triggered.

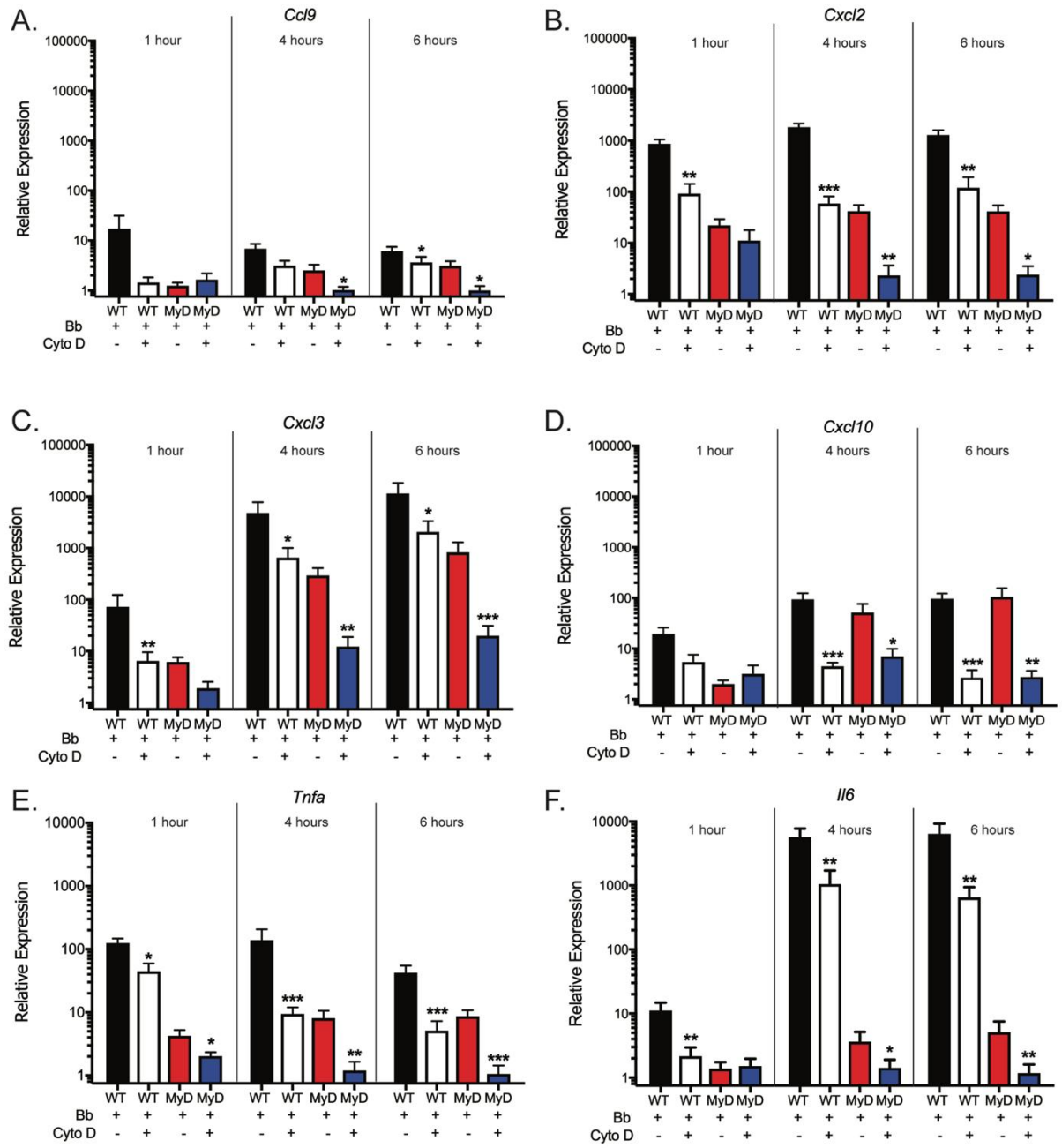

Figure 7: MyD88-independent chemokine production requires uptake of Bb. (A-D) Transcript analysis of WT (black and white bars) and MyD88-/- (red and blue bars) BMDMs stimulated with Bb in the presence or absence of Cytochalasin D for 1, 4 or 6 hours. Cells were pre-treated with Cytochalasin D for 1 hour prior to addition of Bb. Transcript production of *Ccl9* (A), *Cxcl2* (B), *Cxcl3* (C), *Cxcl10* (D), *Tnfa* (E) and *Il6* (F) were measured by qRT-PCR from total BMDM RNA. *p-value<0.05, **p-value<0.01, ***p-value<0.001, NS=not significant

CHAPTER 5: MYD88 DEPENDENT AND INDEPENDENT PHAGOSOMAL SIGNALING IN MURINE MACROPHAGES

IMPORTANCE

Our results in the preceding chapters emphasize the changes in inflammatory cell infiltrate and chemokine upregulation in tissues due to MyD88 signaling and show that MyD88 enhanced the capacity of macrophages to capture spirochetes. The purpose of the following experiments was to investigate MyD88-independent inflammatory responses and MyD88-dependent signaling in driving enhanced phagocytosis. To accomplish this, we used an RNA-sequencing approach (see methods in Chapter 2 and **Figure 1**) on Bb-stimulated BMDMs.

RESULTS

MyD88-dependent signaling causes differential expression of genes in macrophages that promote the inflammatory response.

To gain a better understanding of events that occur downstream of signaling by MyD88 which result in this phenotype presentation, we performed RNA sequencing on WT and MyD88-/- BMDMs stimulated with Bb for 6 hours. This time point was selected based on data showing comparable maturation in both WT and MyD88-/- BMDM phagosomes (**Figure 2A**). To establish comparable levels of phagocytic cargo despite the reduced uptake seen in the absence of MyD88, we stimulated WT BMDMs at a MOI of 10:1 and MyD88-/- BMDMs at a MOI of 100:1. The uptake percentages were not significantly different between the two cell phenotypes under these conditions. Both WT and MyD88-/- BMDMs showed differentially expressed genes (DEGs) when compared to their

respective unstimulated controls. We noted that the number of DEGs in WT BMDMs was much higher compared to MyD88-/- BMDMs (2818 genes vs 141 genes respectively) (**Figure 2B**). We saw similar numbers of up- and down-regulated DEGs in WT BMDMs (**Figure 2B**). In the MyD88-/- BMDMs, approximately 83% of the DEGs were up-regulated (**Figure 2B**). We classified the DEGs into three categories for further analysis: genes differentially expressed only in WT BMDMs (MyD88-dependent); genes differentially expressed in both WT and MyD88-/- BMDMs (MyD88-independent); and genes that were differentially expressed only in MyD88-/- BMDMs (MyD88-privative) (**Figure 2C**).

Using these data, we performed a Gene Ontology (GO) enrichment analysis of each group of DEGs (**Figure 2**). Because we showed above that in macrophages MyD88 affects both the inflammatory response and uptake of spirochetes we focused on biological processes relating to inflammation and phagocytosis in the MyD88-dependent DEGs. Multiple inflammatory biological processes were enriched (see supplemental files) but we concentrated on five processes with high numbers of gene hits: (i) Positive Regulation of Immune System Process; (ii) Positive Regulation of Cytokine Production; (iii) Immune System Process; (iv) Immune Response; and (v) Defense Response. The MyD88-dependent GO analysis resulted in the DEGs being broadly characterized into two different subsets. The first is comprised of DEGs enriched in all or almost all five processes and includes classic inflammatory genes, such as *Il6*, *Il12b*, *Il1b*, *Il23a* and *Tlr9* (**Figure 2D**). The second is comprised of DEGs that were enriched in only one or two of the five biological processes (**Figure 2D**). Examples of these DEGs included *Prdm1* (Positive Regulation of Immune System Process), which is involved in suppression of

IFN-β production (Keller and Maniatis 1991) and *Il17ra* (Positive Regulation of Cytokine Production), which facilitates the differentiation of neutrophils in response to IL-17 (Yao, Spriggs et al. 1997). The MyD88-independent DEGs also significantly enriched to the same five biological processes in their GO analysis but had fewer numbers of hits for each process. The GO analysis of the MyD88-privative genes also showed significant enrichment to four of these inflammatory processes; Positive Regulation of Cytokine Production was not enriched in the MyD88-privative DEGs. Overall this analysis indicates that MyD88 signaling triggers a more robust transcriptional inflammatory response to Bb which involves many processes and cellular elements that can result in immune cell activation.

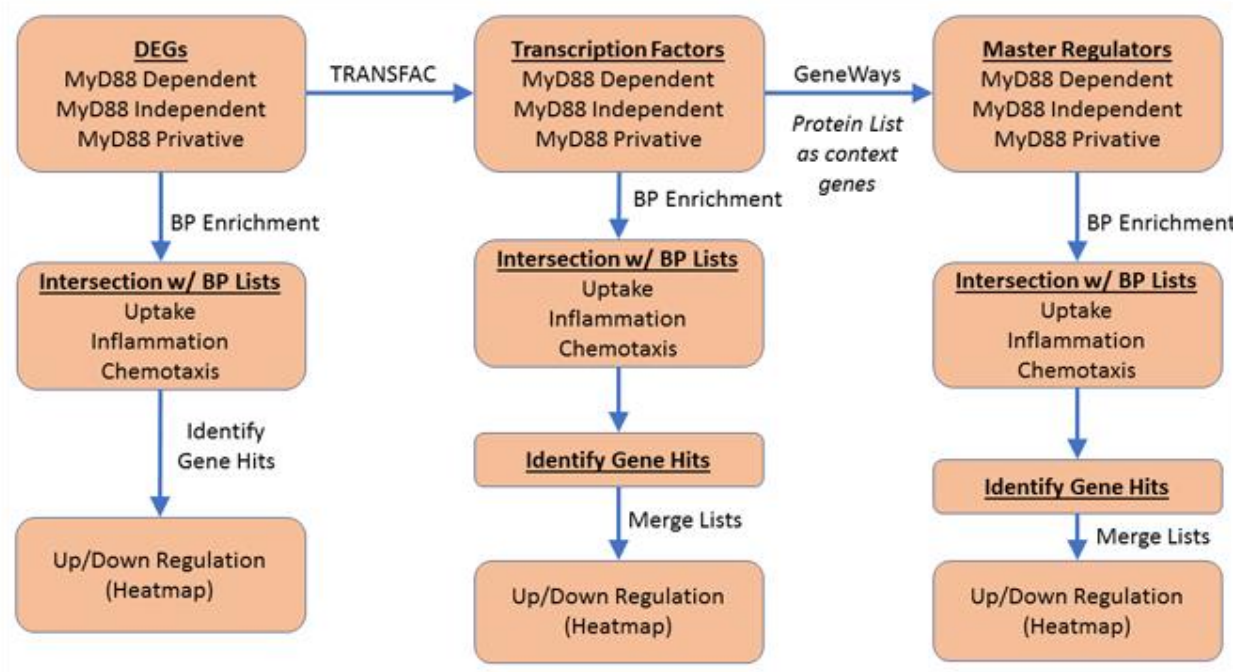

Figure 1: Analysis pipeline for analysis of RNA sequencing data. Based on identified DEGs transcription factors were mapped to promotor regions using the TRANSFAC database. Once transcription factors were identified for each subgroup of DEGs, master regulators were identified using the GeneWays database, using a list of known proteins expressed in MyD88-/- BMDMs as context genes. At each step of analysis (DEG, transcription factor, master regulator) an enrichment analysis for biological processes was completed and intersected with the list of relevant biological processes. The gene hits for each biological process were then merged into one list and exported into a heat map to determine whether they were up or down regulated.

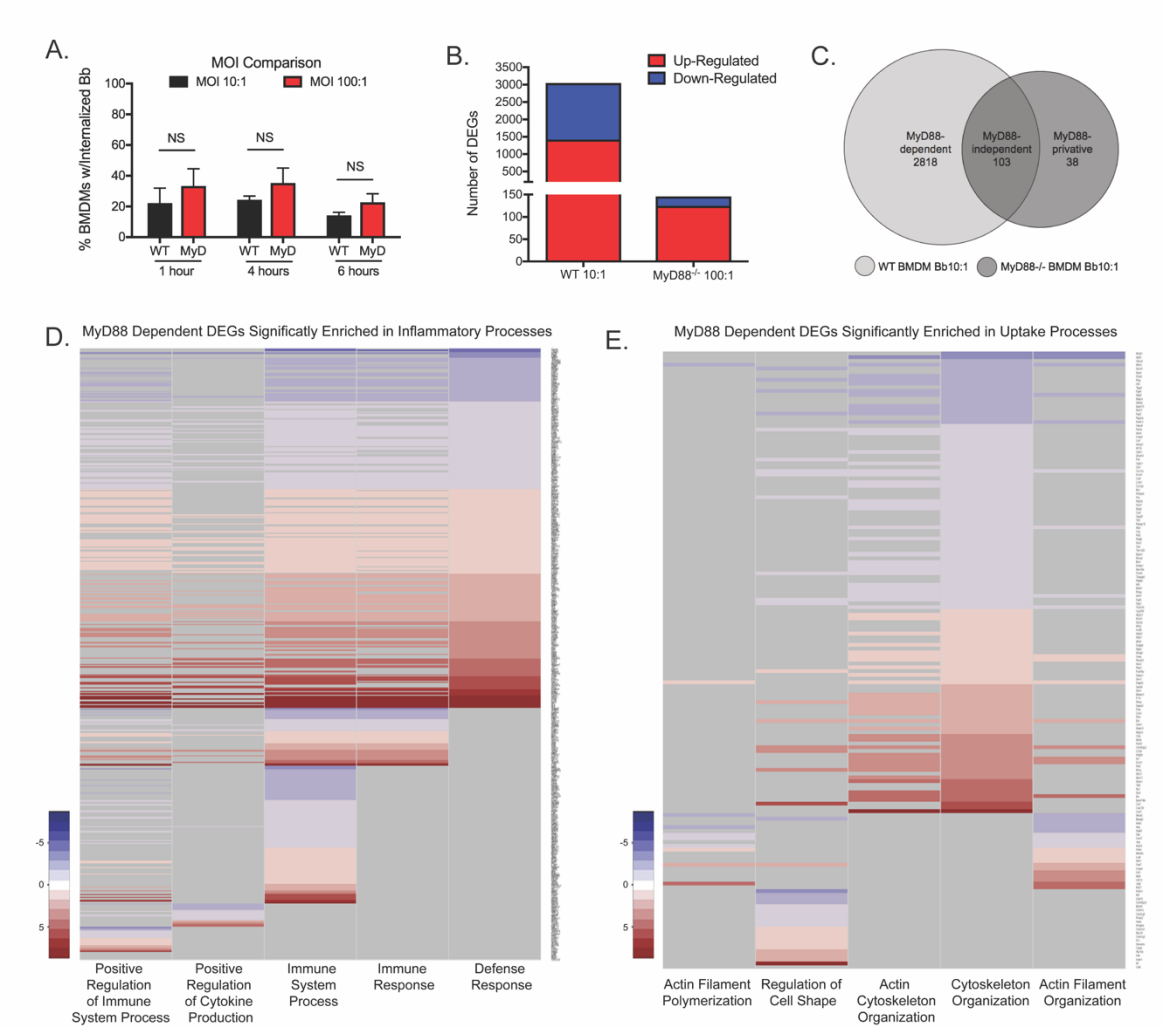

Figure 2: MyD88-dependent DEGs are significantly enriched in biological processes related to inflammation and uptake. (A) Bb uptake comparison between WT BMDMs stimulated at a MOI 10:1 and MyD88-/- BMDMs stimulated at a MOI 100:1 for 6 hours. (B) Number of differentially expressed genes (DEGs) in Bb-infected WT and MyD88-/- BMDMs determined by RNA-sequencing. Red bar indicates number of upregulated DEGs and blue bar indicates number of down-regulated DEGs. Bar height represents total number of DEGs in each condition. (C) Venn diagram depicting DEG classification. MyD88-dependent genes (light gray, left) are only differentially expressed in WT BMDMs. MyD88-independent genes (center) are expressed in both cell types. MyD88-privative genes (dark gray, right) are only differentially expressed in MyD88-/- BMDMs. (D and E) Heat maps depicting fold-change values of MyD88-dependent DEGs enriched in specific biological processes. Red indicates positive fold-change increase, blue indicates negative fold-change increase, gray indicates no enrichment to biological process. (D) MyD88-dependent DEGs that significantly enriched to 5 indicated biological processes relating to inflammation. (E) MyD88-dependent DEGs that significantly enriched to 5 indicated biological processes relating to uptake.

Multiple genes associated with biological processes involved with phagocytosis are MyD88-dependent.

Based on our observation that the presence of MyD88 enhances phagocytosis we also analyzed whether any of the MyD88-dependent DEGs enriched to biological processes related to pathogen uptake. We identified 164 MyD88-dependent DEGs that enriched to five different biological processes relating to phagocytosis (Actin Filament Polymerization, Regulation of Cell Shape, Actin Cytoskeleton Organization, Cytoskeleton Organization, and Actin Filament Organization) (**Figure 2E**). Of particular interest, *Daam1* and *Fmnl1*, two genes shown to play a role in phagocytosis of Bb (Naj, Hoffmann et al. 2013, Hoffmann, Naj et al. 2014, Williams, Weiner et al. 2018), were differentially expressed in a MyD88-dependent manner (**Figure 2E**). Daam1, which was upregulated, is a formin protein that bundles actin fibers together to increase stability of coiling pseudopods, which are more adept at capturing the highly motile spirochetes (Naj and Linder 2017). Fmnl1, which was down-regulated, is also a formin protein that severs actin branches to promote polymerization and increase filopodia protrusion (Naj and Linder 2017, Williams, Weiner et al. 2018).To better understand how these genes relate to other genes commonly associated with phagocytosis, and to understand which pathways are turned on or off, we first separated the 164 genes into two groups based on upregulation or downregulation. We then entered the list of genes from each group into the GeneXplain software to determine how they interact with each other. Pathways including the uptake genes with up to 10 intermediates between them were computed. Because Daam1 and Fmnl1 have been previously implicated in phagocytosis of Bb, we then merged all pathways that included either *Daam1* or *Fmnl1* into networks (**Figure 3**). The network mapping *Daam1*

chains (**Figure 3A**) shows related pathways that are upregulated and includes *Rhoa*, *Akt1*, *Rac1* and *Cdc42* as intermediates. *Daam1* regulates *Rhoa* expression, which controls *Cdc42*, *Rac1* and *Akt1*. *Cdc42* is activating a Rho GTPase, *Rhoq*, which is upregulated in response to Bb. *Rac1* and *Akt1* both activate multiple genes that are also upregulated, indicating that while these intermediate proteins aren't differentially expressed they are still active in macrophages that have been stimulated with Bb. In contrast to *Daam1*, *Fmnl1* was downregulated in response to Bb. The network mapping *Fmnl1* chains (**Figure 3B**) also highlights other pathways and genes that are downregulated. This network also includes *Cdc42* and *Akt1* as intermediate proteins. However, the network shows that the genes which inactivate these proteins are being downregulated in an MyD88-dependent manner. The downregulation of these inhibitors indicates that the activity of these proteins is important in the macrophage response to Bb, consistent with the Daam1 network above. Taken together, these data suggest that MyD88 signaling upregulates multiple genes involved in regulating macrophage membrane protrusions. Upregulation of these genes likely contributes to the reorganization of cell machinery that enhances the capability of the WT macrophage to take up spirochetes.

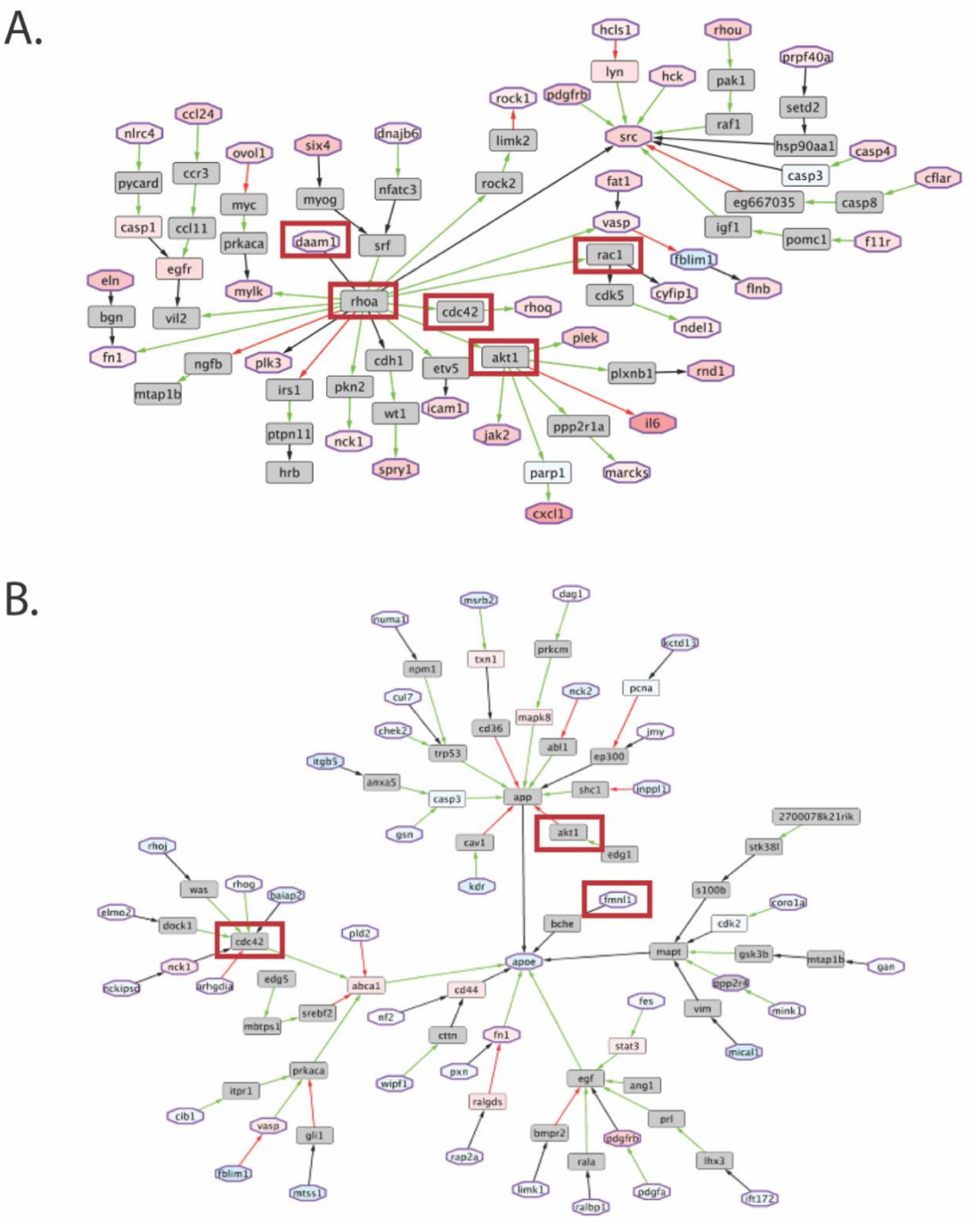

Figure 3: MyD88-dependent DEGs that significantly enrich to uptake processes show direct and indirect connections with key proteins involved in Bb phagocytosis. (A) Network of MyD88-dependent uptake DEGs that are upregulated. The varying degree of red or blue hue in select nodes correlates with the gene's Log2 Fold Change value. Red indicates positive fold change and blue indicates negative fold change. Gray nodes represent genes that were not differentially expressed. (B) Network of MyD88-dependent uptake DEGs that are upregulated. The same parameters and color scale applied in (A) was used.

Similar inflammatory and chemotactic processes are enriched regardless of MyD88-mediated signaling, but utilize different regulatory proteins

MyD88-dependent mechanisms of inflammation have been well characterized, but little work has been done to understand the drivers of Bb-induced inflammation in the absence of MyD88. To address this issue, we next completed a comprehensive analysis to determine how the DEGs are regulated within Bb-infected macrophages in the presence or absence of MyD88. We first identified transcription factors with potential binding sites in the promoter regions of the DEGs for each of the three subsets (66 MyD88-dependent, 201 MyD88-independent, and 39 MyD88-privative). We then identified master regulator proteins upstream of these transcription factors and performed a GO enrichment analysis using the same parameters described in **Figure 1**. The enrichment analysis of MyD88-independent master regulators revealed processes involved in cell metabolism and homeostasis, which did not give much insight into differences in mechanisms of inflammation driven by the presence or absence of MyD88. Therefore, we focused on analysis of MyD88-dependent and MyD88-privative master regulators. In light of our findings that Bb-infected MyD88-/- mice showed increased macrophage and neutrophil infiltrate in heart tissue, we investigated whether any master regulators enriched to inflammatory and/or chemotactic biological processes. Interestingly, similar biological processes significantly enriched in inflammation were both identified in the MyD88-dependent (including *MyD88*, *Irak2* and *Ly96*) and MyD88-privative (including *Vcam1* and *Cxcl2*) master regulators (**Figure 4A and 4C**), but the individual master regulators involved were different for each subset (**Figure 4A**). Importantly, over three times as many master regulators were identified for the MyD88-dependent DEGs than the MyD88-

privative DEGs (**Figure 4C**), suggesting that MyD88 signaling controls activation of more master regulators in the cell to initiate DEGs (see **Figure 2**) and enables the cell to perform unique processes in response to Bb.

MyD88 is a master regulator for transcription factors that control the MyD88-dependent DEGs enriched in uptake processes.

To better understand the phenotypic differences related to phagocytosis between the two genotypes (see **Figure 2)**, we identified transcription factors that map to promoter regions of DEGs related to phagocytosis. We then used OCSANA in Cytoscape to link MyD88 (as a master regulator) with transcription factors that map to DEGs in this specific subset. Of these transcription factors, three were expressed exclusively in WT BMDMs; *Zic1*, *Zeb1* and *Gata3*. Based on this information we constructed a network illustrating potential links between MyD88-mediated signaling and enhanced phagocytic capability seen in WT cells (**Figure 4E**). Of particular interest, the network predicts that Zic1, but not Zeb1 or Gata3, has the capacity to bind to the promoter regions of several of the MyD88-dependent DEGs that significantly enriched to processes associated with bacterial uptake. Zic1 is controlled by the intermediate protein ApoE, which is known to play a role in cholesterol metabolism in macrophages (Toledo, Monzon et al. 2015) and the absence of ApoE increases Bb burdens in experimentally infected mice (Toledo, Monzon et al. 2015).

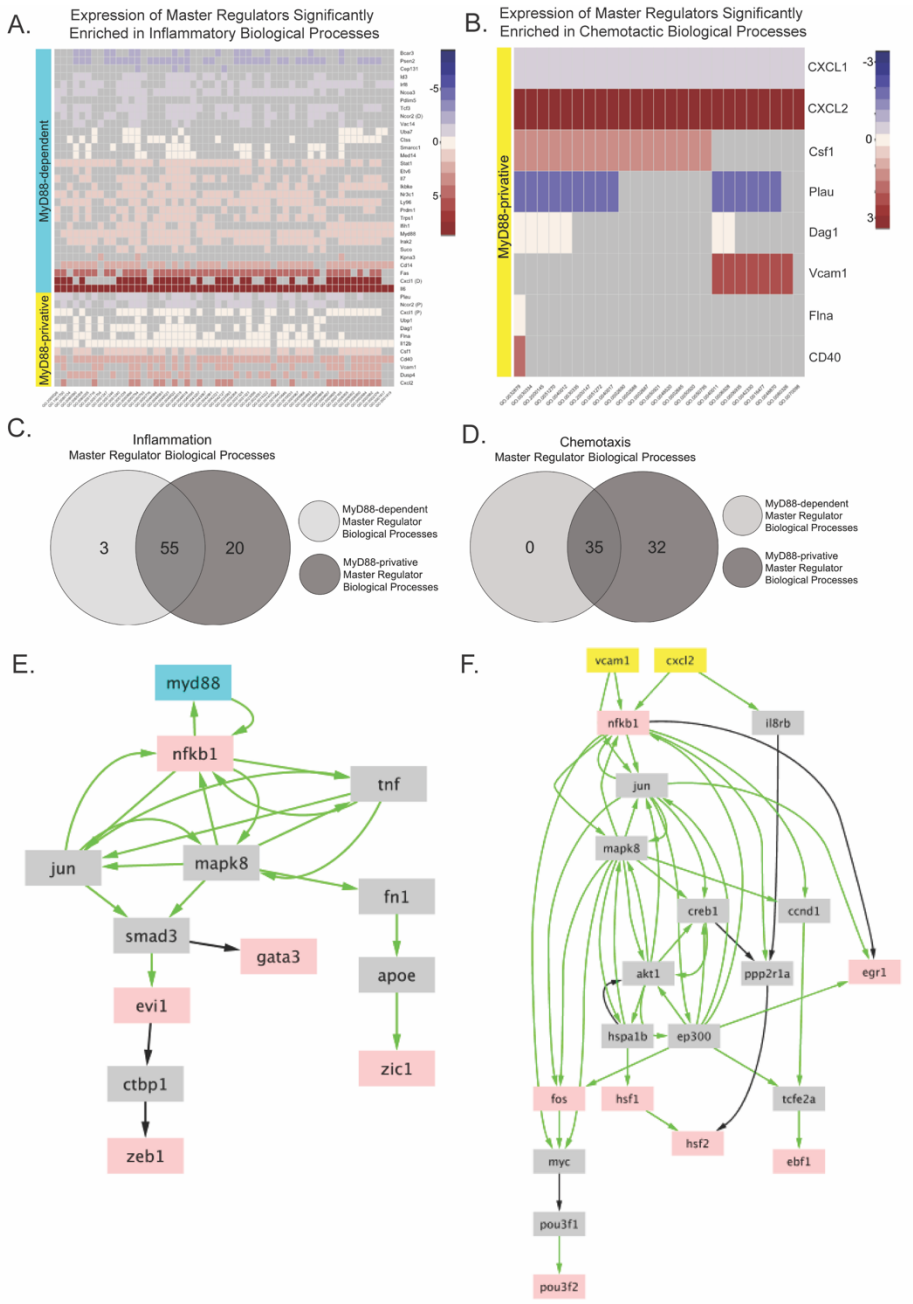

Figure 4: Master regulators of MyD88-dependent and MyD88-privative DEGs control similar inflammatory processes but different chemotactic processes. (A and B) Venn diagrams comparing biological processes (BP) relating to inflammation (A) or chemotaxis (B) significantly enriched between MyD88-dependent (light gray) and MyD88-privative (dark gray) master regulators. (C and D) Heat map showing fold change of master regulators enriched in inflammation (C) or chemotaxis (D) in WT (cyan) or MyD88-/- (yellow) BMDMs. GO numbers for significantly enriched BP are indicated on the x-axis. (E-F) Protein networks of significant master regulator proteins. Green arrows indicate positive regulation from one protein to another. Black arrows indicate unknown effect of one protein on another. Proteins in gray boxes represent intermediates and red boxes indicate transcription factors. (E) Protein network of MyD88 (blue box) and downstream intermediates. (F) Protein network of MyD88-privative master regulators (yellow boxes) that significantly enriched to chemotaxis-related BP.

MyD88-privative master regulators are involved in multiple chemotactic biological processes not enriched in WT BMDMs.

We also observed significant overlap between the chemotactic biological processes enriched in MyD88-dependent and MyD88-privative master regulators. However, MyD88-privative master regulators significantly enriched to multiple biological processes involved in chemotaxis that were not enriched in MyD88-dependent master regulators (**Figure 4B and 4D**), suggesting that the lack of MyD88 signaling allows for increased up-regulation of processes to facilitate cell migration into the tissues. The MyD88-privative master regulators involved in these chemotactic processes also enriched to inflammatory processes (**Figure 4B and 4D**), suggesting that Bb may trigger other signaling cascades which induce inflammation more skewed to cell recruitment and localization. We then generated a network of two MyD88-privative master regulators that were up-regulated and significantly enriched to multiple chemotactic biological processes (**Figure 4F**). Interestingly, *Cxcl2* was differentially expressed in the absence of MyD88 and also mapped as a master regulator in the network. Most importantly, both networks shown in **Figure 4E and 4F** provide potential targets for mutagenesis to test if they contribute to inflammation in humans.

CHAPTER 6: DISCUSSION

Lyme disease affects approximately 25,000 people in the United States each year, with an additional 10,000 unconfirmed but probable cases (Adrion, Aucott et al. 2015, CDC 2016). The spectrum of clinical manifestations seen in patients varies between asymptomatic, mild and more severe disease. Patients with severe LD can present with varying degrees of carditis, meningitis, optic neuritis and increased intracranial pressure (Steere and Glickstein 2004, Radolf, Caimano et al. 2012, CDC 2016, Steere, Strle et al. 2016). It is also well established that some patients develop a wide spectrum of poorly understood post LD treatment inflammatory signs and symptoms (CDC 2016), as well as post-treatment arthritis. Thus, it is essential to gain a complete understanding for how the human immune system responds to Bb, facilitates clearance of the spirochete and contributes to the inflammatory clinical manifestation of the disease. Previous studies by our group have emphasized that uptake and degradation of Bb by phagocytic cells, including monocytes and macrophages, are critical in eliciting the inflammatory response to the bacterium (Moore, Cruz et al. 2007, Salazar, Duhnam-Ems et al. 2009, Cervantes, Dunham-Ems et al. 2011, Cervantes, La Vake et al. 2013, Cervantes, Hawley et al. 2014). The findings from these studies, as well as others (Shin, Isberg et al. 2008), show that the adaptor protein MyD88 plays a critical role in bacterial uptake and phagosomal signaling. in macrophages. In the current study we provide further evidence that the macrophage is a key driver of inflammation, even in the absence of MyD88. We also showed that while MyD88 has a significant impact on spirochetal uptake, phagosome maturation and bacteria degradation are not affected. Of particular novelty, phagosomal signaling cascades induced by Bb ligands in macrophages trigger a number of

inflammatory and chemotactic processes. Inflammatory processes are mediated by different regulatory proteins depending on whether MyD88 is present or absent, but similar processes are upregulated in both genotypes. Induction of several chemotactic processes occurs independently of MyD88. Moreover, inflammatory and chemotactic signals in macrophages can also be emitted from within the phagosome, independently of MyD88, through interaction with a yet to be characterized receptor. In depth analysis of these signaling cascades allowed us to identify unique master regulators and transcription factors which need to be further explored to understand their potential role affecting the wide diversity of the clinical manifestations seen in human LD. In the current study we provide further evidence that the macrophage is a key driver of inflammation, even in the absence of MyD88. We also showed that while MyD88 has a significant impact on spirochetal uptake, phagosome maturation and bacteria degradation are not affected. These phenotypic changes are driven by the signaling cascades induced by MyD88 as a result of bacterial ligands engaging TLR receptors in the phagosome, triggering phagosomal signaling.

The importance of MyD88 signaling in tissues to facilitate Bb clearance is a concept that has been well-studied, but the mechanisms that account for this effect have not been defined. Our results demonstrate that MyD88 signaling in Bb-infected mice affects spirochete clearance from multiple tissues. In bladder, skin, ear, and joint tissue the lack of MyD88 results in Bb burdens that remain elevated even 56 DPI. This finding is consistent with results from several previously recognized (Bolz, Sundsbak et al. 2004, Liu, Montgomery et al. 2004, Behera, Hildebrand et al. 2006). Liu et al demonstrated.

demonstrated increased bacterial burdens in MyD88-/- mouse bladders at 14 and 45 DPI, as well as blood culture positivity at 45 DPI (Liu, Montgomery et al. 2004). Bolz et al. showed increased spirochete burdens in MyD88-/- mice 2 weeks and 4 weeks post infection in heart, ear and ankle tissue (Bolz, Sundsbak et al. 2004). Behera et al. illustrated increased bacterial burdens in MyD88-/- mice 3 weeks post infection in joint, muscle and kidney tissue (Behera, Hildebrand et al. 2006). Overall these prior studies are comparable to our results shown in **Figure 1,** demonstrating that MyD88 signaling in Bb-infected mice affects spirochete clearance from multiple tissues. In the current study we quantified Bb burdens in multiple target tissues at early (14 DPI), intermediate (28 DPI) and late (56 DPI) time points post-infection to create a more complete depiction of bacterial burden kinetics and how they are affected by the presence of MyD88. In bladder, skin, ear, and joint tissue the lack of MyD88 resulted in high Bb burdens, even 56 DPI. It should be noted that in contrast to prior work (Bolz, Sundsbak et al. 2004, Liu, Montgomery et al. 2004, Behera, Hildebrand et al. 2006), we did not observe significant differences in spirochete burdens at 14 DPI. Of particular importance, our findings suggest that MyD88 signaling enhances but is not required for bacterial control in heart tissue, since there was a reduction in Bb burdens in MyD88-/- mouse hearts 56 DPI. No change in the overall health of the mice was observed despite the high Bb burdens in MyD88-/- mice, indicating that while the mouse model is extremely useful for examining infiltrate at the cellular level, the effect of higher burdens on severity of clinical manifestations is difficult to determine. Whether MyD88 is required for Bb clearance in human tissues, and how it impacts this process in the context of LD is not known.

It is well accepted that infection with Bb triggers an inflammatory response, the robustness of which dictates the severity of human LD. Tissue-specific differences in inflammation in the mouse model of infection have been reported in prior studies (Bolz, Sundsbak et al. 2004, Behera, Hildebrand et al. 2006), but the characterization of the immune cell infiltrate occurring in the absence of MyD88 in those studies was very general. In this study we characterized the types of immune cells observed in Bb-infected tissue infiltrate, focusing on macrophages because of their role in early recognition and clearance. Interestingly, the heart tissue in MyD88-/- mice showed significantly more inflammation, with higher macrophage infiltrate 28 DPI. The robust macrophage recruitment to the heart illustrates the important role these cells have in clearing spirochetes. Montgomery *et al*.(Montgomery, Booth et al. 2007) showed that inhibiting chemotaxis of macrophages to the heart resulted in increased Bb burdens, but our study findings show increased Bb burdens in MyD88-/- hearts 28 DPI despite robust macrophage recruitment. This phenotype is rescued somewhat at 56 DPI when Bb burdens are reduced in MyD88-/- hearts. Taken together, findings from our *in vivo* heart studies suggest three major points. First, immune cell recruitment is not regulated by MyD88, since macrophages readily appear in infected heart tissue despite the lack of MyD88 signaling and chemokine production is significantly upregulated. Second, MyD88 signaling in macrophages is required for them to maintain the ability to effectively control Bb burdens in heart tissue, whether or not they are successfully able to migrate to sites of infection. Third, reduced or delayed spirochete clearance from heart tissue due to the absence of MyD88 signaling results in more phagocytic cells being recruited in attempt to control the infection, as indicated by the increased infiltrate seen in MyD88-/- mouse

hearts. These phagocytic cells, despite their diminished ability to capture spirochetes, eventually begin to control the bacterial loads. This could potentially be due to the availability of antibodies to opsonize spirochetes for uptake via Fc receptors (Liu, Montgomery et al. 2004, Belperron, Liu et al. 2014). However, macrophages are not the only cell driving spirochete clearance *in vivo*. Infected MyD88-/- mouse hearts also showed significant neutrophil infiltration 28 DPI, greater than WT mice, suggesting that, similar to joints, neutrophils also play a role in chemokine production and Bb clearance in the heart (Ritzman, Hughes-Hanks et al. 2010). Whether MyD88 signaling affects the ability of neutrophils to efficiently capture spirochetes is not known.

Unlike heart tissue, we did not observe increased inflammation in MyD88-/- joint tissue, despite seeing significant chemokine upregulation 28 DPI. This is in contrast to prior studies that showed greater neutrophil infiltrate in the joints of Bb-infected MyD88-/- mice (Bolz, Sundsbak et al. 2004). The lack of increased macrophage or neutrophil infiltrate in joints during Bb infection suggests that another cell is driving bacterial clearance in this tissue. This alternative response is not as effective at spirochete clearance because MyD88-/- mouse Bb burdens persist in tibiotarsal joints 56 DPI, providing further support that MyD88 also affects the ability of immune cells besides the macrophage to capture spirochetes. Despite high Bb burdens the inflammation in joint tissue was very mild, indicating that the phenomenon of recruiting more inflammatory in attempt to control the infection, as seen in heart tissue, is not observed in joint tissue. However, macrophages and neutrophils have been identified in synovial fluid and joint space of patients with Lyme

arthritis (Steere and Glickstein 2004), indicating that these cells have a much stronger role in the human inflammatory response in joints rather than heart.

An important step in this process is degradation of the bacteria to expose TLR ligands, which occurs only when the phagosome has matured and acidified. The requirement of MyD88 in this process is questionable; our results indicate that in the context of Bb infection, MyD88 is not required for phagosome maturation, evidenced by the recruitment of LAMP-1 to Bb-containing phagosomes in MyD88-/- BMDMs. Blander et al. published that MyD88-/- BMDMs infected with *S. aureus* or *E. coli* did not colocalize with either Lysotracker or LAMP-1 to the same degree as WT BMDMs (Blander and Medzhitov 2004). One possible explanation for this is that the recruitment of LAMP-1 is delayed in MyD88-/- BMDMs, given that Blander *et al*. measured phagosome maturation 1 hour after stimulation while our analysis was done 6 hours after stimulation. This explanation is supported by Yates *et al*. who showed slightly delayed acidification in MyD88-/- BMDMs stimulated with TLR2 or TLR4 ligands for 40 minutes (Yates and Russell 2005). The fragility of the Bb membranes also suggests that perhaps less acidification of the phagosome is needed to expose Bb PAMPs. Importantly, additional studies in human macrophages, which readily phagocytose Bb (Hawley, Cruz et al. 2017), will reveal whether possible variations in degradation affect recognition of Bb by the human immune system, and thus affect the inflammatory response.

Murine macrophages lacking MyD88 show a phagocytic defect when stimulated with Bb *ex vivo* compared to WT macrophages. Our results reveal that this phagocytic defect is

not dependent on length of stimulation (i.e. time dependent) and is only slightly rescued by increasing the MOI. Thus, in the absence of MyD88, macrophages are still capable of binding and uptake of the LD spirochete, but MyD88 signaling enhances the efficiency of Bb uptake by macrophages (**Figure 1**). This phenotype has been previously demonstrated with other bacteria (Edelson and Unanue 2002, Blander and Medzhitov 2004, Ip, Sokolovska et al. 2010, Shen, Kawamura et al. 2010). The direct correlation between MyD88 signaling and enhanced bacterial uptake has yet to be identified, but several advances have been made in determining proteins that link these cellular processes. Addition of TLR3 ligands to Bb stimulation of MyD88-/- BMDMs significantly rescues uptake (Shin, Miller et al. 2009), suggesting that in the absence of MyD88 TRIF signaling can activate pathways that result in similar actin rearrangement in the cell. Additional studies indicating that TLR2 can utilize TRIF have also been completed, but this interaction only appears to contribute to the inflammatory response rather than spirochete uptake (Salazar, Duhnam-Ems et al. 2009, Petnicki-Ocwieja, Chung et al. 2013). More recently, work by Killpack *et al.* (2017) showed an important role for spleen tyrosine kinase (Syk) in phagocytosis of Bb via integrin binding. The Syk gene (*Syk*) is significantly upregulated in an MyD88-dependent manner, suggesting that MyD88 drives over-expression of *Syk* to increase phosphorylation and activation of proteins involved in generating actin branches. In our GO analysis *Syk* was not one of the 164 MyD88-dependent genes that enriched to uptake biological processes, and the transcription factor Zic1, which has binding sites in the promoter regions of a significant number of these genes, is not predicted to bind in the promoter region of *Syk*. Zic1 was of particular interest to us because it appeared downstream of MyD88 in our network analysis and is

controlled by the intermediate protein ApoE. Mice lacking ApoE have increased bacterial burdens when infected with Bb (Toledo, Monzon et al. 2015), suggesting that ApoE signaling plays a role in cell remodeling processes necessary to enhance uptake. In addition, a link between Bb phagocytosis and cholesterol has been postulated by Hawley *et al.* (Hawley, Martin-Ruiz et al. 2013) who showed that CR3, a known phagocytic receptor for Bb, is recruited to lipid rafts with the co-receptor CD14. Thus, it is possible that MyD88 upregulates ApoE to enhance lipid rafts on the macrophage membrane, which can potentiate signaling to enhance uptake and provide scaffolding for proteins involved in actin remodeling.

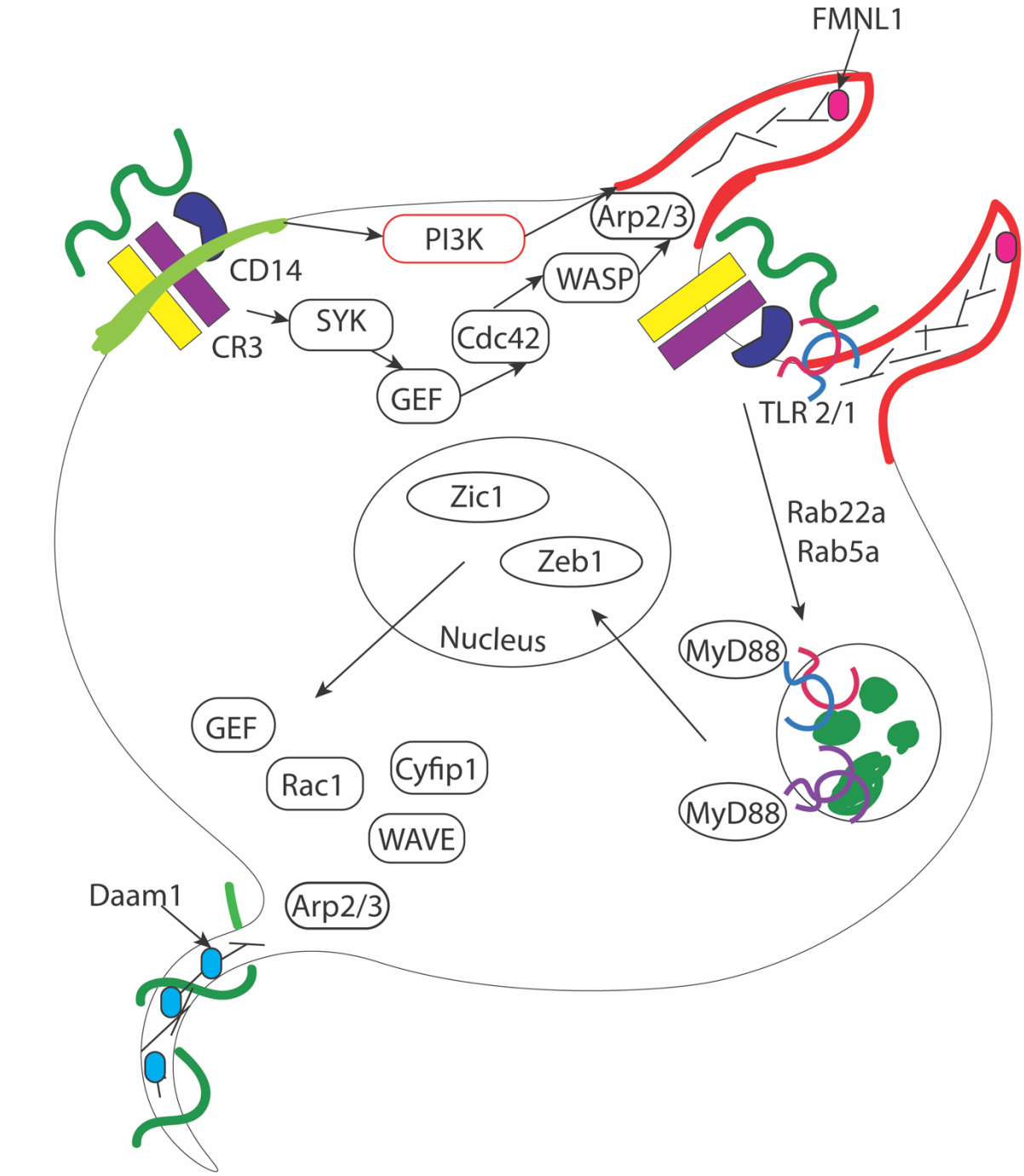

Figure 1: Model of phagocytic processes associated with Bb uptake. Initial interaction of Bb with surface integrins results in recruitment of kinases to phosphorylate the plasma membrane and activate guanine exchange factors (GEFs). GEFs activate Rho GTPases to induce actin polymerization and filopodia protrusions which form the phagocytic cup. Rab proteins facilitate coiling of Bb into a phagosome where degradation releases bacterial ligands for recognition by endosomal TLRs. MyD88 signaling downstream of these TLRs potentially activates transcription factors that control genes which affect coiling pseudopod protrusion for more efficient spirochete uptake.

Another important question raised by the RNA sequencing data is the non-canonical sources of inflammation seen in MyD88-/- mice. Our model traditionally predicts that due to the lack of TLR signaling Bb ligands cannot be recognized in the phagosome to trigger inflammatory signals. However, chemokine production by macrophages suggests that there is possibly another receptor recruited the phagosome that initiates chemokine production. The Bb ligand for this receptor is exposed in the phagosome, as indicated by **Figure 7**. Another mechanism for triggering chemokine production may be that the TLR receptors are utilizing another adaptor protein to transmit signals out of the phagosome, as postulated by Petnicki-Ocwieja *et al.* (Petnicki-Ocwieja, Chung et al. 2013). The production of chemokines facilitates recruitment of cells to spirochetes infected tissues, but the increased cell recruitment in MyD88-/- mice, coupled with higher Bb burdens suggests that the infiltrating immune cells are not efficient at clearing spirochetes. To compensate for their lack of efficiency at uptake, more cells are recruited. This progression of events may not be true for joint tissue compared to heart tissue, since our results show that the chemokine responses are different in both tissues and different cell types are recruited to each tissue. Network analysis of DEGs from macrophages identified multiple master regulators that could be controlling production of these chemokines, but further work needs to be done to determine if these master regulators are in fact active in macrophages containing Bb. Additional studies to test whether acidification of the phagosome is required for Bb-induced chemokine production will also give insight into which ligand-receptor interaction induces this response.

In summary, our results emphasize that the macrophage has a very important role in both recognition and clearance of Bb and is at the epicenter of the immunologic response to spirochete infection, particularly in relation to Lyme carditis. We also identified multiple factors that play a role in the efficiency of these processes. One crucial step is the recruitment of cells to the tissue via production of chemokines, which does not require MyD88 signaling but does require uptake of spirochetes. The necessity of uptake for significant chemokine upregulation is supported by our data showing that MyD88 is not required for phagosome maturation, a key step in exposing Bb ligands for recognition. Another aspect of this response requires MyD88 signaling cascades to elicit an inflammatory response that results in cell remodeling to enhance phagocytosis, as indicated by our *ex vivo* data. This allows macrophages to efficiently take up and clear spirochetes. The robustness of both the macrophage response and MyD88 signaling in human cells could also play a significant role in symptom severity and manifestation spectrum seen in patients with LD, affecting whether increased recruitment and activity of these cells plays a role in the long-term inflammation that develops in some individuals. Once translated in to human cells, these studies identify potential targets for treatment of Lyme disease in humans and increased understanding of the clinical spectrum of Lyme disease.

REFERENCES

Adachi, O., T. Kawai, K. Takeda, M. Matsumoto, H. Tsutsui, M. Sakagami, K. Nakanishi and S. Akira (1998). "Targeted disruption of the MyD88 gene results in loss of IL-1- and IL-18-mediated function." Immunity **9**(1): 143-150.

Adrion, E. R., J. Aucott, K. W. Lemke and J. P. Weiner (2015). "Health care costs, utilization and patterns of care following Lyme disease." PLoS One **10**(2): e0116767.

Ahuja, S. K. and P. M. Murphy (1996). "The CXC chemokines growth-regulated oncogene (GRO) alpha, GRObeta, GROgamma, neutrophil-activating peptide-2, and epithelial cell-derived neutrophil-activating peptide-78 are potent agonists for the type B, but not the type A, human interleukin-8 receptor." J Biol Chem **271**(34): 20545-20550.

Anders, S. and W. Huber (2010). "Differential expression analysis for sequence count data." Genome Biol **11**(10): R106.

Armstrong, A. L., S. W. Barthold, D. H. Persing and D. S. Beck (1992). "Carditis in Lyme disease susceptible and resistant strains of laboratory mice infected with Borrelia burgdorferi." Am J Trop Med Hyg **47**(2): 249-258.

Barthold, S. W., D. S. Beck, G. M. Hansen, G. A. Terwilliger and K. D. Moody (1990). "Lyme borreliosis in selected strains and ages of laboratory mice." J Infect Dis **162**(1): 133-138.

Barthold, S. W., D. H. Persing, A. L. Armstrong and R. A. Peeples (1991). "Kinetics of Borrelia burgdorferi dissemination and evolution of disease after intradermal inoculation of mice." Am J Pathol **139**(2): 263-273.

Behera, A. K., E. Hildebrand, R. T. Bronson, G. Perides, S. Uematsu, S. Akira and L. T. Hu (2006). "MyD88 deficiency results in tissue-specific changes in cytokine induction and inflammation in interleukin-18-independent mice infected with Borrelia burgdorferi." Infect Immun **74**(3): 1462-1470.

Behera, A. K., E. Hildebrand, S. Uematsu, S. Akira, J. Coburn and L. T. Hu (2006). "Identification of a TLR-independent pathway for Borrelia burgdorferi-induced expression of matrix metalloproteinases and inflammatory mediators through binding to integrin alpha 3 beta 1." J Immunol **177**(1): 657-664.

Belperron, A. A., N. Liu, C. J. Booth and L. K. Bockenstedt (2014). "Dual role for Fcgamma receptors in host defense and disease in Borrelia burgdorferi-infected mice." Front Cell Infect Microbiol **4**: 75.

Benhnia, M. R., D. Wroblewski, M. N. Akhtar, R. A. Patel, W. Lavezzi, S. C. Gangloff, S. M. Goyert, M. J. Caimano, J. D. Radolf and T. J. Sellati (2005). "Signaling through CD14 attenuates the inflammatory response to Borrelia burgdorferi, the agent of Lyme disease." J Immunol **174**(3): 1539-1548.

Blander, J. M. (2007). "Coupling Toll-like receptor signaling with phagocytosis: potentiation of antigen presentation." Trends Immunol **28**(1): 19-25.

Blander, J. M. and R. Medzhitov (2004). "Regulation of phagosome maturation by signals from toll-like receptors." Science **304**(5673): 1014-1018.

Bockenstedt, J. J. W. a. L. K. (2010). Host Response. Borrelia: Molecular Biology, Host Interaction and Pathogenesis. D. S. S. a. J. D. Radolf. Norfolk UK, Caister Academic Press**:** 413-441.

Bolz, D. D., R. S. Sundsbak, Y. Ma, S. Akira, C. J. Kirschning, J. F. Zachary, J. H. Weis and J. J. Weis (2004). "MyD88 plays a unique role in host defense but not arthritis development in Lyme disease." J Immunol **173**(3): 2003-2010.

Brandt, M. E., B. S. Riley, J. D. Radolf and M. V. Norgard (1990). "Immunogenic integral membrane proteins of Borrelia burgdorferi are lipoproteins." Infect Immun **58**(4): 983-991.

CDC. (2016). "Lyme Disease Incidence Rates by State 2004-2015." from http://www.cdc.gov/lyme/stats/chartstables/incidencebystate.html.

CDC. (2016). "Post Treatment Lyme Disease Syndrome." from http://www.cdc.gov/lyme/postlds/index.html.

CDC. (2016). "Signs and Symptoms of Untreated Lyme Disease." from http://www.cdc.gov/lyme/signs_symptoms/index.html.

Cervantes, J. L., S. M. Dunham-Ems, C. J. La Vake, M. M. Petzke, B. Sahay, T. J. Sellati, J. D. Radolf and J. C. Salazar (2011). "Phagosomal signaling by Borrelia burgdorferi in human monocytes involves Toll-like receptor (TLR) 2 and TLR8 cooperativity and TLR8-mediated induction of IFN-beta." Proc Natl Acad Sci U S A **108**(9): 3683-3688.

Cervantes, J. L., K. L. Hawley, S. J. Benjamin, B. Weinerman, S. M. Luu and J. C. Salazar (2014). "Phagosomal TLR signaling upon Borrelia burgdorferi infection." Front Cell Infect Microbiol **4**: 55.

Cervantes, J. L., C. J. La Vake, B. Weinerman, S. Luu, C. O'Connell, P. H. Verardi and J. C. Salazar (2013). "Human TLR8 is activated upon recognition of Borrelia burgdorferi RNA in the phagosome of human monocytes." J Leukoc Biol **94**(6): 1231-1241.

Coburn, J., L. Magoun, S. C. Bodary and J. M. Leong (1998). "Integrins alpha(v)beta3 and alpha5beta1 mediate attachment of lyme disease spirochetes to human cells." Infect Immun **66**(5): 1946-1952.

Curtis, M. W., B. L. Hahn, K. Zhang, C. Li, R. T. Robinson and J. Coburn (2018). "Characterization of Stress and Innate Immunity Resistance of Wild-Type and Deltap66 Borrelia burgdorferi." Infect Immun **86**(2).

de Souza, M. S., A. L. Smith, D. S. Beck, L. J. Kim, G. M. Hansen, Jr. and S. W. Barthold (1993). "Variant responses of mice to Borrelia burgdorferi depending on the site of intradermal inoculation." Infect Immun **61**(10): 4493-4497.

Devreotes, P. and A. R. Horwitz (2015). "Signaling networks that regulate cell migration." Cold Spring Harb Perspect Biol **7**(8): a005959.

Dunham-Ems, S. M., M. J. Caimano, C. H. Eggers and J. D. Radolf (2012). "Borrelia burgdorferi requires the alternative sigma factor RpoS for dissemination within the vector during tick-to-mammal transmission." PLoS Pathog **8**(2): e1002532.

Dunham-Ems, S. M., M. J. Caimano, U. Pal, C. W. Wolgemuth, C. H. Eggers, A. Balic and J. D. Radolf (2009). "Live imaging reveals a biphasic mode of dissemination of Borrelia burgdorferi within ticks." J Clin Invest **119**(12): 3652-3665.

Edelson, B. T. and E. R. Unanue (2002). "MyD88-dependent but Toll-like receptor 2-independent innate immunity to Listeria: no role for either in macrophage listericidal activity." J Immunol **169**(7): 3869-3875.

Elsner, R. A., C. J. Hastey and N. Baumgarth (2015). "CD4+ T cells promote antibody production but not sustained affinity maturation during Borrelia burgdorferi infection." Infect Immun **83**(1): 48-56.

Fortune, D. E., Y. P. Lin, R. K. Deka, A. M. Groshong, B. P. Moore, K. E. Hagman, J. M. Leong, D. R. Tomchick and J. S. Blevins (2014). "Identification of lysine residues in the Borrelia burgdorferi DbpA adhesin required for murine infection." Infect Immun **82**(8): 3186-3198.

Fraser, C. M., S. Casjens, W. M. Huang, G. G. Sutton, R. Clayton, R. Lathigra, O. White, K. A. Ketchum, R. Dodson, E. K. Hickey, M. Gwinn, B. Dougherty, J. F. Tomb, R. D. Fleischmann, D. Richardson, J. Peterson, A. R. Kerlavage, J. Quackenbush, S. Salzberg, M. Hanson, R. van Vugt, N. Palmer, M. D. Adams, J. Gocayne, J. Weidman, T. Utterback, L. Watthey, L. McDonald, P. Artiach, C. Bowman, S. Garland, C. Fuji, M. D. Cotton, K. Horst, K. Roberts, B. Hatch, H. O. Smith and J. C. Venter (1997). "Genomic sequence of a Lyme disease spirochaete, Borrelia burgdorferi." Nature **390**(6660): 580-586.

Gebbia, J. A., J. L. Coleman and J. L. Benach (2001). "Borrelia spirochetes upregulate release and activation of matrix metalloproteinase gelatinase B (MMP-9) and collagenase 1 (MMP-1) in human cells." Infect Immun **69**(1): 456-462.

Guo, B. P., E. L. Brown, D. W. Dorward, L. C. Rosenberg and M. Hook (1998). "Decorin-binding adhesins from Borrelia burgdorferi." Mol Microbiol **30**(4): 711-723.

Hartmann, K., C. Corvey, C. Skerka, M. Kirschfink, M. Karas, V. Brade, J. C. Miller, B. Stevenson, R. Wallich, P. F. Zipfel and P. Kraiczy (2006). "Functional characterization of BbCRASP-2, a distinct outer membrane protein of Borrelia burgdorferi that binds host complement regulators factor H and FHL-1." Mol Microbiol **61**(5): 1220-1236.

Hastey, C. J., J. Ochoa, K. J. Olsen, S. W. Barthold and N. Baumgarth (2014). "MyD88- and TRIF-independent induction of type I interferon drives naive B cell accumulation but not loss of lymph node architecture in Lyme disease." Infect Immun **82**(4): 1548-1558.

Hawley, K., N. Navasa, C. M. Olson, Jr., T. C. Bates, R. Garg, M. N. Hedrick, D. Conze, M. Rincon and J. Anguita (2012). "Macrophage p38 mitogen-activated protein kinase activity regulates invariant natural killer T-cell responses during Borrelia burgdorferi infection." J Infect Dis **206**(2): 283-291.

Hawley, K. L., A. R. Cruz, S. J. Benjamin, C. J. La Vake, J. L. Cervantes, M. LeDoyt, L. G. Ramirez, D. Mandich, M. Fiel-Gan, M. J. Caimano, J. D. Radolf and J. C. Salazar (2017). "IFNgamma Enhances CD64-Potentiated Phagocytosis of Treponema pallidum Opsonized with Human Syphilitic Serum by Human Macrophages." Front Immunol **8**: 1227.

Hawley, K. L., I. Martin-Ruiz, J. M. Iglesias-Pedraz, B. Berwin and J. Anguita (2013). "CD14 targets complement receptor 3 to lipid rafts during phagocytosis of Borrelia burgdorferi." Int J Biol Sci **9**(8): 803-810.

Hawley, K. L., C. M. Olson, Jr., J. M. Iglesias-Pedraz, N. Navasa, J. L. Cervantes, M. J. Caimano, H. Izadi, R. R. Ingalls, U. Pal, J. C. Salazar, J. D. Radolf and J. Anguita (2012). "CD14 cooperates with complement receptor 3 to mediate MyD88-independent phagocytosis of Borrelia burgdorferi." Proc Natl Acad Sci U S A **109**(4): 1228-1232.

Heil, F., H. Hemmi, H. Hochrein, F. Ampenberger, C. Kirschning, S. Akira, G. Lipford, H. Wagner and S. Bauer (2004). "Species-specific recognition of single-stranded RNA via toll-like receptor 7 and 8." Science **303**(5663): 1526-1529.

Hellwage, J., T. Meri, T. Heikkila, A. Alitalo, J. Panelius, P. Lahdenne, I. J. Seppala and S. Meri (2001). "The complement regulator factor H binds to the surface protein OspE of Borrelia burgdorferi." J Biol Chem **276**(11): 8427-8435.

Hirschfeld, M., C. J. Kirschning, R. Schwandner, H. Wesche, J. H. Weis, R. M. Wooten and J. J. Weis (1999). "Cutting edge: inflammatory signaling by Borrelia burgdorferi lipoproteins is mediated by toll-like receptor 2." J Immunol **163**(5): 2382-2386.

Hoffmann, A. K., X. Naj and S. Linder (2014). "Daam1 is a regulator of filopodia formation and phagocytic uptake of Borrelia burgdorferi by primary human macrophages." FASEB J **28**(7): 3075-3089.

Hyde, J. A., E. H. Weening, M. Chang, J. P. Trzeciakowski, M. Hook, J. D. Cirillo and J. T. Skare (2011). "Bioluminescent imaging of Borrelia burgdorferi in vivo demonstrates that the fibronectin-binding protein BBK32 is required for optimal infectivity." Mol Microbiol **82**(1): 99-113.

Ip, W. K., A. Sokolovska, G. M. Charriere, L. Boyer, S. Dejardin, M. P. Cappillino, L. M. Yantosca, K. Takahashi, K. J. Moore, A. Lacy-Hulbert and L. M. Stuart (2010). "Phagocytosis and phagosome acidification are required for pathogen processing and MyD88-dependent responses to Staphylococcus aureus." J Immunol **184**(12): 7071-7081.

Keller, A. D. and T. Maniatis (1991). "Identification and characterization of a novel repressor of beta-interferon gene expression." Genes Dev **5**(5): 868-879.

Kenedy, M. R., T. R. Lenhart and D. R. Akins (2012). "The role of Borrelia burgdorferi outer surface proteins." FEMS Immunol Med Microbiol **66**(1): 1-19.

Kim, D., G. Pertea, C. Trapnell, H. Pimentel, R. Kelley and S. L. Salzberg (2013). "TopHat2: accurate alignment of transcriptomes in the presence of insertions, deletions and gene fusions." Genome Biol **14**(4): R36.

Kraiczy, P., J. Hellwage, C. Skerka, H. Becker, M. Kirschfink, M. M. Simon, V. Brade, P. F. Zipfel and R. Wallich (2004). "Complement resistance of Borrelia burgdorferi correlates with the expression of BbCRASP-1, a novel linear plasmid-encoded surface protein that interacts with human factor H and FHL-1 and is unrelated to Erp proteins." J Biol Chem **279**(4): 2421-2429.

Krull, M., S. Pistor, N. Voss, A. Kel, I. Reuter, D. Kronenberg, H. Michael, K. Schwarzer, A. Potapov, C. Choi, O. Kel-Margoulis and E. Wingender (2006). "TRANSPATH: an information

resource for storing and visualizing signaling pathways and their pathological aberrations." Nucleic Acids Res **34**(Database issue): D546-551.

Kurtenbach, K., K. Hanincova, J. I. Tsao, G. Margos, D. Fish and N. H. Ogden (2006). "Fundamental processes in the evolutionary ecology of Lyme borreliosis." Nat Rev Microbiol **4**(9): 660-669.

Lasky, C. E., R. M. Olson and C. R. Brown (2015). "Macrophage Polarization during Murine Lyme Borreliosis." Infect Immun **83**(7): 2627-2635.

Levin, R., S. Grinstein and J. Canton (2016). "The life cycle of phagosomes: formation, maturation, and resolution." Immunol Rev **273**(1): 156-179.

Lister, R., B. D. Gregory and J. R. Ecker (2009). "Next is now: new technologies for sequencing of genomes, transcriptomes, and beyond." Curr Opin Plant Biol **12**(2): 107-118.

Liu, N., R. R. Montgomery, S. W. Barthold and L. K. Bockenstedt (2004). "Myeloid differentiation antigen 88 deficiency impairs pathogen clearance but does not alter inflammation in Borrelia burgdorferi-infected mice." Infect Immun **72**(6): 3195-3203.

Mantovani, A., A. Sica, S. Sozzani, P. Allavena, A. Vecchi and M. Locati (2004). "The chemokine system in diverse forms of macrophage activation and polarization." Trends Immunol **25**(12): 677-686.

Matys, V., O. V. Kel-Margoulis, E. Fricke, I. Liebich, S. Land, A. Barre-Dirrie, I. Reuter, D. Chekmenev, M. Krull, K. Hornischer, N. Voss, P. Stegmaier, B. Lewicki-Potapov, H. Saxel, A. E. Kel and E. Wingender (2006). "TRANSFAC and its module TRANSCompel: transcriptional gene regulation in eukaryotes." Nucleic Acids Res **34**(Database issue): D108-110.

Mead, P. S. (2015). "Epidemiology of Lyme disease." Infect Dis Clin North Am **29**(2): 187-210.

Montgomery, R. R., C. J. Booth, X. Wang, V. A. Blaho, S. E. Malawista and C. R. Brown (2007). "Recruitment of macrophages and polymorphonuclear leukocytes in Lyme carditis." Infect Immun **75**(2): 613-620.

Moore, M. W., A. R. Cruz, C. J. LaVake, A. L. Marzo, C. H. Eggers, J. C. Salazar and J. D. Radolf (2007). "Phagocytosis of Borrelia burgdorferi and Treponema pallidum potentiates innate immune activation and induces gamma interferon production." Infect Immun **75**(4): 2046-2062.

Muehlenbachs, A., B. C. Bollweg, T. J. Schulz, J. D. Forrester, M. DeLeon Carnes, C. Molins, G. S. Ray, P. M. Cummings, J. M. Ritter, D. M. Blau, T. A. Andrew, M. Prial, D. L. Ng, J. A. Prahlow, J. H. Sanders, W. J. Shieh, C. D. Paddock, M. E. Schriefer, P. Mead and S. R. Zaki (2016). "Cardiac Tropism of Borrelia burgdorferi: An Autopsy Study of Sudden Cardiac Death Associated with Lyme Carditis." Am J Pathol **186**(5): 1195-1205.

Naj, X., A. K. Hoffmann, M. Himmel and S. Linder (2013). "The formins FMNL1 and mDia1 regulate coiling phagocytosis of Borrelia burgdorferi by primary human macrophages." Infect Immun **81**(5): 1683-1695.

Naj, X. and S. Linder (2015). "ER-Coordinated Activities of Rab22a and Rab5a Drive Phagosomal Compaction and Intracellular Processing of Borrelia burgdorferi by Macrophages." Cell Rep **12**(11): 1816-1830.

Naj, X. and S. Linder (2017). "Actin-Dependent Regulation of Borrelia burgdorferi Phagocytosis by Macrophages." Curr Top Microbiol Immunol **399**: 133-154.

Niedergang, F. and S. Grinstein (2018). "How to build a phagosome: new concepts for an old process." Curr Opin Cell Biol **50**: 57-63.

Norgard, M. V., L. L. Arndt, D. R. Akins, L. L. Curetty, D. A. Harrich and J. D. Radolf (1996). "Activation of human monocytic cells by Treponema pallidum and Borrelia burgdorferi lipoproteins and synthetic lipopeptides proceeds via a pathway distinct from that of lipopolysaccharide but involves the transcriptional activator NF-kappa B." Infect Immun **64**(9): 3845-3852.

Oosting, M., A. Berende, P. Sturm, H. J. Ter Hofstede, D. J. de Jong, T. D. Kanneganti, J. W. van der Meer, B. J. Kullberg, M. G. Netea and L. A. Joosten (2010). "Recognition of Borrelia burgdorferi by NOD2 is central for the induction of an inflammatory reaction." J Infect Dis **201**(12): 1849-1858.

Oosting, M., F. L. van de Veerdonk, T. D. Kanneganti, P. Sturm, I. Verschueren, A. Berende, J. W. van der Meer, B. J. Kullberg, M. G. Netea and L. A. Joosten (2011). "Borrelia species induce inflammasome activation and IL-17 production through a caspase-1-dependent mechanism." Eur J Immunol **41**(1): 172-181.

Pal, U., A. M. de Silva, R. R. Montgomery, D. Fish, J. Anguita, J. F. Anderson, Y. Lobet and E. Fikrig (2000). "Attachment of Borrelia burgdorferi within Ixodes scapularis mediated by outer surface protein A." J Clin Invest **106**(4): 561-569.

Pal, U., X. Li, T. Wang, R. R. Montgomery, N. Ramamoorthi, A. M. Desilva, F. Bao, X. Yang, M. Pypaert, D. Pradhan, F. S. Kantor, S. Telford, J. F. Anderson and E. Fikrig (2004). "TROSPA, an Ixodes scapularis receptor for Borrelia burgdorferi." Cell **119**(4): 457-468.

Pawlik, A., D. Kotrych, E. Paczkowska, D. Roginska, V. Dziedziejko, K. Safranow and B. Machalinski (2016). "Expression of allograft inflammatory factor-1 in peripheral blood monocytes and synovial membranes in patients with rheumatoid arthritis." Hum Immunol **77**(1): 131-136.

Petnicki-Ocwieja, T., E. Chung, D. I. Acosta, L. T. Ramos, O. S. Shin, S. Ghosh, L. Kobzik, X. Li and L. T. Hu (2013). "TRIF mediates Toll-like receptor 2-dependent inflammatory responses to Borrelia burgdorferi." Infect Immun **81**(2): 402-410.

Petzke, M. M., A. Brooks, M. A. Krupna, D. Mordue and I. Schwartz (2009). "Recognition of Borrelia burgdorferi, the Lyme disease spirochete, by TLR7 and TLR9 induces a type I IFN response by human immune cells." J Immunol **183**(8): 5279-5292.

Radolf, J. D., L. L. Arndt, D. R. Akins, L. L. Curetty, M. E. Levi, Y. Shen, L. S. Davis and M. V. Norgard (1995). "Treponema pallidum and Borrelia burgdorferi lipoproteins and synthetic lipopeptides activate monocytes/macrophages." J Immunol **154**(6): 2866-2877.

Radolf, J. D., M. J. Caimano, B. Stevenson and L. T. Hu (2012). "Of ticks, mice and men: understanding the dual-host lifestyle of Lyme disease spirochaetes." Nat Rev Microbiol **10**(2): 87-99.

Radolf, J. D., M. S. Goldberg, K. Bourell, S. I. Baker, J. D. Jones and M. V. Norgard (1995). "Characterization of outer membranes isolated from Borrelia burgdorferi, the Lyme disease spirochete." Infect Immun **63**(6): 2154-2163.

Radolf, J. D., M. V. Norgard, M. E. Brandt, R. D. Isaacs, P. A. Thompson and B. Beutler (1991). "Lipoproteins of Borrelia burgdorferi and Treponema pallidum activate cachectin/tumor necrosis factor synthesis. Analysis using a CAT reporter construct." J Immunol **147**(6): 1968-1974.

Ribes, S., T. Regen, T. Meister, S. C. Tauber, S. Schutze, A. Mildner, M. Mack, U. K. Hanisch and R. Nau (2013). "Resistance of the brain to Escherichia coli K1 infection depends on MyD88 signaling and the contribution of neutrophils and monocytes." Infect Immun **81**(5): 1810-1819.

Ristow, L. C., H. E. Miller, L. J. Padmore, R. Chettri, N. Salzman, M. J. Caimano, P. A. Rosa and J. Coburn (2012). "The beta(3)-integrin ligand of Borrelia burgdorferi is critical for infection of mice but not ticks." Mol Microbiol **85**(6): 1105-1118.

Ritzman, A. M., J. M. Hughes-Hanks, V. A. Blaho, L. E. Wax, W. J. Mitchell and C. R. Brown (2010). "The chemokine receptor CXCR2 ligand KC (CXCL1) mediates neutrophil recruitment and is critical for development of experimental Lyme arthritis and carditis." Infect Immun **78**(11): 4593-4600.

Russell, T. M., M. J. Delorey and B. J. Johnson (2013). "Borrelia burgdorferi BbHtrA degrades host ECM proteins and stimulates release of inflammatory cytokines in vitro." Mol Microbiol **90**(2): 241-251.

Salazar, J. C., S. Duhnam-Ems, C. La Vake, A. R. Cruz, M. W. Moore, M. J. Caimano, L. Velez-Climent, J. Shupe, W. Krueger and J. D. Radolf (2009). "Activation of human monocytes by live Borrelia burgdorferi generates TLR2-dependent and -independent responses which include induction of IFN-beta." PLoS Pathog **5**(5): e1000444.

Salazar, J. C., C. D. Pope, T. J. Sellati, H. M. Feder, Jr., T. G. Kiely, K. R. Dardick, R. L. Buckman, M. W. Moore, M. J. Caimano, J. G. Pope, P. J. Krause, J. D. Radolf and N. Lyme Disease (2003). "Coevolution of markers of innate and adaptive immunity in skin and peripheral blood of patients with erythema migrans." J Immunol **171**(5): 2660-2670.

Schenk, M., J. T. Belisle and R. L. Modlin (2009). "TLR2 looks at lipoproteins." Immunity **31**(6): 847-849.

Schmittgen, T. D. and K. J. Livak (2008). "Analyzing real-time PCR data by the comparative C(T) method." Nat Protoc **3**(6): 1101-1108.

Schwan, T. G. (2003). "Temporal regulation of outer surface proteins of the Lyme-disease spirochaete Borrelia burgdorferi." Biochem Soc Trans **31**(Pt 1): 108-112.

Schwan, T. G. and J. Piesman (2000). "Temporal changes in outer surface proteins A and C of the lyme disease-associated spirochete, Borrelia burgdorferi, during the chain of infection in ticks and mice." J Clin Microbiol **38**(1): 382-388.

Sellati, T. J., D. A. Bouis, M. J. Caimano, J. A. Feulner, C. Ayers, E. Lien and J. D. Radolf (1999). "Activation of human monocytic cells by Borrelia burgdorferi and Treponema pallidum is facilitated by CD14 and correlates with surface exposure of spirochetal lipoproteins." J Immunol **163**(4): 2049-2056.

Shannon, P., A. Markiel, O. Ozier, N. S. Baliga, J. T. Wang, D. Ramage, N. Amin, B. Schwikowski and T. Ideker (2003). "Cytoscape: a software environment for integrated models of biomolecular interaction networks." Genome Res **13**(11): 2498-2504.

Shen, Y., I. Kawamura, T. Nomura, K. Tsuchiya, H. Hara, S. R. Dewamitta, S. Sakai, H. Qu, S. Daim, T. Yamamoto and M. Mitsuyama (2010). "Toll-like receptor 2- and MyD88-dependent phosphatidylinositol 3-kinase and Rac1 activation facilitates the phagocytosis of Listeria monocytogenes by murine macrophages." Infect Immun **78**(6): 2857-2867.

Shin, J. J., K. Strle, L. J. Glickstein, A. D. Luster and A. C. Steere (2010). "Borrelia burgdorferi stimulation of chemokine secretion by cells of monocyte lineage in patients with Lyme arthritis." Arthritis Res Ther **12**(5): R168.

Shin, O. S., R. R. Isberg, S. Akira, S. Uematsu, A. K. Behera and L. T. Hu (2008). "Distinct roles for MyD88 and Toll-like receptors 2, 5, and 9 in phagocytosis of Borrelia burgdorferi and cytokine induction." Infect Immun **76**(6): 2341-2351.

Shin, O. S., L. S. Miller, R. L. Modlin, S. Akira, S. Uematsu and L. T. Hu (2009). "Downstream signals for MyD88-mediated phagocytosis of Borrelia burgdorferi can be initiated by TRIF and are dependent on PI3K." J Immunol **183**(1): 491-498.

Skare, J. T., T. A. Mirzabekov, E. S. Shang, D. R. Blanco, H. Erdjument-Bromage, J. Bunikis, S. Bergstrom, P. Tempst, B. L. Kagan, J. N. Miller and M. A. Lovett (1997). "The Oms66 (p66) protein is a Borrelia burgdorferi porin." Infect Immun **65**(9): 3654-3661.

Sokolovska, A., C. E. Becker, W. K. Ip, V. A. Rathinam, M. Brudner, N. Paquette, A. Tanne, S. K. Vanaja, K. J. Moore, K. A. Fitzgerald, A. Lacy-Hulbert and L. M. Stuart (2013). "Activation of caspase-1 by the NLRP3 inflammasome regulates the NADPH oxidase NOX2 to control phagosome function." Nat Immunol **14**(6): 543-553.

Steere, A. C. and S. L. Arvikar (2015). "Editorial commentary: what constitutes appropriate treatment of post-Lyme disease symptoms and other pain and fatigue syndromes?" Clin Infect Dis **60**(12): 1783-1785.

Steere, A. C. and L. Glickstein (2004). "Elucidation of Lyme arthritis." Nat Rev Immunol **4**(2): 143-152.

Steere, A. C., R. L. Grodzicki, J. E. Craft, M. Shrestha, A. N. Kornblatt and S. E. Malawista (1984). "Recovery of Lyme disease spirochetes from patients." Yale J Biol Med **57**(4): 557-560.

Steere, A. C., F. Strle, G. P. Wormser, L. T. Hu, J. A. Branda, J. W. Hovius, X. Li and P. S. Mead (2016). "Lyme borreliosis." Nat Rev Dis Primers **2**: 16090.

Takenawa, T. and S. Suetsugu (2007). "The WASP-WAVE protein network: connecting the membrane to the cytoskeleton." Nat Rev Mol Cell Biol **8**(1): 37-48.

Takeuchi, O., K. Hoshino and S. Akira (2000). "Cutting edge: TLR2-deficient and MyD88-deficient mice are highly susceptible to Staphylococcus aureus infection." J Immunol **165**(10): 5392-5396.

Tilly, K., J. G. Krum, A. Bestor, M. W. Jewett, D. Grimm, D. Bueschel, R. Byram, D. Dorward, M. J. Vanraden, P. Stewart and P. Rosa (2006). "Borrelia burgdorferi OspC protein required exclusively in a crucial early stage of mammalian infection." Infect Immun **74**(6): 3554-3564.

Toledo, A., J. D. Monzon, J. L. Coleman, J. C. Garcia-Monco and J. L. Benach (2015). "Hypercholesterolemia and ApoE deficiency result in severe infection with Lyme disease and relapsing-fever Borrelia." Proc Natl Acad Sci U S A **112**(17): 5491-5496.

Tunev, S. S., C. J. Hastey, E. Hodzic, S. Feng, S. W. Barthold and N. Baumgarth (2011). "Lymphoadenopathy during lyme borreliosis is caused by spirochete migration-induced specific B cell activation." PLoS Pathog **7**(5): e1002066.

Utans, U., R. J. Arceci, Y. Yamashita and M. E. Russell (1995). "Cloning and characterization of allograft inflammatory factor-1: a novel macrophage factor identified in rat cardiac allografts with chronic rejection." J Clin Invest **95**(6): 2954-2962.

Vera-Licona, P., E. Bonnet, E. Barillot and A. Zinovyev (2013). "OCSANA: optimal combinations of interventions from network analysis." Bioinformatics **29**(12): 1571-1573.

Vudattu, N. K., K. Strle, A. C. Steere and E. E. Drouin (2013). "Dysregulation of CD4+CD25(high) T cells in the synovial fluid of patients with antibiotic-refractory Lyme arthritis." Arthritis Rheum **65**(6): 1643-1653.

Westphal, A., W. Cheng, J. Yu, G. Grassl, M. Krautkramer, O. Holst, N. Foger and K. H. Lee (2017). "Lysosomal trafficking regulator Lyst links membrane trafficking to toll-like receptor-mediated inflammatory responses." J Exp Med **214**(1): 227-244.

Whiteside, S. K., J. P. Snook, Y. Ma, F. L. Sonderegger, C. Fisher, C. Petersen, J. F. Zachary, J. L. Round, M. A. Williams and J. J. Weis (2018). "IL-10 Deficiency Reveals a Role for TLR2-Dependent Bystander Activation of T Cells in Lyme Arthritis." J Immunol **200**(4): 1457-1470.

Williams, S. K., Z. P. Weiner and R. D. Gilmore (2018). "Human neuroglial cells internalize Borrelia burgdorferi by coiling phagocytosis mediated by Daam1." PLoS One **13**(5): e0197413.

Wooten, R. M., Y. Ma, R. A. Yoder, J. P. Brown, J. H. Weis, J. F. Zachary, C. J. Kirschning and J. J. Weis (2002). "Toll-like receptor 2 is required for innate, but not acquired, host defense to Borrelia burgdorferi." J Immunol **168**(1): 348-355.

Wormser, G. P. (2006). "Hematogenous dissemination in early Lyme disease." Wien Klin Wochenschr **118**(21-22): 634-637.

Yang, X. F., U. Pal, S. M. Alani, E. Fikrig and M. V. Norgard (2004). "Essential role for OspA/B in the life cycle of the Lyme disease spirochete." J Exp Med **199**(5): 641-648.

Yao, Z., M. K. Spriggs, J. M. Derry, L. Strockbine, L. S. Park, T. VandenBos, J. D. Zappone, S. L. Painter and R. J. Armitage (1997). "Molecular characterization of the human interleukin (IL)-17 receptor." Cytokine **9**(11): 794-800.

Yates, R. M. and D. G. Russell (2005). "Phagosome maturation proceeds independently of stimulation of toll-like receptors 2 and 4." Immunity **23**(4): 409-417.

Zinovyev, A., E. Viara, L. Calzone and E. Barillot (2008). "BiNoM: a Cytoscape plugin for manipulating and analyzing biological networks." Bioinformatics **24**(6): 876-877.